Westfälische
Wilhelms-Universität
Münster

Master Thesis

Electroweak neutralino annihilation processes in DM@NLO

Saskia Schmiemann
student number: 370256

28th January 2016

Münster

Abstract

Today there are several pieces of evidence for dark matter. One well-known experiment is the measurement of the Dark Matter relic density by the Planck satellite.

The thesis introduces the *Dark Matter at next-to-leading order* (DM@NLO) project which provides predictions for the dark matter relic density in the MSSM including higher-order corrections. Specifically the thesis will deal with the implementation of the processes $\tilde{\chi}_i^0 \tilde{\chi}_j^0 \to H_k H_l$ within DM@NLO. The second part will be the calculation of the relic density, by solving the numerical integration of the Boltzmann equation within DM@NLO.

Zusammenfassung

Heutzutage gibt es viele Hinweise auf die Existenz von Dunkler Materie. Ein bekanntes Experiment ist die Vermessung der Reliktdichte dunkler Materie mit dem Planck Satelieten.

Diese Arbeit gibt einen Einblick in das Projekt *Dark Matter at next-to-leading order* (DM@NLO). Mit DM@NLO werden Vorhergesagen über die Reliktdichte dunkler Materie im MSSM gemacht unter Berücksichtigung von Korrekturen nächster Ordnung. Das Augenmerk dieser Arbeit wird auf die Berechnung und Einbindung elektroschwacher Prozesse in DM@NLO liegen. Des weiteren wird die Berechnung der Reliktdichte genauer diskutiert und eine eigenständige Integrationsroutine zur Lösung der Boltzmann Gleichung in DM@NLO programmiert.

Contents

1. Introduction

Theoretical particle physics has still few open questions. One open question deals with the content the Universe. Only around 5% of the content of the Universe is from the luminous matter. The rest of the content is split into dark matter ($\sim 27\%$) and dark energy($\sim 68\%$) [17]. This begs the question, what is dark matter and dark energy.

Today there are several observational indications for dark matter. One well-known experiment is the measurement of the Dark Matter relic density by the Planck satellite [15].

Within the *Minimal supersymmetric Standard Model* (MSSM) a dark matter candidate is predicted, namely the *lightest supersymmetric particle* (LSP). This is due to the fact that in the MSSM the R-parity conservation force that one supersymmetric particles can only decay to another supersymmetric particle. The lightest particle is therefore stable [25].

Dark Matter at next-to-leading order (DM@NLO) is a code which provides predictions for the dark matter relic density in the MSSM including higher-order corrections.

There are two main objects of this work. The first part is the calculation and implementation of the neutralino annihilation into Higgs and vector bosons $\tilde{\chi}_i^0\tilde{\chi}_j^0 \to H_k H_l$, $\tilde{\chi}_i^0\tilde{\chi}_j^0 \to H_k V_l$, $\tilde{\chi}_i^0\tilde{\chi}_j^0 \to V_k V_l$ in DM@NLO. The second part is the calculation of the relic density by solving the numerically the Boltzmann equation in order to make DM@NLO a stand alone code.

The thesis is organized as follows, first there is a short overview, explaining the main aspects of the Standard Model and its remaining unsolved issues. Focusing on one weak point of the Standard Model the sector of Dark Matter will be discussed in more detail citing experimental evidence and possible dark matter candidates. Furthermore, the supersymmetric extension of Standard Model will be introduced, which provides a dark matter candidate, the neutralino of the MSSM.

Afterwards, the project *Dark Matter at next to leading order* (DM@NLO) will be presented with an overview of the included processes within DM@NLO.

This part starts with, the calculation and implementation of the electroweak processes and their comparison (analytically and numerically) with FormCalc [34] [35] and micrOMEGAs [20].

Second part is devoted to the stand alone code for DM@NLO for the calculation of the relic density. First the Boltzmann equation will be introduced and later on the numerical integration routine to solve the Boltzmann equation will be discussed. Finally the integration routine will be compared numerically with results from micrOMEGAs [19]. At the end the results will be summarized and a short outlook will be given.

2. Theoretical Background

2.1. The Standard Model

The Standard Model (SM) is the current model used to describe elementary particles and their interactions [14] [16].

The elementary particles are split into two groups, the fermions, with a spin of $\frac{1}{2}$ and the bosons with a spin of 1 (see figure 2.1). The fermions include quarks with six different flavors and leptons, all ordered in three families. To each particle there is a corresponding antiparticle with the opposite quantum numbers (unless the particle is its own anti-particle). The first generation represents the lightest particles of each group, while the third generation represents the heaviest ones. The second and third generation particles have a very short life time, that means, they decay very quickly into particles of a lighter generation.

There are four different ways for the elementary particles to interact with each other. The interactions can be separated into strong, electromagnetic, weak and gravitational. However, the gravitational interaction is not included in the SM.

All fermions interact weakly and the electrically charged ones interact also electromagnetically. The quarks are also affected by the strong interaction because of their color charge. Quarks do not exist as free particles, they have only been found experimentally in bounded states so called hadrons.

The gauge bosons are the mediators of the interactions. In an electromagnetic interaction between electrically charged particles a massless photon is transferred. In the weak interaction, the massive $W^{\pm}$- and Z-bosons represent the mediators. There are eight types of gluons. They all carry color charge, which induces them to interact. The Higgs boson is an indicator for the Higgs mechanism inducing some particles to be massive.

Despite the experimental success of the SM, several problems arise that cannot be explained within the SM. One of the main problems is the so-called *hierarchy problem*. In addition to the hierarchy problem, in the SM, it is not possible to unify all three interactions and form a grand unitary theory (GUT). The last problem, which is mentioned here is that the SM does not have candidate for *dark matter*[1]. To solve these problems, one has to extend the SM.

[1] see section 2.2

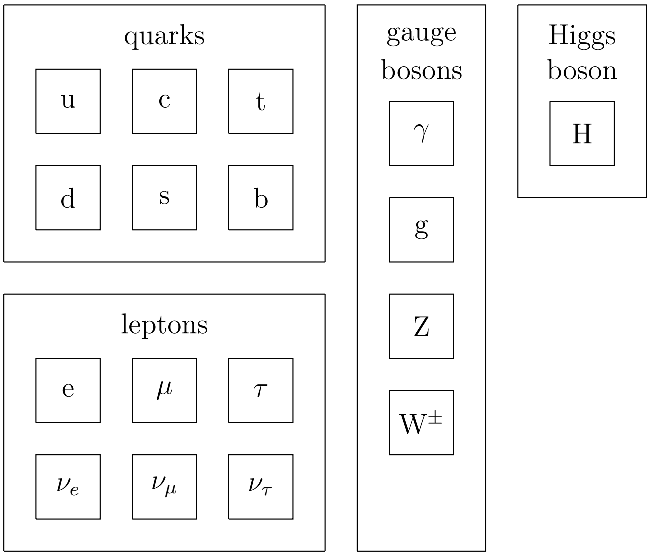

u: up
d: down
c: charm
s: strang
t: top
b: bottom

ν_e: electron neutrino
ν_μ: muon neutrino
ν_τ: tau neutrino
e: elektron
μ: muon
τ: tau

γ: photon
g: gluon
Z: Z boson
$W^\pm$: W boson
h^0: Higgs boson

Figure 2.1.: The elementary particles of the Standard Model

2.2. Dark Matter

Today one still does not know what dark matter really is. There are several efforts to explain dark matter. As far as we know dark matter is some kind of matter that does not interact electro-magnetically and is therefore invisible for most observations. Several pieces of evidence predict the existence of dark matter and indicate attributes for possible dark matter candidates.

2.2.1. Evidence

One of the earliest evidence for dark matter was given by F. Zwicky in 1933 [37]. He measured the red shift of the galaxies in the Coma Cluster. Within his calculations, he discovered that the luminous matter is not massive enough to explain the observed high velocities of the galaxies in the Coma Cluster. He discovered that there has to be around four hundred times more matter than luminous matter to explain the observed red shift. Until now, there a several more observations which show the existence of dark matter.

Rotation curves

One important evidence for dark matter is given by the analysis of galactic rotation curves. The rotation velocity of a star in a galaxy depends on its distance r from the galactic center. Using Newtonian mechanics the velocity can be determined as

$$m\frac{v^2}{r} = \frac{GmM(r)}{r^2} \qquad \Rightarrow v = \sqrt{\frac{GM(r)}{r}}, \tag{2.1}$$

where m is the mass of the stars, G the gravitational constant and $M(r)$ is the mass of the galaxy up to the distance r from the center. The rotation velocity can be experimentally determined by the measurement of the red shift of the stars. The light spectrum of the stars is red shifted because of the Doppler effect. To keep it simple, the mass density of the galaxy $\rho(r)$ is set to be radial in the following

$$M(r) = 4\pi \int_0^r dr' r'^2 \rho(r'). \tag{2.2}$$

The mass is concentrated around the center of the galaxy (black hole), so the stars further away from the center do not contribute radial to the mass any more. The mass starts to be r independent. As a result the star velocity v is anti-proportional to the distance from the center of the galaxy for large distances r. Figure 2.2 shows the measurement of the rotation curve of the galaxy MGC 6503. The theoretical prediction is the lowest curve, named as ‘disk’ The measurement of the galaxy MGC 6503 shows a plateau at higher distances, which does not agree with the theoretical prediction.

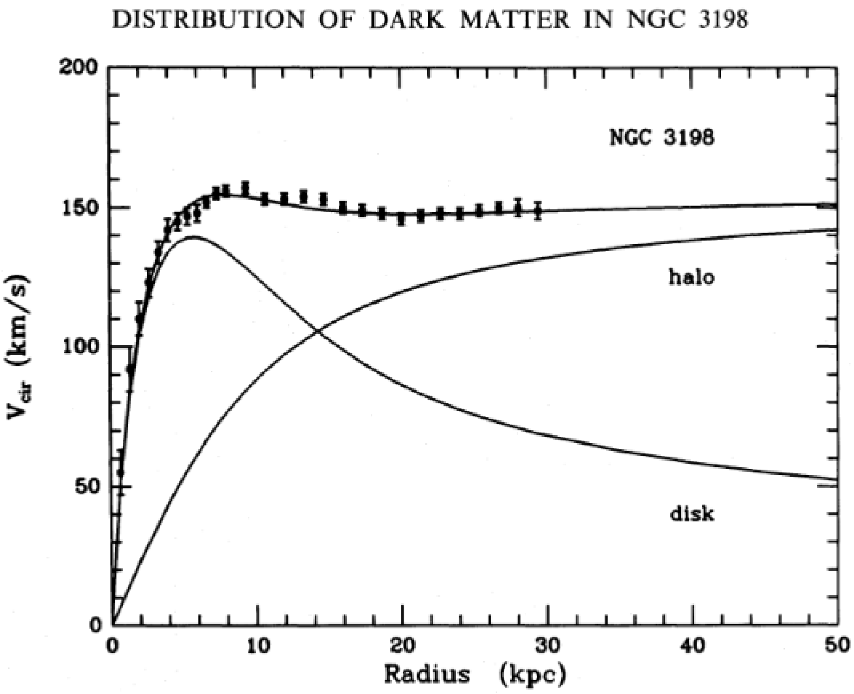

Figure 2.2.: Rotation curves of the MGC 6503 [10]

There are two possible approaches for this discrepancy. One idea is that the Newtonian mechanics is not valid for such small accelerations. The other approach is that there is still mass in the outer area of the galaxies, which interacts gravitationally. In Fig. 2.2 the theoretical prediction for this invisible massive matter is shown as 'halo'. Adding the effect of the 'halo' to the Newtonian prediction, the newly obtained prediction describes experimental data.

The Bullet-Cluster

Another evidence for dark matter is the observation of the Bullet Cluster [18]. The Bullet Cluster, such as in Fig. 2.3 accrues by the collision of two galaxy clusters 100 million years ago.

The most mass contained in the cluster is in the interstellar dust, which is visible via the X-ray radiation (colored red in Fig. 2.3). Total (even invisible) mass can be reconstructed by looking at gravitational lensing[2] which distorts the image of stars. It is to mention that the interstellar dust is affected by the collision of the galaxies because of electro-magnetically interactions. While for the blue colored matter, which is measured

[2]Gravitational lenses is the name of the effect that in the present of heavy masses the light is deflected by gravitational fields. This can be observed by blurred or shifted objects behind heavy masses. With statistical methods one can determine the mass of the gravitational lenses.

by gravitational lensing, the mass in unaffected by the collision and therefore interacts only weakly.

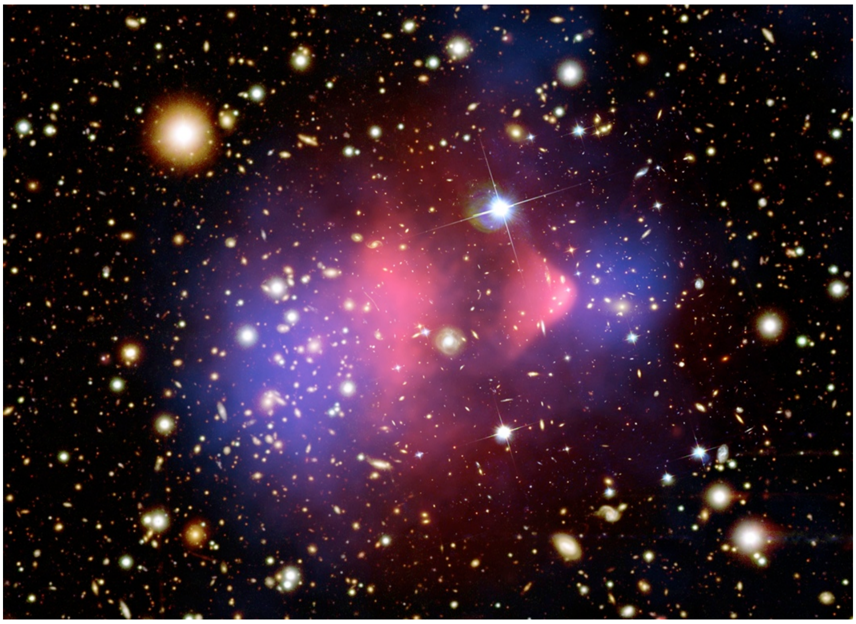

Figure 2.3.: Coloured Bullet-Cluster 1E0657-558 [1]

Cosmic Background

The cosmic microwave has its background origins in the epoch of the evolution of the Universe when the radiation and matter decoupled.The cosmic microwave background (CMB) was measured by several experiments (COBE, WMAP, Planck...). The CMB was identified with the black body radiation with a temperature of 2.7 K. The CMB is more or less isotropic on large scale, with temperature anisotropies around 60 μK. In Fig. 2.4 the fluctuations of the temperature are shown. These fluctuations are essential for our understanding of the universe. Without these fluctuation, the universe would not have any structure, like galaxies. These anisotropies can be also used to calculate the relic density of dark matter and of the baryonic matter [15]

$$\Omega_{\mathrm{CDM}} = 0.1186 \pm 0.0020 \qquad \Omega_{\mathrm{baryonic}} = 0.02226 \pm 0.00023 \tag{2.3}$$

2.2.2. Candidates

Today several theories exist which describes possible dark matter candidates. Some theoretical candidates will be named in the following.

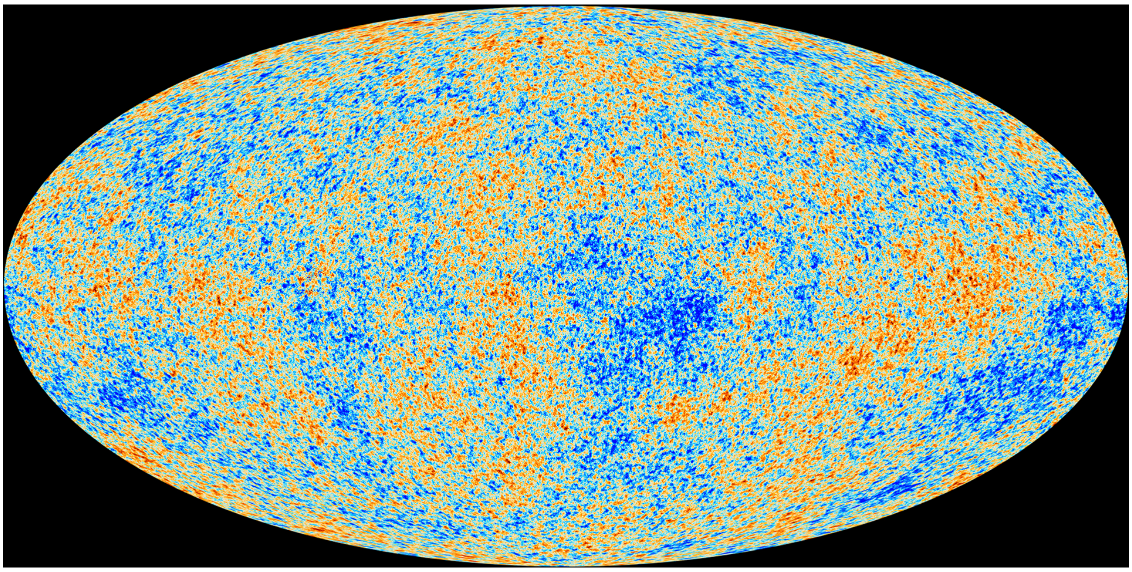

Figure 2.4.: Measurement of the cosmic background by Planck [2] [15]

MACHOs

Massive Astronomical Compact Halo Objects (MACHO's) are heavy compact but not bright objects. Known MACHO's are brown and white dwarfs, neutron stars and black holes. In the outer region of the galaxies,there has to be an enormous number of MACHO's to explain the observed phenomena. But there are still some infirmities in MACHO's. One of the main weak points is that this objects did not exist in the early universe, so that they can not explain phenomena like the structure formation. Another point is that MACHO's can be detected via the gravitational lensing effect[3], but by now there are not enough MACHO's observed to explain the amount of dark matter.

WIMPs

Weakly Interacting Massive Particles (WIMPs) are particles which do not interact electromagnetically. They have to be massive, stable and not relativistic. There are three different possibilities for WIMPs to interact:

- they interact only gravitational
- they interact gravitational and weakly only with themselves
- they interact gravitational and weakly with SM particles.

WIMPs can not interact strongly, because then they should already be detected within the search for anomalous protons.

[3] If a light signal pass the MACHO there is a flash up of the beam

MOND

Modified Newtonan Dynamics (MOND) [28] is the approach to extend Newtonian mechanics by modifying the 2nd Newton law of motion

$$F = ma. \tag{2.4}$$

With a correction term $\mu(x)$ the modified Newtonian mechanics becomes

$$F = ma\mu(\frac{a}{a_0}), \tag{2.5}$$

where

$$\mu(x >> 1) = 1 \qquad \mu(x << 1) = x. \tag{2.6}$$

With the condition for $\mu(x)$, one ensures that the Newtonian mechanics is a limiting case of the modified theory. Typical functions for $\mu(x)$ are

$$\mu(x) = \frac{x}{1+x}, \qquad \mu(x) = \frac{x}{\sqrt{1+x^2}}. \tag{2.7}$$

This correction leads to a modified velocity

$$\frac{GmM}{r^2} = m\frac{a^2}{a_0} \quad \Rightarrow \quad v = \sqrt[4]{a_0 GM}, \tag{2.8}$$

which is independent of distance. This modification of the Newtonian mechanics would explain the behavior of the rotation curves. But other phenomena, like the Bullet Cluster, can not be explained by MOND. Another important point is that until now the modified theory cannot be extended to the relativistic case, which is necessary for a valid theory.

2.3. Supersymmetry

Supersymmetry (SUSY)[25] [9] [8] is one of the most popular ideas on extending the SM. Supersymmetry was introduced in order to solve the hierachy problem but it has other nice features such that it allows the grand unification of coupling constants and introduces a dark matter candidate.

2.4. Formulation of SUSY

In SUSY the SM is extended by a symmetry between fermions and bosons

$$Q|\text{Boson} >= |\text{Fermion} > \qquad Q|\text{Fermion} >= |\text{Boson} > . \tag{2.9}$$

The generator of SUSY Q transform fermionic states into bosonic states and vice versa. Within the extension of the SM with SUSY, new particles are included, the so called super-partners of the SM (sparticles).

If SUSY would be an exakt symmetry the superpartners should have the same mass as their corresponding SM partner. But by now there was no sparticle found , the sparticles have to be much heavier. SUSY have to be broken.

2.4.1. The Minimal Supersymmetric Standardmodel (MSSM)

The *Minimal Supersymmetric Standard Model* (MSSM) takes the SM and extends the symmetry to a minimal amount of sparticles. That means, only one set of generator is considered, the so called $N = 1$ SUSY.

The Higgs sector is also extended in a minimal way.

The full Lagrangian describing all SUSY interaction in the MSSM is given in [26]. In the following the structure of the MSSM will be discussed (see Fig. 2.5).

The fermions of the SM receive a scalar (spin 0) partner, sfermions (quarks→squarks, leptons→ sleptons). The bosonic and fermionic degrees of freedom have to be the same, therefore each fermion becomes two superpartners $\tilde{f}_L, \tilde{f}_R$ in the MSSM, for each chiral component one superpartner (up- and down-typ).

The gauge bosons have the gauginos (spin $\frac{1}{2}$) as their superpartners(gluon→gluino, Z→Zino, W →Wino...)

Taking a look on the Higgs sector, the SM Higgs is extended into two complex Higgs doublets, to give mass to the up- and down-type fermions. The included superpartners of the Higgs fields with spin $\frac{1}{2}$ are called higgsinos.

The new particles of the MSSM inherit gauge interactions from their SM counterparts and the only additional interaction is given by the MSSM superpotential. The MSSM superpotential is characterized by the choice

$$W = y_u^{ij}\overline{u}_i Q_j \cdot H_u - y_d^{ij}\overline{d}_i Q_j \cdot H_d - y_e^{ij}\overline{e}_i L_j \cdot H_d + \mu H_u \cdot H_d. \tag{2.10}$$

2.4.2. R-Parity

Taking a deeper look at the superpotential (2.10) of the MSSM, the superpotential could be extended by other gauge invariant and renormalizable terms, like

$$W_{\Delta L=1} = \lambda_e^{ijk} L_i \cdot L_j \overline{e}_k + \lambda_L^{ijk} L_i \cdot Q_j \overline{d}_k + \mu_L^i L_i \cdot H_u \tag{2.11}$$

or

$$W_{\Delta B=1} = \lambda_B^{ijk} \overline{u}_i \overline{d}_j \overline{d}_k. \tag{2.12}$$

The superfields Q_i carry the baryon number $B = \frac{1}{3}$, $\overline{u}, \overline{d}$ carry $B = -\frac{1}{3}$. The lepton number $L = 1$ is carried by the superfield L_i and $\overline{e}$ carries $L = -1$. Therefore the

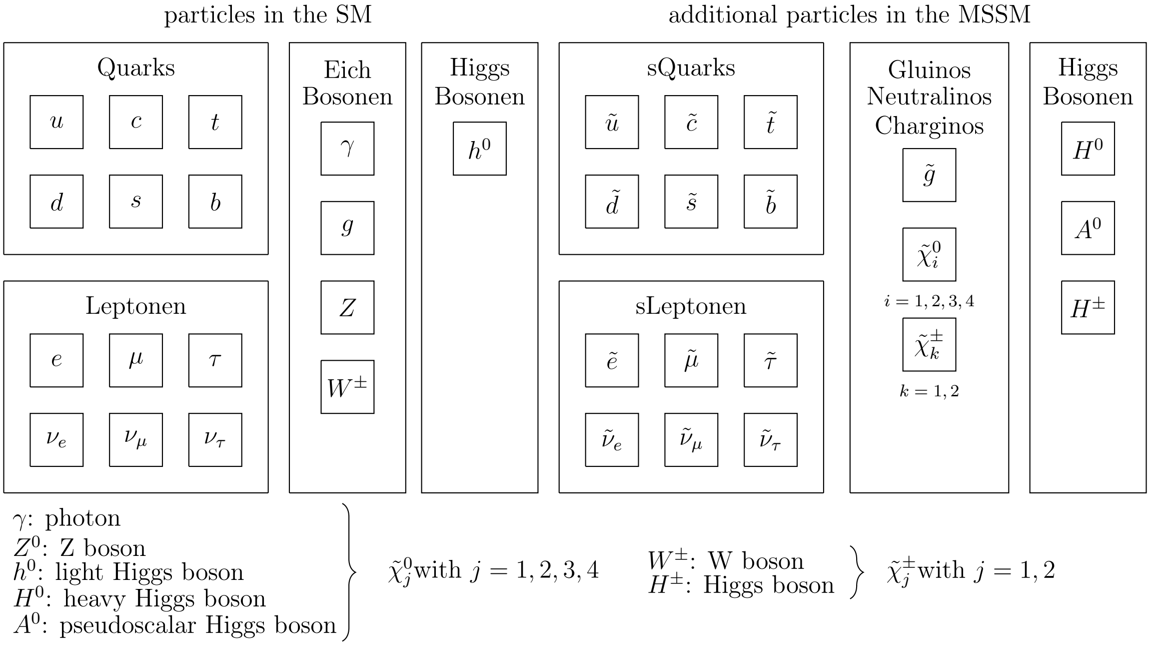

Figure 2.5.: Particles in the MSSM

Lepton number conservation would be violated by the terms (2.11) and (2.12). Furthermore, if λ_e^{ijk} and λ_B^{ijk} would exist the proton could decay via $e^+\pi^0, \mu^+\pi^0, \ldots$. So far this decays were not observed, therefore the two extensions of the superpotential should be forbidden. Introducing a new conservation law, the R-parity conservation

$$R = (-1)^{3B+L+2S} \tag{2.13}$$

with S as the spin of the particles, the formula (2.11) and (2.12) are forbidden, whereas the superpotential (2.10) conserve R-parity.

R-parity has important phenomenological consequences:

- for R-parity conservation there has to be an even number of sparticles in an interaction
- There exist a *lightest supersymmetric particle* (LSP) which is absolutly stable. It can not decay in a lighter sparticle any more and the decay in two SM particles is forbidden by R-party conservation.
- The decay products of all other sparticles must contain an odd number of LSP's .
- In accelerator experiments sparticles can only be produced in pairs.

2.4.3. Higgs sector

Due to consistency reasons, in MSSM an additional Higgs doublet has to be added to the theory. The new doublet has an opposite hypercharge to the original Higgs doublet and is used to give masses to the up-type fermions. The Higgs potential in the MSSM is

$$\begin{aligned} V &= m_1^2|H_1|^2 + m_2^2|H_2|^2 - m_{12}^2(H_1H_2 + H_1^\dagger H_2^\dagger) && (2.14)\\ &\quad + \frac{1}{8}(g^2+g'^2)(|H_1|^2 - |H_2|^2)^2 + \frac{1}{2}g^2|H_1^\dagger H_2|^2\,, && (2.15)\end{aligned}$$

where $m_{1,2}^2 = m_{H_{1,2}}^2 + |\mu|^2$. In the MSSM the self-interaction of the Higgs fields is determined by the gauge couplings.

The neutral Higgs boson fields acquire a vacuum expectation value (VEV)

$$\langle H_1\rangle = \begin{pmatrix} \frac{v_1}{\sqrt{2}} \\ 0 \end{pmatrix}, \qquad \langle H_2\rangle = \begin{pmatrix} 0 \\ \frac{v_2}{\sqrt{2}} \end{pmatrix}. \tag{2.16}$$

The doublets are parametrized as

$$H_1 \equiv \begin{pmatrix} H_1^0 \\ H_1^- \end{pmatrix} = \begin{pmatrix} (v_1 + \phi_1^0 + i\chi_1^0)/\sqrt{2} \\ \phi_1^- \end{pmatrix}, \qquad Y_{H_1} = -1\,, \tag{2.17}$$

$$H_2 \equiv \begin{pmatrix} H_1^0 \\ H_1^- \end{pmatrix} = \begin{pmatrix} \phi_2^+ \\ (v_2 + \phi_2^0 + i\chi_2^0)/\sqrt{2} \end{pmatrix}, \qquad Y_{H_2} = +1\,. \tag{2.18}$$

The electro-weak symmetry breaking makes the gauge bosons massive and one of the VEVs can be related to the masses of the gauge bosons and the gauge couplings as

$$m_Z^2 = \frac{g^2+g'^2}{4}(v_1^2+v_2^2)\,, \qquad m_W^2 = \frac{g^2}{4}(v_1^2+v_2^2)\,, \tag{2.19}$$

$$v^2 \equiv (v_1^2+v_2^2) = \frac{4m_Z^2}{g^2+g'^2} \approx (246\text{GeV})^2\,. \tag{2.20}$$

The other VEV remains a free parameter of the theory and is conventionally replaced by the mixing angle β which is defined as

$$\tan\beta \equiv \frac{v_2}{v_1} \geq 0\,, \qquad 0 \leq \beta \leq \frac{\pi}{2}\,. \tag{2.21}$$

The Higgs mass matrix is defined as

$$M_{ij}^{2,\text{Higgs}} = \frac{1}{2}\left.\frac{\partial^2 V}{\partial H_i \partial H_j}\right|_{\langle H_n^0\rangle = v_n}. \tag{2.22}$$

The mass matrix is split into four independent 2×2 blocks

$$\begin{pmatrix} H^0 \\ h^0 \end{pmatrix} = \begin{pmatrix} \cos\alpha & \sin\alpha \\ -\sin\alpha & \cos\alpha \end{pmatrix} \begin{pmatrix} \phi_1^0 \\ \phi_2^0 \end{pmatrix}, \tag{2.23}$$

$$\begin{pmatrix} G^0 \\ A^0 \end{pmatrix} = \begin{pmatrix} -\cos\beta & \sin\beta \\ \sin\beta & \cos\beta \end{pmatrix} \begin{pmatrix} \chi_1^0 \\ \chi_2^0 \end{pmatrix}, \tag{2.24}$$

$$\begin{pmatrix} G^\pm \\ H^\pm \end{pmatrix} = \begin{pmatrix} -\cos\beta & \sin\beta \\ \sin\beta & \cos\beta \end{pmatrix} \begin{pmatrix} \phi_1^\pm \\ \phi_2^\pm \end{pmatrix}. \tag{2.25}$$

After the vector bosons absorb the Goldstone bosons G^0 and $G^\pm$ as their longitudinal components, three neutral Higgs bosons– two CP even states (h^0, H^0) and one CP odd state A^0– and two charged $(H^\pm)$ Higgs bosons remain. There are three free parameters in the Higgs sector and these are conventionally chosen to be

$$m_{A^0}\,, \qquad \tan\beta\,, \quad \text{and} \quad \mu\,. \tag{2.26}$$

All parameters for example the masses of the Higgs bosons can be expressed using these free parameters as

$$m^2_{h^0,H^0} = \frac{1}{2}\left[m^2_{A^0} + m^2_Z \mp \sqrt{(m^2_{A^0} + m^2_Z)^2 - 4m^2_{A^0} m^2_Z \cos^2\beta}\right], \tag{2.27}$$

$$m^2_{H^\pm} = m^2_{A^0} + m^2_W\,, \tag{2.28}$$

The masses in the Higgs sector are modified by loop corrections. The most obvious example is the mass of the lightest Higgs which should be lower than the mass of the Z-boson according to Eq. (2.27).

2.4.4. Sfermion sector

The sfermions are scalar superpartners of the fermions. Each chiral part of a fermion get one scalar superpartner i.e. for each fermion there are two scalar sfermions $\tilde{f}_{L,R}$. These scalar fermions are not the mass eigenstates though. The sfermion mass matrix is off-diagonal in the basis $(\tilde{f}_L, \tilde{f}_R)$ and it has the form

$$\mathcal{M}^2_{\tilde{f}} = \begin{pmatrix} m^2_{\tilde{f}_L} & a_f\, m_f \\ a_f\, m_f & m^2_{\tilde{f}_R} \end{pmatrix}, \tag{2.29}$$

where

$$m^2_{\tilde{f}_L} = M^2_{\{\tilde{Q},\tilde{L}\}} + (I_f^{3L} - e_f\, s_W^2)\cos 2\beta\, m_Z^2 + m_f^2\,, \tag{2.30}$$

$$m^2_{\tilde{f}_R} = M^2_{\{\tilde{U},\tilde{D},\tilde{E}\}} + e_f\, s_W^2 \cos 2\beta\, m_Z^2 + m_f^2\,, \tag{2.31}$$

$$a_f = A_f - \mu\,(\tan\beta)^{-2I_f^{3L}}\,. \tag{2.32}$$

$M_{\tilde{Q}}$, $M_{\tilde{L}}$, $M_{\tilde{U}}$, $M_{\tilde{D}}$ and $M_{\tilde{E}}$ are the soft SUSY-breaking masses, A_f is the trilinear scalar coupling parameter, μ the higgsino mass parameter, $\tan\beta = \frac{v_2}{v_1}$ is the ratio of the vacuum expectation values of the two neutral Higgs doublet states , I_f^{3L} denotes the third component of the weak isospin of the fermion f, e_f the electric charge in terms of the elementary charge e, and s_W is the sine of the Weinberg angle $\tan\theta_W$.
The mass eigenstates are obtained by diagonalizing the mass matrix. In the process we introduce the mixing angle $\theta_{\tilde{f}}$ (i.e. the mixing matrix $R^{\tilde{f}}$).

$$\mathcal{M}_{\tilde{f}}^2 \;=\; \begin{pmatrix} m_{\tilde{f}_L}^2 & a_f\, m_f \\ a_f\, m_f & m_{\tilde{f}_R}^2 \end{pmatrix} = \left(R^{\tilde{f}}\right)^{\dagger} \begin{pmatrix} m_{\tilde{f}_1}^2 & 0 \\ 0 & m_{\tilde{f}_2}^2 \end{pmatrix} R^{\tilde{f}}\,, \tag{2.33}$$

where

$$R^{\tilde{f}} = \begin{pmatrix} \cos\theta_{\tilde{f}} & \sin\theta_{\tilde{f}} \\ -\sin\theta_{\tilde{f}} & \cos\theta_{\tilde{f}} \end{pmatrix}. \tag{2.34}$$

The masses of the sfermions and the mixing angle are

$$m_{\tilde{f_{1,2}}}^2 \;=\; \frac{1}{2}\left(m_{\tilde{f}_L}^2 + m_{\tilde{f}_R}^2 \mp \sqrt{(m_{\tilde{f}_L}^2 - m_{\tilde{f}_R}^2)^2 + 4a_f^2 m_f^2}\,\right), \tag{2.35}$$

$$\cos\theta_{\tilde{f}} \;=\; \frac{-a_f\, m_f}{\sqrt{(m_{\tilde{f}_L}^2 - m_{\tilde{f}_1}^2)^2 + a_f^2 m_f^2}} \qquad (0 \le \theta_{\tilde{f}} < \pi)\,. \tag{2.36}$$

2.4.5. Chargino sector

The fermionic superpartners of the charged gauge bosons, the gauginos, and the superpartners of the charged Higgs bosons, the higgsinos, mix to form mass eigenstates called charginos.
The Weyl spinor chargino fields are

$$\psi^+ = (-i\tilde{W}^+, \tilde{H}_2^+)\,, \qquad \psi^- = (-i\tilde{W}^-, \tilde{H}_1^-)\,. \tag{2.37}$$

The mass Lagrangian in this basis is

$$\mathcal{L} = -\frac{1}{2}\left(\psi^+, \psi^-\right) \cdot \begin{pmatrix} 0 & X^T \\ X & 0 \end{pmatrix} \cdot \begin{pmatrix} \psi^+ \\ \psi^- \end{pmatrix} + h.c.\,, \tag{2.38}$$

with the chargino mass matrix

$$X = \begin{pmatrix} M & \sqrt{2} m_W \sin\beta \\ \sqrt{2} m_W \cos\beta & \mu \end{pmatrix}. \tag{2.39}$$

This mass matrix is made diagonal by using two unitary matrices U and V as

$$U X V^{-1} = \mathrm{diag}(m_{\chi_1^\pm}, m_{\chi_2^\pm}), \qquad |m_{\chi_1^\pm}| \le |m_{\chi_2^\pm}|\,. \tag{2.40}$$

The Dirac mass eigenstates are constructed as follows

$$\tilde{\chi}_i^{\pm} \equiv \begin{pmatrix} V_{ij}\,\psi_j^+ \\ U_{ij}\,\bar{\psi}_j^- \end{pmatrix} . \tag{2.41}$$

The mass eigenvalues are given by

$$m^2_{\chi^{\pm}_{1,2}} = \frac{1}{2}\left[M^2 + \mu^2 + 2m_W^2 \mp \sqrt{(M^2+\mu^2+2m_W^2)^2 - 4(m_W^2 \sin 2\beta - \mu M)^2}\right] . \tag{2.42}$$

2.4.6. Neutralino sector

The neutralinos are a mixing between the gauginos and higgsinos. The mass Lagrangian of the four Weyl states

$$\varphi_j^0 = (-\mathrm{i}\tilde{B}, -\mathrm{i}\tilde{W}_3^0, \tilde{H}_1^0, \tilde{H}_2^0) \tag{2.43}$$

is given as

$$\mathcal{L} = -\frac{1}{2}(\varphi^0)^T Y \varphi^0 + h.c. \tag{2.44}$$

Y is the neutralino mass matrix

$$Y = \begin{pmatrix} M' & 0 & -m_Z s_W \cos\beta & m_Z s_W \sin\beta \\ 0 & M & m_Z c_W \cos\beta & -m_Z c_W \sin\beta \\ -m_Z s_W \cos\beta & m_Z c_W \cos\beta & 0 & -\mu \\ m_Z s_W \sin\beta & -m_Z c_W \sin\beta & -\mu & 0 \end{pmatrix} . \tag{2.45}$$

s_W and c_W are short forms of $\sin\theta_W$ and $\cos\theta_W$, with the Weinberg angel θ_W. The neutralinos are Majorana particles and therefore the matrix can be diagonalized using only one rotation matrix

$$ZYZ^{-1} = \mathrm{diag}(m_{\tilde{\chi}_1^0}, m_{\tilde{\chi}_2^0}, m_{\tilde{\chi}_3^0}, m_{\tilde{\chi}_4^0}) \qquad \left|m_{\tilde{\chi}_1^0}\right| \leq \left|m_{\tilde{\chi}_2^0}\right| \leq \left|m_{\tilde{\chi}_3^0}\right| \leq \left|m_{\tilde{\chi}_4^0}\right| . \tag{2.46}$$

Concluding the 4-component Majorana spinors for the neutralino fields can be constructed as

$$\tilde{\chi}_i^0 = \begin{pmatrix} Z_{ij}\varphi_j^0 \\ Z_{ij}\overline{\varphi}_j^0 \end{pmatrix} . \tag{2.47}$$

3. DM@NLO

Dark Matter at next-to-leading order (DM@NLO) is a program which provides predictions for the dark matter relic density in MSSM including higher order corrections. There are already other existing codes for the calculation of the relic density, like *micrOMEGAs* [20] and *DarkSUSY* [30]. But the programs do not include full next-to-leading order corrections. In the following, the project DM@NLO will be introduced in more detail.

3.1. Structure of the project

DM@NLO [13] [23] [29] [12] is a FORTRAN-based code which calculates several (co-)annihilation cross section including next-to-leading (NLO) SUSY-QCD corrections within the MSSM. The included processes will be discussed in section 3.2.

For the calculation of the relic density it is important to specify a particular scenario. One specifies a scenario via a set of input parameters at a given input scale M_{in} (e.g. $M_{in} \sim$ GUT). The parameters a given in a format, specified by the SUSY *Les Houches Accord* (SLHA) [38]. These parameters are passed further to the spectrum calculator *SPheno* [**SPheno**], which calculates the spectrum of the MSSM. The spectrum calculator calculates the masses and couplings of the SUSY and Higgs sector at an output scale M_{out} (e.g. $M_{out} \sim \mathcal{O}(\mathsf{TeV})$. The mass spectrum is then used by micrOMEGAs for the calculation of the relic density. The relic density is calculated via solving the Boltzmann equation, which will be discussed in more detail in chapter 5. For the calculation of the relic density the cross section of the important processes are essential. In micrOMEGAs these cross sections are calculated by *CalcHEP* [33] [7]. DM@NLO provides an alternative calculation of annihilation processes which are then used by micrOMEGAs to calculate the relic density instead of those of CalcHEP.

To make DM@NLO a stand alone code, there is the need of an own integration routine for the Boltzmann equation. The new structure of DM@NLO is shown in 3.2. How far this step was taken will be discussed later within chapter 5.

The difference between figure 3.1 and 3.2 is obviously that micrOMEGAs is replaced by an integration routine, which first calculates the thermal average of the cross section.Afterwards the Boltzmann equation is solved which is discussed in chapter 5 in more detail. Moreover CalcHEP is no longer included in the software chain. Therefore DM@NLO is the only source for the cross section. Within the step of going over to a stand alone code, the most relevant processes should be included in DM@NLO.

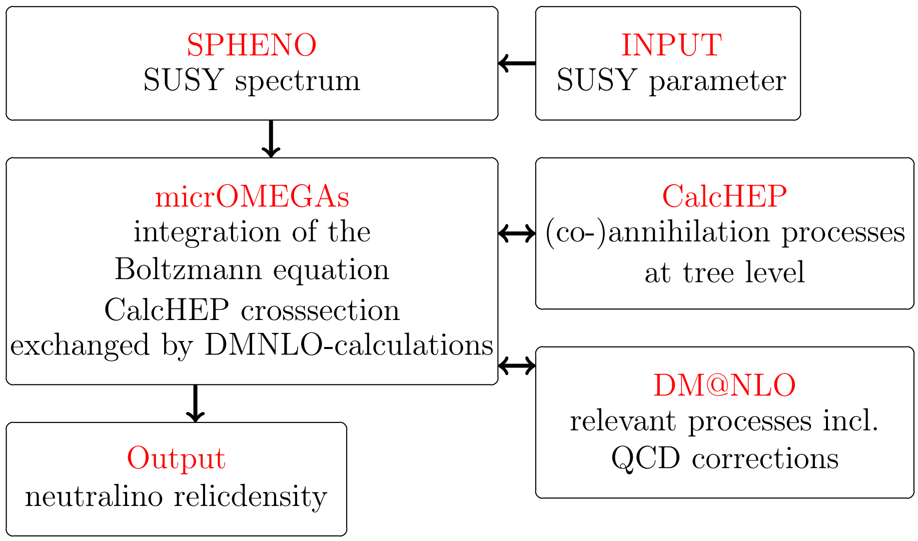

Figure 3.1.: Visualization of the software chain by including DM@NLO to micrOMEGAs for the calculation of the relic density.

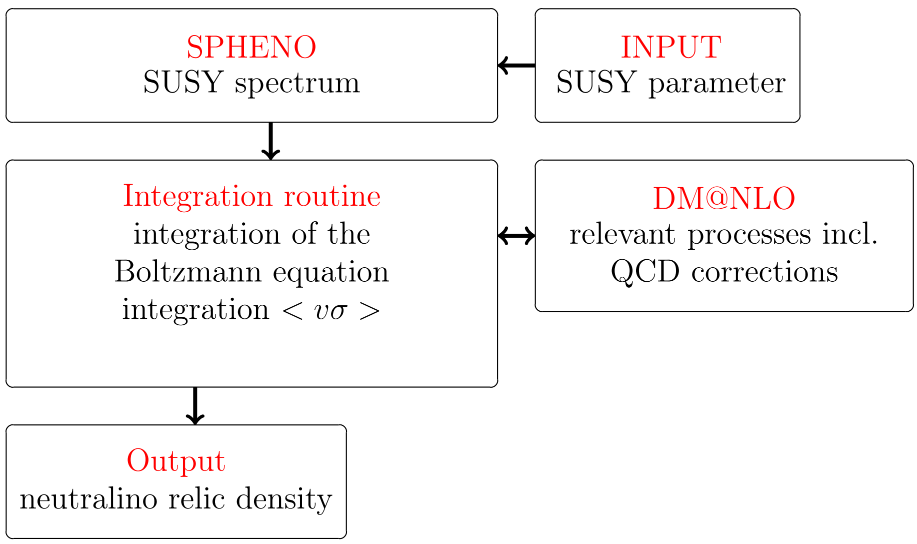

Figure 3.2.: Visualization of the software chain by including an routine which solves the Boltzmann equation within DM@NLO.

3.2. Included processes

By know there are several processes included in DM@NLO. The included processes are listed below.

ChiChi2QQ [11] [13] [12]

- neutralino annihilation to quark antiquark pair:

$$\tilde{\chi}_i^0 \tilde{\chi}_j^0 \to q\bar{q} \quad (i, j \in \{1, 2, 3, 4\}) \tag{3.1}$$

- gaugino annihiation extended to chargino annihilation

$$\tilde{\chi}_k^{\pm} \tilde{\chi}_l^{\pm} \to q\bar{q} \quad (k, l \in \{1, 2\}) \tag{3.2}$$

- co-annihilation of neutralino chargino initial states included

$$\tilde{\chi}_i^0 \tilde{\chi}_k^{\pm} \to q\bar{q}\prime \quad (i \in \{1, 2, 3, 4\}, k \in \{1, 2\}) \tag{3.3}$$

NeuQ2qx [23]

- neutralino-squark co-annihilation to quark vector boson final state

$$\tilde{\chi}_i^0 \tilde{q} \to qV \quad (i \in \{1, 2, 3, 4\}, q \in \{u, d, c, s, t, b\}, V \in \{G, \gamma, Z^0, W^{\pm}\}) \tag{3.4}$$

- gaugino squark initial state

$$\tilde{\chi}_k^{\pm} \tilde{q} \to qV \quad (k \in \{1, 2\}, q \in \{u, d, c, s, t, b\}, V \in \{G, \gamma, Z^0, W^{\pm}\}) \tag{3.5}$$

- modification of squark and Higgs in final state

$$\tilde{\chi}_i^0 \tilde{q} \to qH \quad (i \in \{1, 2, 3, 4\}, q \in \{u, d, c, s, t, b\}, H \in \{h^0, H^0, A^0, H^{\pm}\}) \tag{3.6}$$

$$\tilde{\chi}_k^{\pm} \tilde{q} \to qH \quad (k \in \{1, 2\}, q \in \{u, d, c, s, t, b\}, H \in \{h^0, H^0, A^0, H^{\pm}\}) \tag{3.7}$$

QQ2xx [24]

- squark pair annihilation to vector boson final state

$$\tilde{q}\tilde{q}^{\star} \to VV \quad (q \in \{u, d, c, s, t, b\}, V \in \{G, \gamma, Z^0, W^{\pm}\}) \tag{3.8}$$

- extended to Higgs final state

$$\tilde{q}\tilde{q}^{\star} \to HH \quad (q \in \{u, d, c, s, t, b\}, H \in \{h^0, H^0, A^0, H^{\pm}\}) \tag{3.9}$$

- including mixed final state

$$\tilde{q}\tilde{q}^{\star} \to HV \quad (q \in \{u, d, c, s, t, b\}, H \in \{h^0, H^0, A^0, H^{\pm}\}, V \in \{G, \gamma, Z^0, W^{\pm}\}) \tag{3.10}$$

NeuNeu2EW at tree level (see chapter 4)

- neutralino annihilation to Higgs final state

$$\tilde{\chi}_i^0\tilde{\chi}_j^0 \to HH \quad (i \in \{1, 2, 3, 4\}, H \in \{h^0, H^0, A^0, H^{\pm}\}) \tag{3.11}$$

- neutralino annihilation to mixed Higgs vector boson final state

$$\tilde{\chi}_i^0\tilde{\chi}_j^0 \to HV \quad (i \in \{1, 2, 3, 4\}, H \in \{h^0, H^0, A^0, H^{\pm}\}, V \in \{\gamma, Z^0, W^{\pm}\}) \tag{3.12}$$

- neutralino annihilation to vector boson final state

$$\tilde{\chi}_i^0\tilde{\chi}_j^0 \to VV \quad (i \in \{1, 2, 3, 4\}, V \in \{\gamma, Z^0, W^{\pm}\}) \tag{3.13}$$

4. Electroweak Processes

In Fig. 4 is shown a typical DM@NLO relic scan. The input parameters are shown in table 4. The scan includes a variation of the masses $M1$, $M2$ of the initial particles. The scanned regions are colored in green, this shows how many of the dominant processes are included in DM@NLO. At the top of the right side there is a more or less white area. In this region the electroweak processes are dominant.

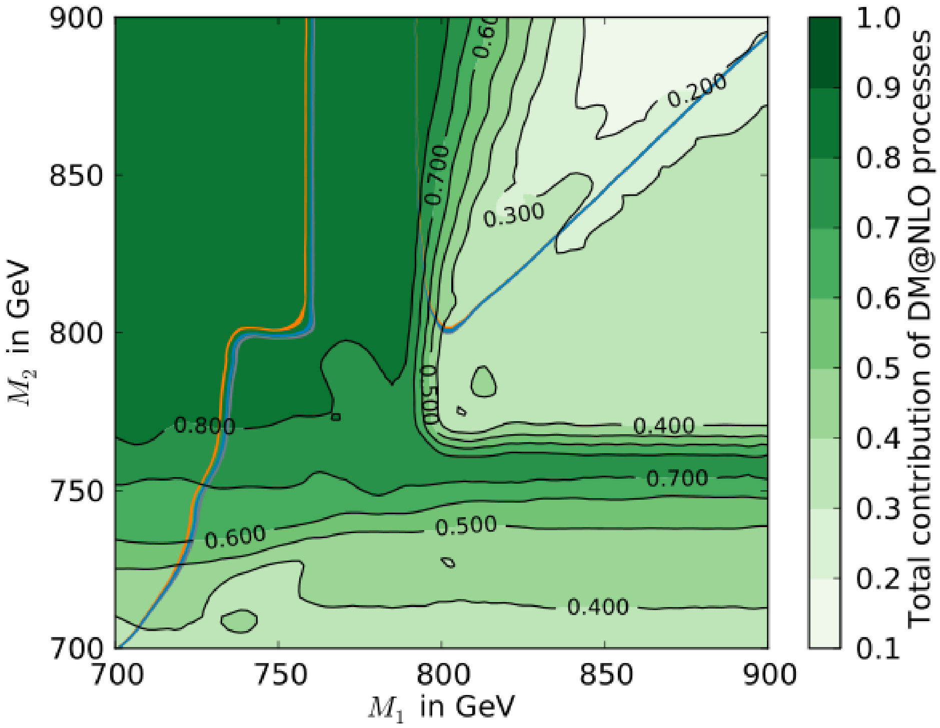

Figure 4.1.: DM@NLO relic scan for the scenario in Tab. 4 [12]

This Chapter will deal with a several kind of electroweak processes, the neutralino annihilation to Higgs boson final state (NeuNeu2HH), mixed Higgs vector boson final state (NeuNeu2HV) and pure vector boson final state (NeuNeu2VV), see Fig.4.2. It is useful to start with the Higgs process because the calculation of the vector bosons is based on the calculation of the Goldstone bosons, which are included in the Higgs

Table 4.1.: MSSM input parameter for the selected scenario, the unit of the parameters is all given in GeV, except $\tan\beta$

$\tan\beta$	μ	m_A	M_1	M_2	M_3	$M_{\tilde{q}_{1,2}}$	$M_{\tilde{q}_3}$	$M_{\tilde{u}_3}$	$M_{\tilde{l}}$	A_t
13.4	1286.3	1592.9	731.0	766.0	1906.3	3252.6	1634.3	1054.4	3589.6	-2792.3

process. Within the feynman gauge one does not only deal with the vector bosons but also with Faddeev-Popov ghosts and Goldstone bosons in the final state[22]. The implementation of the Higgs bosons can later be used for the calculation of the Goldstone bosons within the vector boson final state.

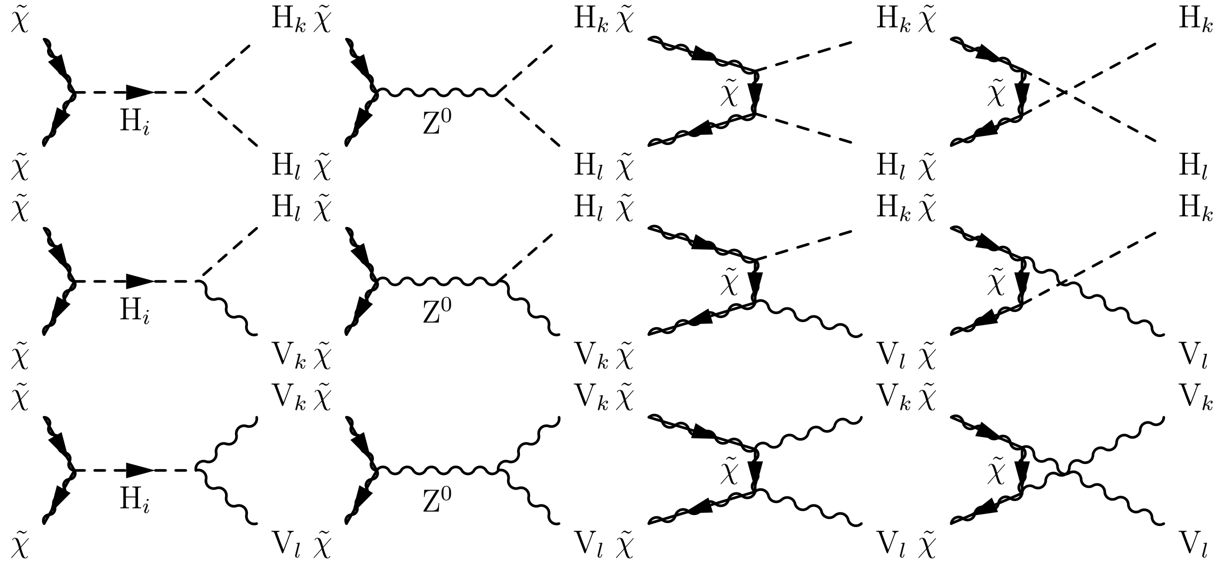

Figure 4.2.: Overview of calculated processes within the electroweak neutralino annihilation

4.1. NeuNeu2HH

In Fig.4.3 all possible annihilation channels for the neutralino annihilation to Higgs final states are shown. There are three different channels within this annihilation. In the first two diagramms the s-channel is shown with a Higgs and a vectorboson as the mediator. The other two processes are the t-channel (diagram at the bottom left) which is mediated by a neutralino or chargino, depending on the final states. On the right side there is also the u-channel. One can not distinguished between the possibility that the first Higgs comes from the vertice of the first neutralino or from the second neutralino. So both channels have to be taken into account. In the following will be

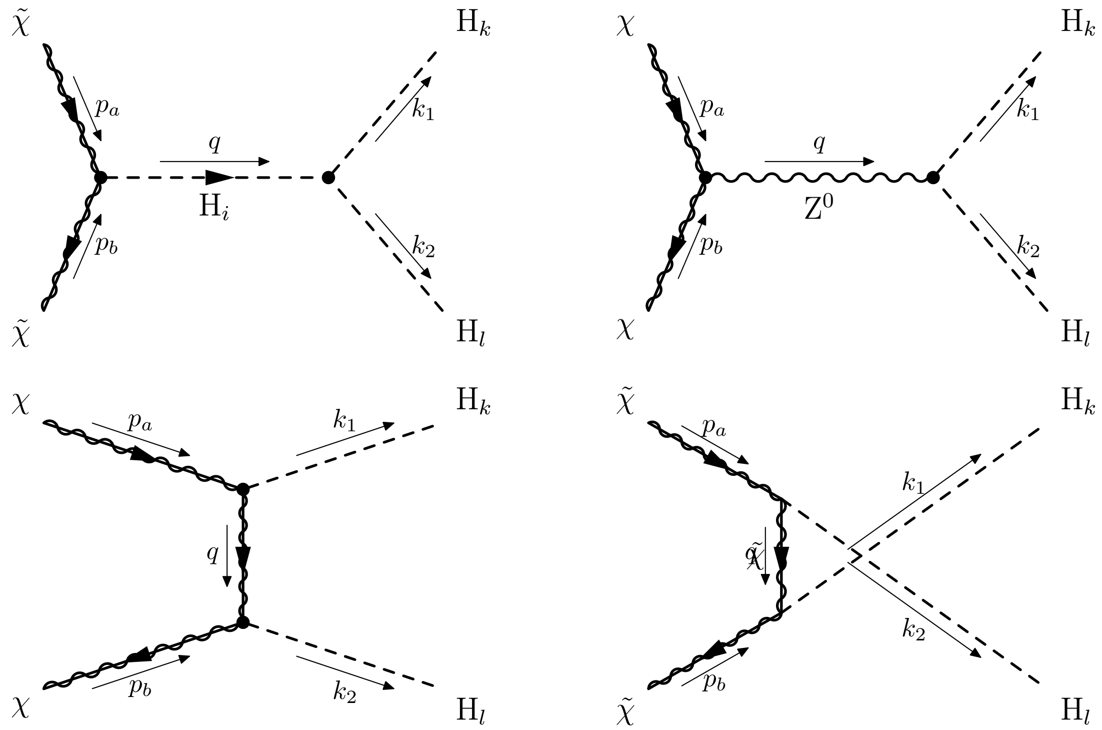

Figure 4.3.: Neutralino annihilation to Higgs

4.1.1. Neutralino annihilation in the s-channel via Higgs propagator

In figure 4.4 you see the Feynman diagram of the s-channel contribution with a Higgs particle in the propagator. Two neutralinos annihilate to a Higgs particle which decays again into two Higgs particles.

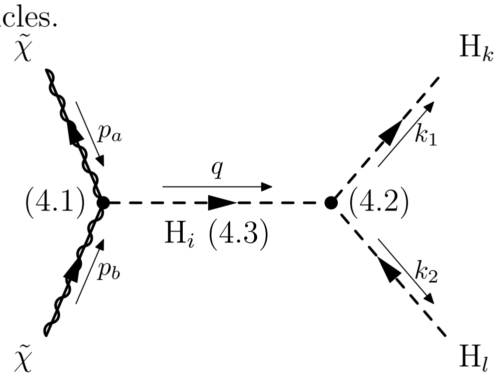

Figure 4.4.: Neutralino annihilation to two Higgs in the s-chanel via Higgs as a propagator

The couplings of the two vertices are

$$-\mathrm{i}(C_L(i)P_L + C_R(i)P_R) \tag{4.1}$$

where P_R, P_L are chirality operators and

$$-\mathrm{i}ILR(i,k,l). \tag{4.2}$$

C_L, C_R and I_{LR} are given in appendix **??** explicitly. With the Higgs-propagator

$$\frac{\mathrm{i}}{(s-m_i^2)+\mathrm{i}m_i w_{h_i}} \tag{4.3}$$

where m_i is the mass of the propagating Higgs particle and w_{h_i} is the width of the propagating Higgs particle. One receives the invariant amplitude

$$\begin{aligned} \mathrm{i}M &= \overline{v}(p_b)(-\mathrm{i})(C_L(i)P_L + C_R(i)P_R)u(p_a)\frac{\mathrm{i}}{(s-m_i^2)}(-\mathrm{i}ILR(i,k,l)) \\ &= \overline{v}(p_b)(C_L(i)P_L + C_R(i)P_R)u(p_a)\frac{-\mathrm{i}}{(s-m_i^2)+\mathrm{i}m_i w_{h_i}}ILR(i,k,l) \end{aligned} \tag{4.4}$$

To write the formula in a shorter way, the indices of the couplings will be neglected in the following. The squared amplitude is given by the product of the invariant amplitude and its complex conjugated

$$M^2 = \mathrm{i}M(\mathrm{i}M)^\star. \tag{4.5}$$

The complex conjugated of the invariant Amplitude is given by (skip the imaginary part of the denominator)

$$\begin{aligned} (\mathrm{i}M)^\star &= u^+(p_a)(C_L^\star P_L + C_R^\star P_R)(\overline{v}(p_b))^+\frac{\mathrm{i}}{(s-m_i^2)}ILR^\star \\ &= \overline{u}(p_a)(C_L^\star P_R + C_R^\star P_L)v(p_b)\frac{\mathrm{i}}{(s-m_i^2)}ILR^\star. \end{aligned} \tag{4.6}$$

$$\begin{aligned} |M|^2 =& \mathrm{i}M(\mathrm{i}M)^\star \\ =& \overline{v}(p_b)(C_L P_L + C_R P_R)u(p_a)\overline{u}(p_a)(C_L^\star P_R + C_R^\star P_L)v(p_b) \\ & \frac{-\mathrm{i}}{(s-m_i^2)+\mathrm{i}m_i w_{h_i}}\frac{\mathrm{i}}{(s-m_j^2)}I_{LR}\cdot I_{LR}^\star \end{aligned} \tag{4.7}$$

$$|M|^2 = \frac{I_{LR}^2}{(s-m_i)^2}\mathrm{Tr}\left[(\not{p}_b - m_{\tilde{\chi}^0})(C_L P_L + C_R P_R)(\not{p}_a + m_{\tilde{\chi}^0})(C_L^\star P_R + C_R^\star P_L)\right]$$

bring $(\not{p}_a + m_{\tilde{\chi}^0})$ to the left side of $(C_L P_L + C_R P_R)$

$$|M|^2 = \frac{I_{LR}^2}{(s-m_i)^2}\mathrm{Tr}\left[(\not{p}_b - m_{\tilde{\chi}^0})(\not{p}_a(C_L P_R + C_R P_L) + m_{\tilde{\chi}^0}(C_L P_L + C_R P_R))(C_L^\star P_R + C_R^\star P_L)\right] \tag{4.8}$$

using(A.27) and (A.26) some terms vanish

$$|M|^2 = \frac{I_{LR}^2}{(s-m_i)^2}\mathrm{Tr}\left[(\not{p}_b - m_{\tilde{\chi}^0})(\not{p}_a(C_L C_L^\star P_R + C_R C_R^\star P_L) + m_{\tilde{\chi}^0}(C_L C_R^\star P_L + C_R C_L^\star P_R))\right]$$

using (A.28)

$$|M|^2 = \frac{I_{LR}^2}{(s-m_i)^2}\left(\mathrm{Tr}\left[\not{p}_b\not{p}_a(C_L C_L^\star P_R + C_R C_R^\star P_L)\right] - 2m_{\tilde{\chi}^0}^2(C_L C_R^\star + C_R C_L^\star)\right) \tag{4.9}$$

with the relations from appendix (A.1.2) one receives

$$|M|^2 = \frac{I_{LR}^2}{(s-m_i)^2}(2p_a p_b(C_L C_L^\star + C_R C_R^\star) - 4m_{\tilde{\chi}^0}^2(C_L C_R^\star + C_R C_L^\star) \tag{4.10}$$

with the Mandelstam variables (see appendix E) the result is

$$|M|^2 = \frac{I_{LR}^2}{(s-m_i)^2}\left[(s-2m_{\tilde{\chi}^0}^2)(C_L C_L^\star + C_R C_R^\star) - 4m_{\tilde{\chi}^0}(C_L C_R^\star + C_R C_L^\star)\right]. \tag{4.11}$$

4.1.2. Complete calculation of the Neutralino annihilation into Higgs final states

In the subsection before, the neutralino annihilation in the s-channel via Higgs propagator was calculated. For the calculation of the complete amplitude square one has to also calculate the s-channel $\left|M_{s(Z)}\right|^2$ with the Z-boson as the propagator and the t- $\left|M_{t(\chi)}\right|^2$ and u-channel$\left|M_{u(\chi)}\right|^2$. Furthermore the interference terms have to be taken into account. Only the real part of the interference terms give a contribution to the complete process. Because of the symmetry between terms like $\left|M_{s(h)}M_{t(\chi)}^\star\right|$ and $\left|M_{t(\chi)}M_{s(h)}^\star\right|$, it is only necessary to calculate one of the interference terms. Summarizing the complete process is given as

$$\begin{aligned}|M_{\tilde{\chi}^0\tilde{\chi}^0\to hh}|^2 = &\left|M_{s(h)}\right|^2 + \left|M_{s(Z)}\right|^2 + \left|M_{t(\chi)}\right|^2 + \left|M_{u(\chi)}\right|^2 \\ &+ 2\mathrm{Re}(\left|M_{s(h)}M_{s(V)}^\star\right|) + 2\mathrm{Re}(\left|M_{s(h)}M_{t(\chi)}^\star\right|) + 2\mathrm{Re}(\left|M_{s(h)}M_{u(\chi)}^\star\right|) \\ &+ 2\mathrm{Re}(\left|M_{s(V)}M_{t(\chi)}^\star\right|) + 2\mathrm{Re}(\left|M_{s(V)}M_{u(\chi)}^\star\right|) + 2\mathrm{Re}(\left|M_{t(\chi)}M_{u(\chi)}^\star\right|)\end{aligned} \tag{4.12}$$

all calculated terms are listed in appendix **??**.

4.2. NeuNeu2HV

In figure 4.4 you see the Feynman diagram of the s-channel contribution with a Higgs particle in the propagator. Two neutralinos annihilate to a Higgs particle which decays again into a Higgs and a verctor boson.

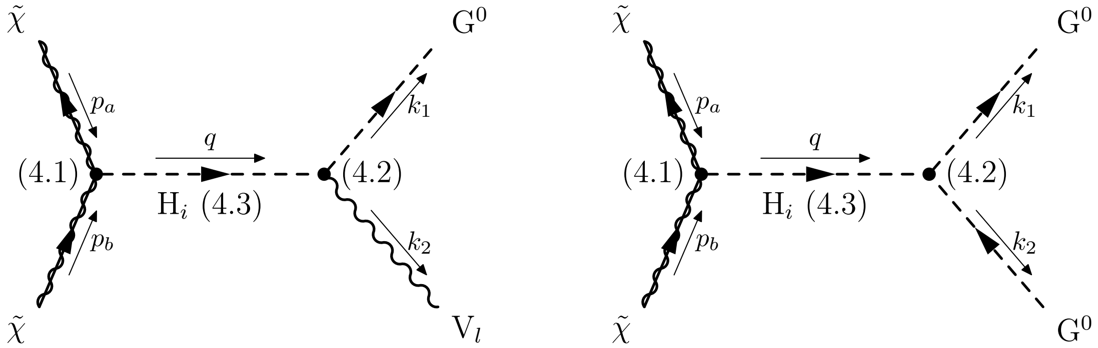

Figure 4.5.: Neutralino annihilation to mixed verctor boson Higgs state in the s-channel via Higgs as a propagator

For the vector boson in the final state one has to take into account that within the Feynman gauge there is a second process which has to be calculated, the neutralino annihilation to a Higgs with a Goldstone boson. This process is completely similar with the Higgs final states. There should only be the couplings exchanged in the squared amplitude.

For the calculation of the full squared amplitude the Eq. (4.12) has to be taken for both processes and summed together. The separate squared amplitudes and interference terms are listed in the appendix D.1 and D.2. The checks on the processes of Higgs and vector bosons in the final state are still work in progress.

4.3. NeuNeu2VV

Taking only a look on the the s-channel one has to take four different diagram into account, see Fig.4.6. In case of the pure Goldstone final state one can again use the squared amplitudes of the Higgs final states and the vector boson Goldstone squared amplitudes are included into the squared amplitudes of the last section. Therefore the remaining part is the calculation of the process $\tilde{\chi}^0\tilde{\chi}^0 \to VV$ in Fermi-gauge. The squared amplitudes of the final states including Goldstone bosons can be added later on.

In addition to the Goldstone bosons one also has to deal with the Faddeev-Popov-ghost, Fig.4.7. Ghost are also scalar particles, therefore the calculation is similar to the calculation of the Higgs final states. The checking of the calculated squared amplitudes is still work in progress.

4.4. Numerical results

In Fig.4.8 the cross section depending on the p_{cm} is shown. The black dashed curve represents the results by DM@NLO and the orange line the results by micrOMEGAs within effective couplings. The behavior depending on the p_{cm} is similar in both results. At around $p_{cm} = 290$ GeV a peak is noticeable. This corresponds to the s-channel

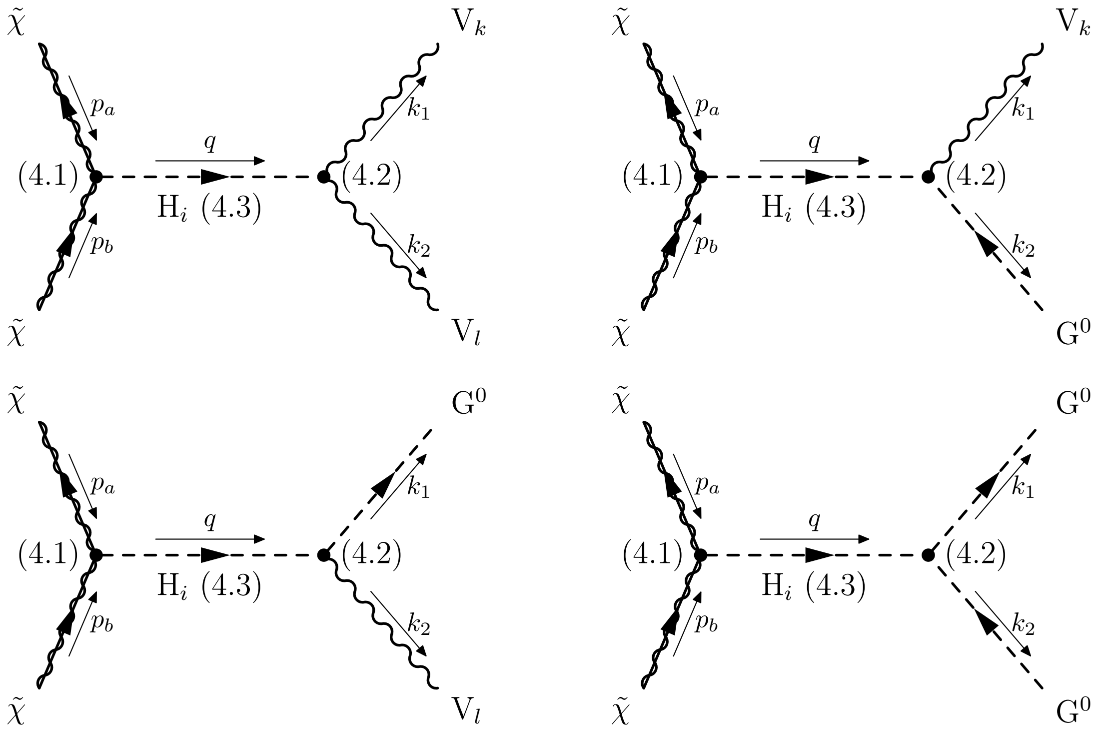

Figure 4.6.: Neutralino annihilation to vector boson final state in the s-channel via Higgs as a propagator, taking Goldstone bosons into account

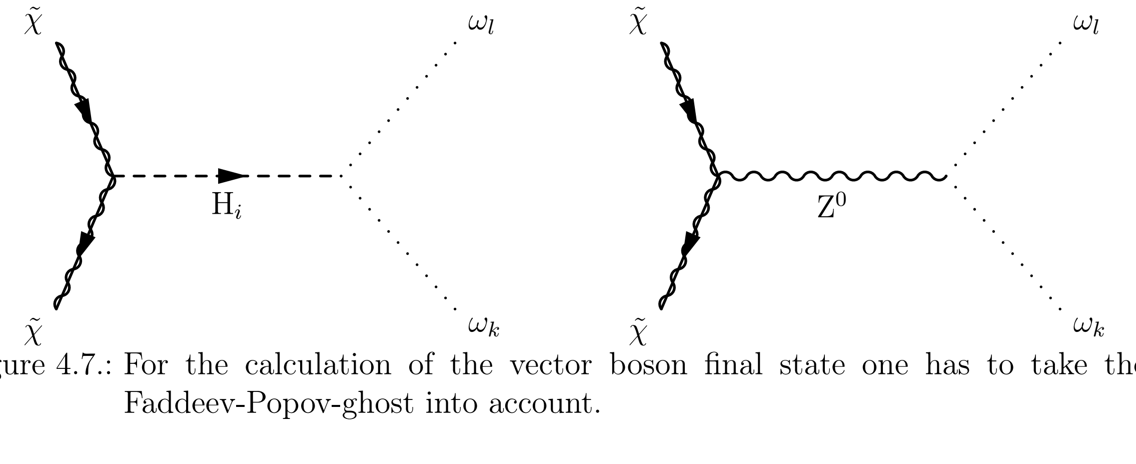

Figure 4.7.: For the calculation of the vector boson final state one has to take the Faddeev-Popov-ghost into account.

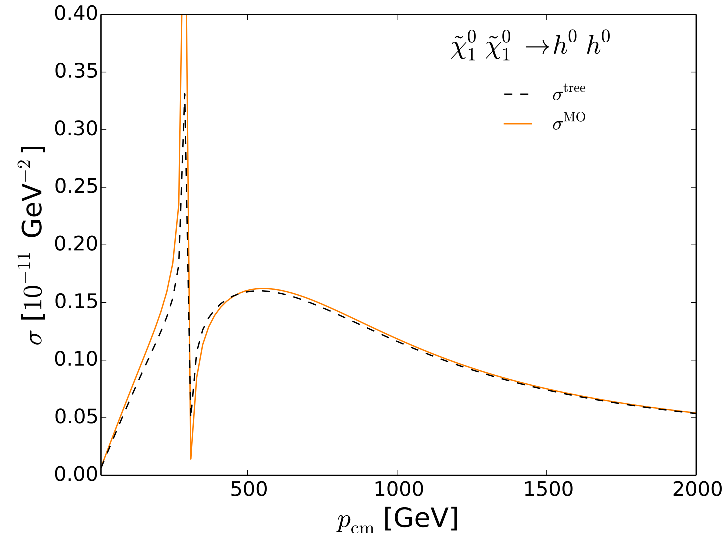

Figure 4.8.: Calculation of the cross section of $\tilde{\chi}_1^0\tilde{\chi}_1^0 \to h^0h^0$, comparing the results of micrOMEGAs (effective couplings) and DM@NLO (pure tree level).

resonance with the H^0 as the propagating particle. The Drop directly after the peak can be a result of the interference term. The interference terms also recognize the resonance, but the interference terms do not have to be positive. Therefore the resonance at the outer region can effect a drop of the curve by a minus sign in the interference terms.

Fig. 4.10(b) shows the process $\tilde{\chi}_1^0\tilde{\chi}_1^0 \to H^+H^-$. In the low p_{cm} regime there are all channels closed until the p_{cm} is high enough that the final Higgs state can be produced. The result of DM@NLO differs only in the highest Peak from the result by micrOMEGAs, this is due to the effective couplings which are used in micrOMEGAs.

Comparing especially $\tilde{\chi}_1^0\tilde{\chi}_1^0 \to h^0A^0$ with $\tilde{\chi}_1^0\tilde{\chi}_1^0 \to H^0A^0$, see Fig. 4.11(a) 4.11(b), or $\tilde{\chi}_1^0\tilde{\chi}_1^0 \to H^0H^0$ with $\tilde{\chi}_1^0\tilde{\chi}_1^0 \to A^0A^0$, see figure 4.9(b) 4.9(a), the behavior of the curves is similar, due to the fact, that $m_{A^0} \sim m_{H^0}$ ($m_{A^0} = 1592.90$ GeV,$m_{H^0} = 1592,66$ GeV). Additionally the channels of the annihilation processes are the same, where just the value of the couplings differ.

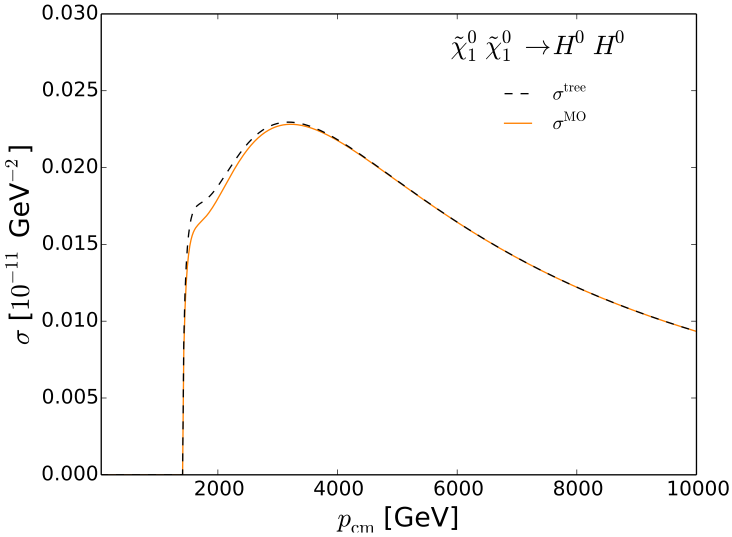

(a)

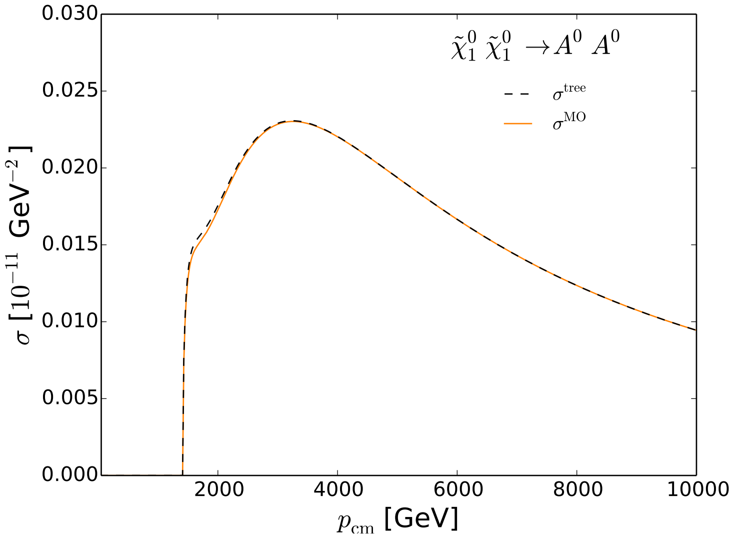

(b)

Figure 4.9.: Calculation of the cross section of a) $\tilde{\chi}_1^0\tilde{\chi}_1^0 \rightarrow H^0H^0$ b) $\tilde{\chi}_1^0\tilde{\chi}_1^0 \rightarrow A^0A^0$, comparing the results of micrOMEGAs (effective couplings) and DM@NLO (pure tree level).

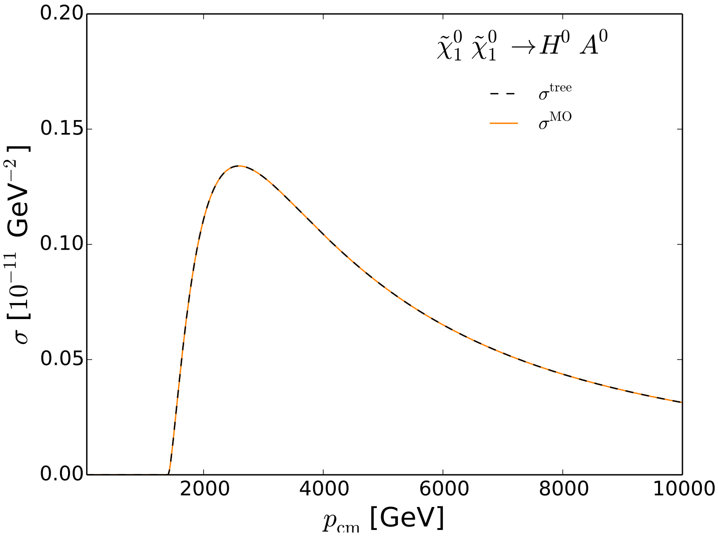

(a)

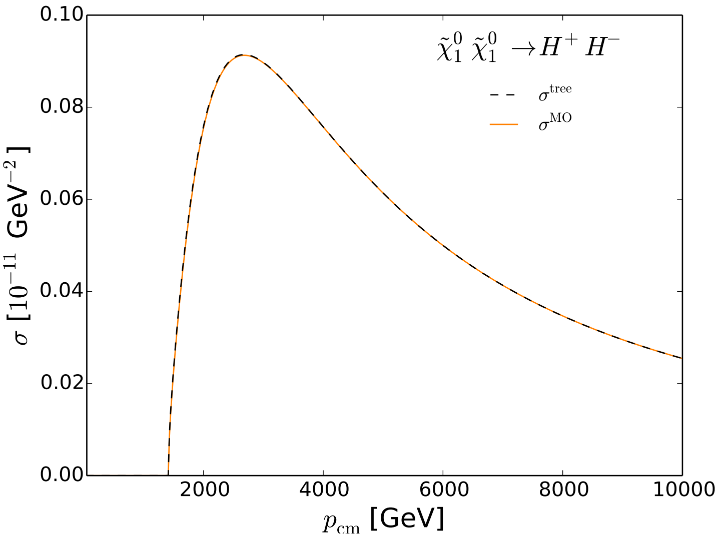

(b)

Figure 4.10.: Calculation of the cross section of a)$\tilde{\chi}_1^0\tilde{\chi}_1^0 \rightarrow H^0 A^0$ b)$\tilde{\chi}_1^0\tilde{\chi}_1^0 \rightarrow H^+ H^-$, comparing the results of micrOMEGAs (effective couplings) and DM@NLO (pure tree level).

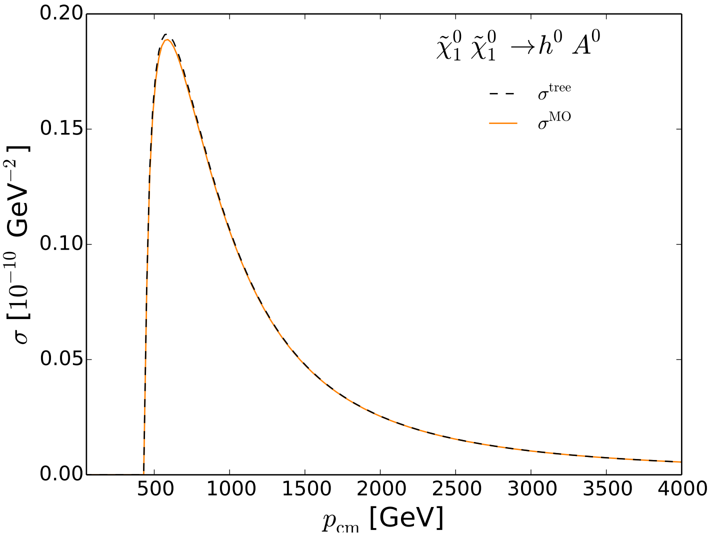

(a)

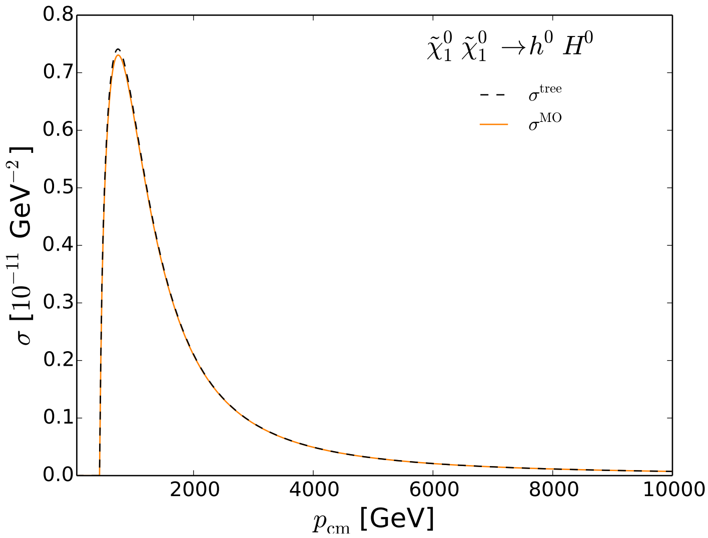

(b)

Figure 4.11.: Calculation of the cross section of a)$\tilde{\chi}_1^0\tilde{\chi}_1^0 \rightarrow h^0 A^0$ b)$\tilde{\chi}_1^0\tilde{\chi}_1^0 \rightarrow h^0 H^0$ comparing the results of micrOMEGAs (effective couplings) and DM@NLO (pure tree level).

5. Calculation of the Relic Density

A way to decide whether a particle can be a dark matter particle or not, is by calculating the relic density. The amount of dark matter particles evolves with the Universe. At the beginning the Universe was very hot. With time as the Universe expanded the Universe cools and depending on the temperature some production processes stop, when the temperature gets too low. When the dark matter particles get diluted even their annihilation stops. This is called the freeze out. The density of the particle is almost constant, because there is no change of the number of particles by annihilation. This state is called equilibrium. In the following the Boltzmann equation is presented. This equation describes the evolution of the phase-space density. As the next step, it is explained how the equation can be solved numerically. Finally the determination of the thermal average of the cross section is explained.

5.1. The Boltzmann equation

The Boltzmann equation [31]

$$L[f] = C[f]. \tag{5.1}$$

describes the evolution of the phase-space density $f(\mathbf{p}, \mathbf{x}, t)$, with L as the Lionville operator and C as the collision operator. The net rate of the change in time of the particle phase-space density is given by the Lionville operator L.

By taking into account that the phase-space density is homogeneous and isotropic, which means, it depends only on the particle energy E and the time t, the Lionville operator becomes

$$L[f] = \frac{\partial f}{\partial t} - H \frac{|\mathbf{p}|^2}{E} \frac{\partial f}{\partial E} \tag{5.2}$$

where $H = \dot{R}/R$ is the Hubble rate and R is the scale factor of the Universe. The dot above the $\dot{R}$ represents the time derivative. On the right hand side of the equation the collision operator C counts the gained or lost particles, via collisions with other particles. The particle number density n is defined as the integral of the phase-space density over all momenta and the sum over all spins

$$n = \int dn = \int f(E, t) \frac{g \, d^3p}{(2\pi)^3}. \tag{5.3}$$

Here g represents the spin degrees of freedom. The evolution function for the particle number density is given by the integrated Boltzmann-equation over all particle momenta and sum over the spin degrees of freedom. For a $2 \to 2$ process (12→34) the Lionville-term becomes

$$g_1 \int L(f_1) \frac{d^3p_1}{(2\pi)^3} = \frac{1}{R}\frac{d}{dt}(R^3 n_1) = \dot{n}_1 + 3Hn_1. \tag{5.4}$$

Only the inelastic terms of the collision term survive the integration

$$\begin{aligned} g_1 \int C(f_1)\frac{d^3p_1}{(2\pi)^3} = -\sum_{\text{Spin}} \int &(f_1 f_2 (1 \pm f_3)(1 \pm f_4)|M_{12\to 34}|^2 \\ &- f_3 f_4 (1 \pm f_1)(1 \pm f_2)|M_{34\to 12}|^2) \cdot (2\pi)^4 \delta(p_1 + p_2 - p_3 - p_4) \\ &\cdot \frac{d^3p_1}{(2\pi)^3 2E_1}\frac{d^3p_2}{(2\pi)^3 2E_2}\frac{d^3p_3}{(2\pi)^3 2E_3}\frac{d^3p_4}{(2\pi)^3 2E_4}, \end{aligned} \tag{5.5}$$

where M is the invariant polarized amplitude. If the initial particle are identical, one gets a factor $\frac{1}{2}$ to avoid double counting and a factor 2 out of the disappearance of two particle in each annihilation. So for identical particles there is no additional factor in the equation. One can replace f_3 and f_4 by their equilibrium distributions f_3^{eq} and f_4^{eq}, because the annihilation product is in equilibrium with the thermal background.The detailed balance allows the replacement

$$f_3^{\text{eq}} f_4^{\text{eq}} = f_1^{\text{eq}} f_2^{\text{eq}}. \tag{5.6}$$

By taking into account unitarity, one receives

$$\sum_{\text{spin}} \int |M_{34\to 12}|^2 (2\pi)^4 \delta^4(p_1 + p_2 - p_3 - p_4) \frac{d^3p_3}{(2\pi)^3 2E_3}\frac{d^3p_4}{(2\pi)^3 2E_4} \tag{5.7}$$

$$= \sum_{\text{spin}} \int |M_{12\to 34}|^2 (2\pi)^4 \delta^4(p_1 + p_2 - p_3 - p_4) \frac{d^3p_3}{(2\pi)^3 2E_3}\frac{d^3p_4}{(2\pi)^3 2E_4}. \tag{5.8}$$

Introducing the unpolarized cross section $\sigma_{12\to 34}$, one gets

$$\sum_{\text{spin}} \int |M_{12\to 34}|^2 (2\pi)^4 \delta^4(p_1 + p_2 - p_3 - p_4) \frac{d^3p_3}{(2\pi)^3 2E_3}\frac{d^3p_4}{(2\pi)^3 2E_4} = 4F g_1 g_2 \sigma_{12\to 34} \tag{5.9}$$

with $F = [(p_1 \cdot p_2)^2 - m_1^2 m_2^2]^{1/2}$ and g_1 and g_2 are the averaged spin factors. To include all accessible final channels, one has to replace $\sigma_{12\to 34}$ with the total annihilation cross section

$$g_1 \int C(f_1)\frac{d^3p_1}{(2\pi)^3} = -\int \sigma v_{\text{Møl}} (dn_1 dn_2 - dn_1^{\text{eq}} dn_2^{\text{eq}}). \tag{5.10}$$

n_1 and n_2 are the particle number densities and their equilibrium values are n_1^{eq} and n_2^{eq}, dn_1 and dn_2 are the momentum-space differentials. The Møller velocity $v_{\text{Møl}} = \frac{F}{E_1 E_2}$ is defined in a way that $v_{\text{Møl}} n_1 n_2$ is invariant under Lorentz transformation. This product equals the product of the relative velocity $v_{\rm lab}$ with the particle densities $n_{1\rm lab}$ and $n_{2\rm lab}$. Using the Møller velocity, the invariant interaction rate per unit volume and unit time can be written in any reference frame as

$$\frac{dN}{dVdt} = \sigma v'_{\rm Møl} n'_1 n'_2. \tag{5.11}$$

The prime on the velocity and the particle densities symbolizes the chosen reference frame, σ is the invariant cross section. If one chose the cosmic comoving frame with the particle velocities $v_1 = \frac{p_1}{E_1}$ and $v_2 = \frac{p_2}{E_2}$ the Møllervelocity becomes

$$v_{\rm Møl} = \left[|v_1 - v_2|^2 - |v_1 \times v_2|^2\right]^{1/2} \tag{5.12}$$

By symmetry consideration, one realizes the distributions in the kinematic equilibrium are proportional to those in chemical equilibrium, where the proportional factor is independent of the momentum. This is true for the species one and two in the kinematic equilibrium through scattering in a thermal bath during the whole evolution even after decoupling, when they are out of the chemical equilibrium.Taking equation (5.10) with comparison of the situation before and after the decoupling, one obtains

$$g_1 \int C(f_1) \frac{d^3 p_1}{(2\pi)^3} = - < \sigma v_{\rm Møl} > (n_1 n_2 - n_1^{\rm eq} n_2^{\rm eq}). \tag{5.13}$$

The thermally averaged total annihilation cross section multiplied by the Møller velocity is given by

$$< \sigma v_{\rm Møl} >= \frac{\int \sigma v_{\rm Møl} dn_1^{\rm eq} dn_2^{\rm eq}}{\int dn_1^{\rm eq} \int dn_1^{\rm eq}}. \tag{5.14}$$

By comparing Eq. (5.10) with Ey. (5.13), one receives

$$\dot{n}_1 + 3Hn_1 = - < \sigma v_{\rm Møl} > (n_1 n_2 - n_1^{\rm eq} n_2^{\rm eq}), \tag{5.15}$$

and an analogous equation for n_2. If the particles one and two are identical it follows

$$\dot{n} + 3Hn = - < \sigma v_{\rm Møl} > (n^2 - n_{\rm eq}^2). \tag{5.16}$$

Where σ is summed over final and averaged over initial spins with no factor of $\frac{1}{2}$ for indentical particles. In the following only identical particles are taken into account. One considers the expansion of the universe corresponds to the ratio of the number of particles to the entropy $Y = \frac{n}{s}$, where s is the total entropy density of the universe, to treat the decrease in the density implicitly. The total entropy per comoving frame is given by $S = R^3 s$. This value is constant if there is no change in entropy. Dividing (5.16) by S, one receives

$$\dot{Y} = -s < \sigma v_{\rm Møl} > (Y^2 - Y_{\rm eq}^2). \tag{5.17}$$

Y_{eq} is the equilibriums abundance and is calculated as

$$Y_{\text{eq}} = \frac{45gx^2K_2(x)}{4\pi^4 h_{eff}(\frac{m}{x})}, \tag{5.18}$$

where g stands for the degrees of freedom of the initial particles and h_{eff} denotes the effective degrees of freedom for the entropy. $K_2(\frac{m}{x})$[27] is the modified bessel function of the second kind. By using the scale factor R as a time variable, one gets

$$\frac{dY}{dR} = \frac{s < \sigma v_{\text{Møl}} >}{RH}(Y^2 - Y_{\text{eq}}^2). \tag{5.19}$$

$H = (\frac{8}{3}\pi G\rho)^{\frac{1}{2}}$ is the Hubble parameter, G the gravitational constant and ρ the total energy density. The function for Y can also be rewritten in terms of the parameter $x = \frac{T}{m}$

$$\frac{dY}{dx} = \frac{1}{3H}\frac{ds}{dx} < \sigma v_{\text{Møl}} > (Y^2 - Y_{\text{eq}}^2), \tag{5.20}$$

where T being the photon temperature. In the following step the effective degrees of freedom for the energy and the entropy density are introduced

$$\rho = g_{\text{eff}}(T)\frac{\pi^2}{30}T^4, \qquad s = h_{\text{eff}}(T)\frac{2\pi^2}{45}T^3. \tag{5.21}$$

For relativistic particles with one internal degrease of freedom, it is $g_{\text{eff}}(T) = h_{\text{eff}} = 1$. Using Eq. (5.21) in (5.20), one receives the final result for the Boltzmann equation

$$\frac{dY}{dx} = -\sqrt{\frac{\pi}{45G}}\frac{g^{*\frac{1}{2}}m}{x^2} < \sigma v_{\text{Møl}} > (Y^2 - Y_{\text{eq}}^2). \tag{5.22}$$

The content of the universe is given by the degrees of freedom parameter

$$g^{*\frac{1}{2}} = \frac{h_{\text{eff}}}{g_{\text{eff}}^{\frac{1}{2}}}\left(1 + \frac{1}{3}\frac{T}{h_{\text{eff}}}\frac{dh_{\text{eff}}}{dT}\right). \tag{5.23}$$

The Eq. (5.22) is only valid as long as the statistical and mechanical factors are neglected, the annihilation products are in thermal equilibrium, the species under consideration remain in kinematic equilibrium after the decoupling and the initial chemical potential of the species is negligible.

5.1.1. Integration Method for the Boltzmann equation

To calculate the relic density one has to solve the Boltzmann equation. This can be done by a numerical integration of the function. In the following a way to do these numerical integration will be explained. The integration routine is based on the routine in *DarkSUSY* [32]. Taking the formula (5.22) and defining the factor λ

$$\lambda = \sqrt{\frac{\pi}{45G}} \frac{\sqrt{g^\star} m_1}{x^2} < \sigma_{eff} v >, \tag{5.24}$$

the Boltzmann equation becomes

$$\frac{dY}{dx} = -\lambda(Y^2 - q^2). \tag{5.25}$$

There is also the thermal equilibrium density renamed to $q = Y_{eq}$. To solve the equation numerically, one can approximate the curve from above and from below and compare both results. With the trapezoidal method one can underestimate the area under the curve, see appendix F. (In the following there will be a short form used for functions with x_i as there argument $f(x_i) = f_i$). Furthermore, the right side of the Eq. (5.25) will be represented by

$$f_i = \lambda_i(Y_i^2 - q_i^2) \tag{5.26}$$

and

$$f_{i+1} = \lambda_{i+1}(Y_{i+1}^2 - q_{i+1}^2) \tag{5.27}$$

with $x_{i+1} = x_i + h$.

The equation which has to be discretized is

$$Y_{i+1} - Y_i = h\frac{f_i + f_{i+1}}{2}. \tag{5.28}$$

This quadratic equation is solved by

$$Y_{i+1} = \frac{c}{1 + \sqrt{1 + uc}} \tag{5.29}$$

with

$$c = 2Y_i + u\left[\left(q_{i+1}^2 + \rho q_i^2\right) - \rho Y_i^2\right] \tag{5.30}$$

$$u = h\lambda_{i+1} \tag{5.31}$$

$$\rho = \frac{\lambda_i}{\lambda_{i+1}}. \tag{5.32}$$

In Eq. (5.29) one has to take into account that the denominator should not be complex. Therefore the step will be repeated with a reduced step width $h = \frac{h}{2}$ if $1 + uc < 0$.

The Euler method is used to overestimate the area under the curve, see appendix G. Therefore, in the next step the Boltzmann equation will be discretized as

$$Y_{i+1} - Y_i = hf_{i+1} \tag{5.33}$$

which leads to the solution

$$Y'_{i+1} = \frac{1}{2}\frac{c'}{1+\sqrt{1+uc'}} \tag{5.34}$$

with

$$c' = 4(Y_i + uq_{i+1}^2). \tag{5.35}$$

As before, it should be checked whether $1 + uc' < 0$, then the step would be repeated with the step width $h = \frac{h}{2}$.

To have an efficient routine, it is useful to use an adaptive method for the step size related to the difference of Y_{i+1} and Y'_{i+1}

$$d = \left|\frac{Y_{i+1} - Y'_{i+1}}{Y_{i+1}}\right|. \tag{5.36}$$

The difference d is then compared to a precision factor ε which should be a fixed value (e.g. 0.01). If $d < \varepsilon$, the step size can be increased by a factor of $\frac{d}{\varepsilon s}$, but the factor should not exceed 5. The factor s is a safety factor, which should be defined on a fixed value (e.g. 0.9). If $d > \varepsilon$, the step size should be reduced by the factor $\frac{d}{\varepsilon s}$, but this time the factor should not be smaller then $\frac{1}{10}$. In the whole calculation one should take care that the step width should not becomes smaller then $h_{min} = 10^-9$. Another check should be that the number of steps is limited by a maximal value (e.g. 10^5). There are two things missing by now. First we need starting values x_i, h. One should take care that x_i is small enough so that the value is not starting after the freeze out. For the step size it is a great choice to start at $h = 0.01$. In Fig. 5.1 one can see what is meant by the freeze out. After a short plateau the comoving number density begins to decrease within time until, the curve ends again on a plateau. This plateau means that the number density is now only depending on the expansion of the universe, this is meant by the freeze out. Secondly there has to be a check for the freeze out. For the freeze out one defines a value x_{end} where the routine starts to check for the freeze out. To check whether the freeze out took place, one compares the old abundance Y_i with the new one Y_{i+1}. If

$$\left|\frac{Y_i - Y_{i+1}}{Y_i}\right| < \varepsilon \tag{5.37}$$

then the freeze out is reached. The relic density is then calculated by

$$\Omega = m \cdot Y_i \cdot 2.742 \cdot 10^8. \tag{5.38}$$

By now the thermal average of the cross section times the velocity was used in the calculation of the relic density. But there is still the question how to calculate the thermal average numerical[31]. This will be done by an integration via the Simpson's rule, see appendix H

$$<\sigma v> = \int_{x_i}^{x_{i+1}} \sigma v(x)dx = \frac{h}{6}\left[\sigma v(x_i) + 4 \cdot \sigma v\left(\frac{x_i + x_{i+1}}{2}\right) + \sigma v(x_{i+1})\right]. \tag{5.39}$$

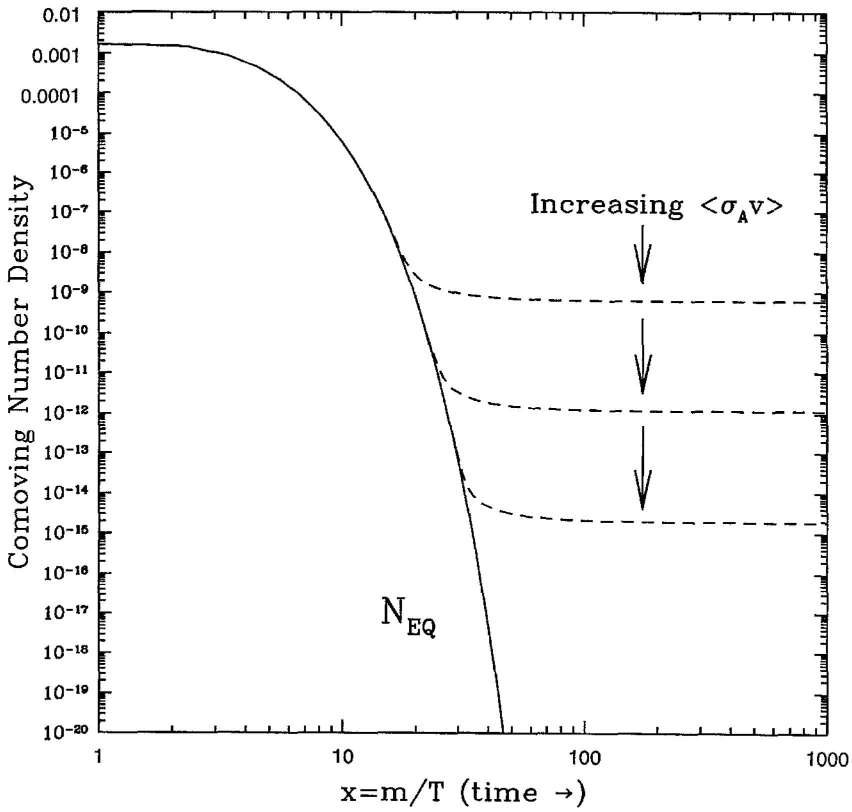

Figure 5.1.: Example for the behavior of the abundance, which is proportional to the number density[21]

Table 5.1.: MSSM input parameter for the selected scenario, the unit of the parameters is all given in GeV, except $\tan\beta$

$\tan\beta$	μ	m_A	M_1	M_2	M_3	$M_{\tilde{q}_{1,2}}$	$M_{\tilde{q}_3}$	$M_{\tilde{u}_3}$	$M_{\tilde{l}}$	A_t
5.8	2925.8	948.8	250.0	1954.1	1945.6	3215.1	1578.0	609.2	3263.9	3033.7

with $x = \sqrt{\frac{S}{4} - m^2}$.

5.2. Comparing DM@NLO with micrOMEGAs

Up until now DM@NLO used micrOMEGAs to calcualte the relic density. Therefor, a routine for the integration is implemented, which uses the thermal average of the cross section times the velocity of micrOMEGAs[1] to compare the results. The routine for the integration was written in C to handle different functions for the thermal average, the equilibriums abundance etc. The integration was implemented in the micrOMEGAs main file as it was explained before.

In the table 5.2 are the MSSM input parameter shown for the test scenario. A special scenario was chosen where 98.8% of the annihilation happens via the process $\tilde{\chi}^0\tilde{\chi}^0 \to t\bar{t}$.

The freeze-out curve of this implementation is shown in figure 5.2. The orange line shows the equilibriums abundance by micrOMEGAs. The dashed black line shows the relic abundance which was calculated by the implemented routine. As it is expected one sees that slowly the annihilation dominates the processes and then the rapid decrease of the equilibriums abundance to zero. Whereas the relic abundance first follows the equilibriums abundance and then freeze out, where the relic abundance of the comoving frame only depends on the expansion of the universe and therefor becoming a flat line.

Comparing the results of the relic abundance Y_{mo} and relic density of micrOMEGAs Ω_{mo} with the new implemented numerical calculation of the relic abundance Y_{te}[2]and the relic density Ω_{te}

$$Y_{mo} = 8.217252 \cdot 10^{-12} \qquad Y_{te} = 8.205265 \cdot 10^{-12}. \tag{5.40}$$

$$\Omega_{mo}h^2 = 0.563 \qquad \Omega_{te}h^2 = 0.5618. \tag{5.41}$$

one sees that the results fit quite well.

As a next step one has to determine the thermal average. Therefore the implemented routine was extended to an integration routine for the calculation of the thermal average, as it was discussed before. Within the comparison of micrOMEGAs and the new integration routine, one has to take into account that we now only deal with 98.8% of the

[1]micrOMEGAs uses a different method to solve the Boltzmann equation, namely the Runge-Kutta-method

[2]The index is chosen to clarify that the trapezoidal and euler method was used

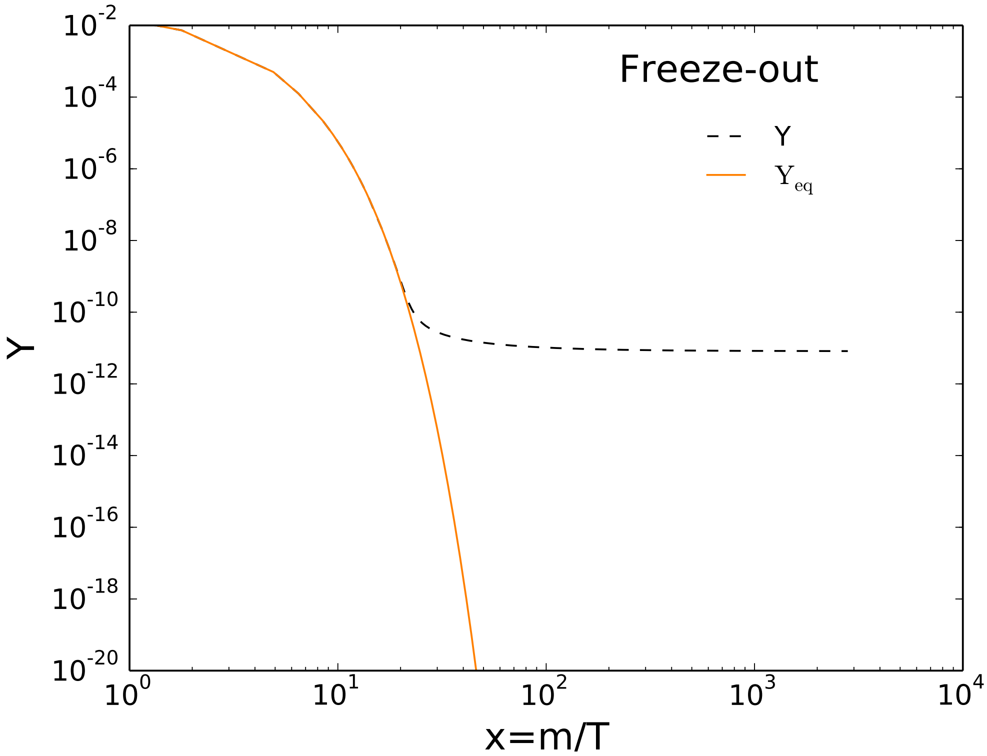

Figure 5.2.: Calculation of the abundance with the new routine within micrOMEGAs, where the thermal average and the equilibriums abundance was used from micrOMEGAs.

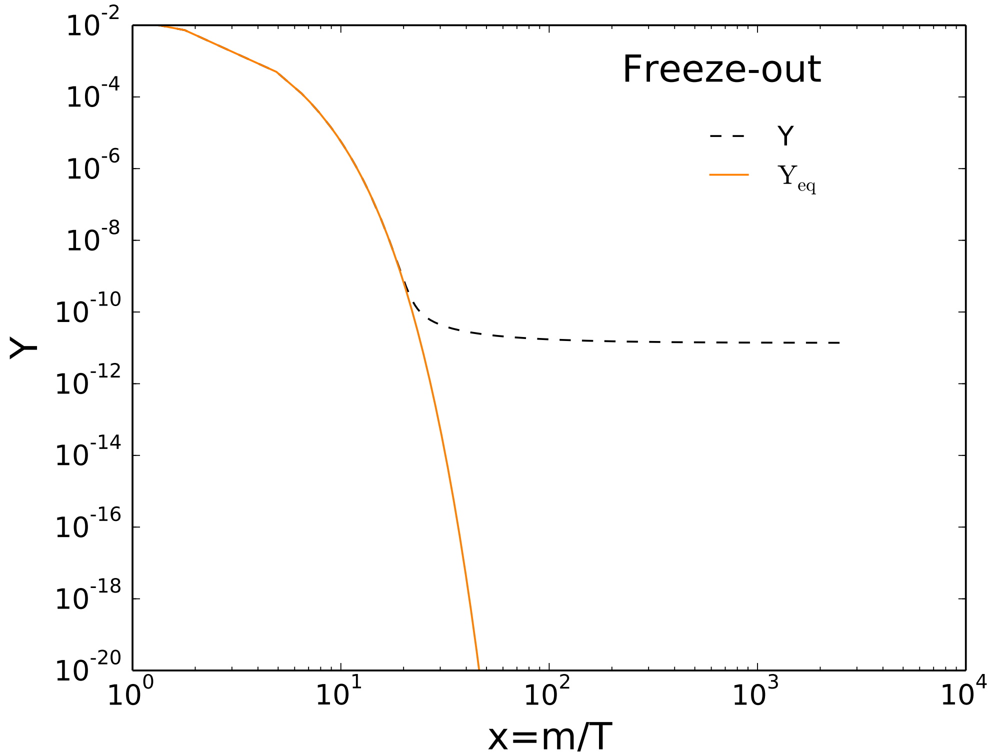

Figure 5.3.: Calculation of the abundance with the new routine within micrOMEGAs, where the equilibriums abundance was used from micrOMEGAs, but the thermal average was calculated within the new routine.

complete cross section. Therefore one can expect differences between the result of micrOMEGAs and the newly implemented routine. In figure 5.3 the freeze out curve of the extended routine is shown. As before the orange line shows the equilibriums abundance, which is exactly the same as before. Still the function for the equilibriums abundance of micrOMEGAs was used. With the new thermal average, there is still the same behavior of the relic abundance. The plateau at the end is now shifted a little higher then before. Again comparing the results from micrOMEGAs and the implementation

$$Y_{mo} = 8.217252 \cdot 10^{-12} \qquad Y_{tes} = 13.81070 \cdot 10^{-12}. \tag{5.42}$$

$$\Omega_{mo}h^2 = 0.563 \qquad \Omega_{tes}h^2 = 0.946. \tag{5.43}$$

As only dominant processes are used the difference between the two relic densities is acceptable.

The next step was to rewrite the routines in a FORTRAN code for the use with DM@NLO. Therefore the equilibriums abundance has to be calculated as well with the formula (5.18). The degrees of freedom $g^\star$, h_{eff} and g_{eff} were implemented in same

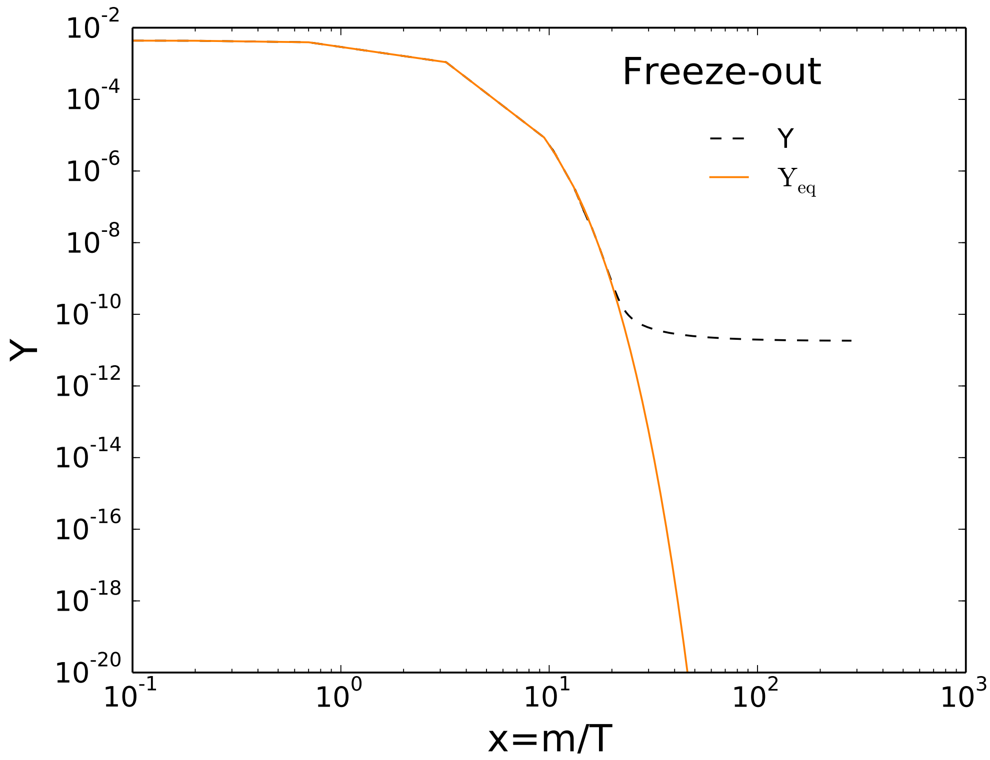

Figure 5.4.: Calculation of the abundance with the new routine implemented in DM@NLO

way as they are in micrOMEGAs [19]. There were also the modified bessel functions implemented from [27].

In figure 5.4 one sees the same behaviour of the equilibriums abundance and relic abundance like before. Comparing the relic density

$$Y_{mo} = 8.217252 \cdot 10^{-12} \qquad Y_{DMNLO} = 18.355548 \cdot 10^{-12}. \tag{5.44}$$

$$\Omega_{mo}h^2 = 0.563 \qquad \Omega_{DMNLO}h^2 = 1.276. \tag{5.45}$$

At the first view it looks like a huge difference. But again one has to take into account that on the first side Ω_{MO} was calculated within micrOMEGAs 4.1 while the relic density of DM@NLO is calculated also on tree level[3] but with the convention of an older version of micrOMEGAs 2.4.

[3]DM@NLO includes an option to decide whether one wants to have NLO correction or not

6. Conclusion

This thesis is a part of an effort to transform the DM@NLO computer code to a stand alone code. As a first step I have implemented the missing process$\tilde{\chi}_1^0\tilde{\chi}_1^0 \rightarrow H_k H_l$. The results were cross-checked analitycally and numerically with other codes such as FormCalc and micrOMEGAs. As was shown in the thesis, the results are in a good agreement in different Higgs regimes. The final states including vector bosons are still work in progress and will be finished as soon as possible.

Another goal was to solve the Boltzmann equation, which is also done and implemented into DM@NLO. At the moment the Boltzmann integration routine uses only one annihilation process to calculate the relic density. As a next step in this project one has to find a efficient way to include all calculated cross section into the Boltzmann routine. The main problem within this is the long calculation time within the integration of the thermal average. A way to reduce the calculation time, would be if DM@NLO runs the first time all cross section should be written into text files, which can be later reused by each relic density calculation.

The transformation of DM@NLO into a stand alone package is still not complete. One needs to implement still missing processes such as the neutralino annihilation into other electroweak final states as well as processes as $\tilde{t}\tilde{t} \rightarrow gg$,including the NLO corrections.

A. Formulary

A.1. Dirac Matrices

[22]

$$\not{p} = \gamma^\mu p_\mu \tag{A.1}$$

$$\{\gamma^\mu, \gamma^\nu\} = 2\mathrm{g}^{\mu\nu} \tag{A.2}$$

$$\not{k}\gamma^\nu = -\gamma^\nu \not{k} + 2k^\nu \tag{A.3}$$

$$\not{a}\not{b} = -\not{b}\not{a} + 2a \cdot b \tag{A.4}$$

$$\gamma_\nu \gamma^\nu = 4 \tag{A.5}$$

$$\gamma_\mu \not{a} \gamma^\mu = -2\not{a} \tag{A.6}$$

$$\gamma_\mu \not{a}\not{b} \gamma^\mu = 4a \cdot b \tag{A.7}$$

$$\gamma_\mu \not{a}\not{b}\not{c} \gamma^\mu = -2\not{c}\not{a}\not{b} \tag{A.8}$$

$$\not{k}\gamma^\nu = -\gamma^\nu \not{k} + 2k^\nu \tag{A.9}$$

$$(a - \gamma_5)\gamma^0 = \gamma^0(1 + \gamma_5) \tag{A.10}$$

A.1.1. Spinors

$$\overline{u}(p) = u^+(p)\gamma_0 \tag{A.11}$$

$$\begin{aligned} \sum_s \overline{u}(p)u(p) &= \mathrm{Tr}(\not{p} + m) \\ \sum_s v(p)\overline{v}(p) &= \mathrm{Tr}(\not{p} - m) \end{aligned} \tag{A.12}$$

$$\sum_s \epsilon^\star_\nu(k)\epsilon_\mu(k) \quad \begin{array}{ll} = (\mathrm{g}^{\mu\nu}) & \text{Fermi-gauge} \\ = (-\mathrm{g}^{\mu\nu} - \frac{k_\mu k_\nu}{m^2}) & \text{unitary gauge} \end{array} \tag{A.13}$$

$$\overline{u}(p)(\not{p} - m) = 0 \tag{A.14}$$

$$(\not{p} - m)v(p) = 0 \tag{A.15}$$

$$\not{k}\epsilon(k) = 0 \tag{A.16}$$

A.1.2. Trace's

$$\mathrm{Tr}(\mathbb{1}) = 4 \tag{A.17}$$

$$\mathrm{Tr}(\gamma_5) = 0 \tag{A.18}$$

$$\mathrm{Tr}(\not{a}\not{b}) = 4ab \tag{A.19}$$

$$\mathrm{Tr}(\not{a}\not{b}\not{c}\not{d}) = 4[(a \cdot b)](c \cdot d) + (a \cdot d)(b \cdot c) - (a \cdot c)(b \cdot d)] \tag{A.20}$$

$$\mathrm{Tr}(\gamma_5 \not{a}\not{b}) = 0 \tag{A.21}$$

$$\mathrm{Tr}(\gamma_5 \not{a}\not{b}\not{c}) = 0 \tag{A.22}$$

$$\mathrm{Tr}(\gamma_5 \not{a}\not{b}\not{c}\not{d}) = 4\mathrm{i}\epsilon_{\alpha\beta\gamma\rho} \tag{A.23}$$

A.2. Polarization

$$P_L = \frac{1}{2}(1 - \gamma_5) \tag{A.24}$$

$$P_R = \frac{1}{2}(1 + \gamma_5) \tag{A.25}$$

$$P_R P_L = 0 \tag{A.26}$$

$$P_R P_R = P_R \qquad P_L P_L = P_L \tag{A.27}$$

$$P_L + P_R = \mathbb{1} \tag{A.28}$$

$$\mathrm{Tr}(P_L) = 2 = \mathrm{Tr}(P_R) \tag{A.29}$$

B. Feynman rules

B.1. Neutralino/chargino-Higgs

[26]

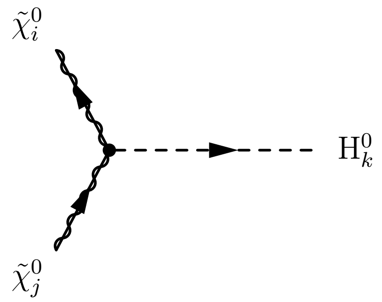

$$-\mathrm{i}g(C_R(k)P_R + C_L(k)P_L)$$

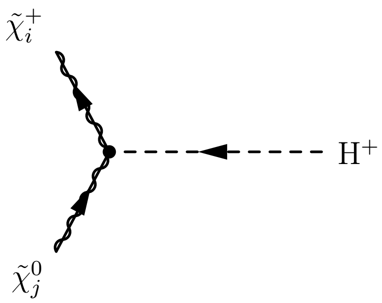

$$-\mathrm{i}g(C_R(k)P_R + C_L(k)P_L)$$

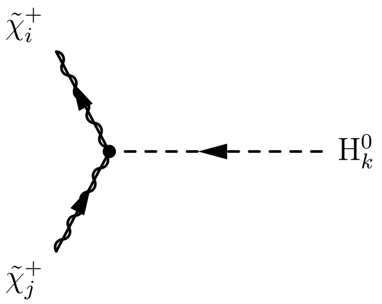

$$-\mathrm{i}g(C_R(k)P_R + C_L(k)P_L)$$

For neutralino annihilation to Higgs:

$$
\begin{aligned}
CL(1) = & -E_L/(2d0S_W)((-S_A)(Z^\star_{\tilde{\chi}^0}(i,3)Z^\star_{\tilde{\chi}^0}(j,2) + Z^\star_{\tilde{\chi}^0}(j,3)Z^\star_{\tilde{\chi}^0}(i,2) \\
& - \frac{S_W}{C_W}(Z^\star_{\tilde{\chi}^0}(i,3)Z^\star_{\tilde{\chi}^0}(j,1) + Z^\star_{\tilde{\chi}^0}(j,3)Z^\star_{\tilde{\chi}^0}(i,1))) \\
& + (-C_A)(Z^\star_{\tilde{\chi}^0}(i,4)Z^\star_{\tilde{\chi}^0}(j,2) + Z^\star_{\tilde{\chi}^0}(j,4)Z^\star_{\tilde{\chi}^0}(i,2) \\
& - \frac{S_W}{C_W}(Z^\star_{\tilde{\chi}^0}(i,4)Z^\star_{\tilde{\chi}^0}(j,1) + Z^\star_{\tilde{\chi}^0}(j,4)Z^\star_{\tilde{\chi}^0}(i,1)))) \\
CR(1) = & -E_L/(2d0S_W)((-S_A)(Z_{\tilde{\chi}^0}(i,3)Z_{\tilde{\chi}^0}(j,2) + Z_{\tilde{\chi}^0}(j,3)Z_{\tilde{\chi}^0}(i,2) \\
& - \frac{S_W}{C_W}(Z_{\tilde{\chi}^0}(i,3)Z_{\tilde{\chi}^0}(j,1) + Z_{\tilde{\chi}^0}(j,3)Z_{\tilde{\chi}^0}(i,1))) \\
& + (-C_A)(Z_{\tilde{\chi}^0}(i,4)Z_{\tilde{\chi}^0}(j,2) + Z_{\tilde{\chi}^0}(j,4)Z_{\tilde{\chi}^0}(i,2) \\
& - \frac{S_W}{C_W}(Z_{\tilde{\chi}^0}(i,4)Z_{\tilde{\chi}^0}(j,1) + Z_{\tilde{\chi}^0}(j,4)Z_{\tilde{\chi}^0}(i,1)))) \\
CL(2) = & -E_L/(2d0S_W)((+C_A)(Z^\star_{\tilde{\chi}^0}(i,3)Z^\star_{\tilde{\chi}^0}(j,2) + Z^\star_{\tilde{\chi}^0}(j,3)Z^\star_{\tilde{\chi}^0}(i,2) \\
& - \frac{S_W}{C_W}(Z^\star_{\tilde{\chi}^0}(i,3)Z^\star_{\tilde{\chi}^0}(j,1) + Z^\star_{\tilde{\chi}^0}(j,3)Z^\star_{\tilde{\chi}^0}(i,1))) \\
& + (-S_A)(Z^\star_{\tilde{\chi}^0}(i,4)Z^\star_{\tilde{\chi}^0}(j,2) + Z^\star_{\tilde{\chi}^0}(j,4)Z^\star_{\tilde{\chi}^0}(i,2) \\
& - \frac{S_W}{C_W}(Z^\star_{\tilde{\chi}^0}(i,4)Z^\star_{\tilde{\chi}^0}(j,1) + Z^\star_{\tilde{\chi}^0}(j,4)Z^\star_{\tilde{\chi}^0}(i,1)))) \\
CR(2) = & -E_L/(2d0S_W)((+C_A)(Z_{\tilde{\chi}^0}(i,3)Z_{\tilde{\chi}^0}(j,2) + Z_{\tilde{\chi}^0}(j,3)Z_{\tilde{\chi}^0}(i,2) \\
& - \frac{S_W}{C_W}(Z_{\tilde{\chi}^0}(i,3)Z_{\tilde{\chi}^0}(j,1) + Z_{\tilde{\chi}^0}(j,3)Z_{\tilde{\chi}^0}(i,1))) \\
& + (-S_A)(Z_{\tilde{\chi}^0}(i,4)Z_{\tilde{\chi}^0}(j,2) + Z_{\tilde{\chi}^0}(j,4)Z_{\tilde{\chi}^0}(i,2) \\
& - \frac{S_W}{C_W}(Z_{\tilde{\chi}^0}(i,4)Z_{\tilde{\chi}^0}(j,1) + Z_{\tilde{\chi}^0}(j,4)Z_{\tilde{\chi}^0}(i,1))))
\end{aligned}
$$

$$
\begin{aligned}
CL(3) = &-\mathrm{i}E_L/(2d0S_W)((-S_B)(Z^\star_{\tilde{\chi}^0}(i,3)Z^\star_{\tilde{\chi}^0}(j,2) + Z^\star_{\tilde{\chi}^0}(j,3)Z^\star_{\tilde{\chi}^0}(i,2) \\
&- \frac{S_W}{C_W}(Z^\star_{\tilde{\chi}^0}(i,3)Z^\star_{\tilde{\chi}^0}(j,1) + Z^\star_{\tilde{\chi}^0}(j,3)Z^\star_{\tilde{\chi}^0}(i,1))) \\
&+ (+C_B)(Z^\star_{\tilde{\chi}^0}(i,4)Z^\star_{\tilde{\chi}^0}(j,2) + Z^\star_{\tilde{\chi}^0}(j,4)Z^\star_{\tilde{\chi}^0}(i,2) \\
&- \frac{S_W}{C_W}(Z^\star_{\tilde{\chi}^0}(i,4)Z^\star_{\tilde{\chi}^0}(j,1) + Z^\star_{\tilde{\chi}^0}(j,4)Z^\star_{\tilde{\chi}^0}(i,1)))) \\
CR(3) = &+\mathrm{i}E_L/(2d0S_W)((-S_B)(Z_{\tilde{\chi}^0}(i,3)Z_{\tilde{\chi}^0}(j,2) + Z_{\tilde{\chi}^0}(j,3)Z_{\tilde{\chi}^0}(i,2) \\
&- \frac{S_W}{C_W}(Z_{\tilde{\chi}^0}(i,3)Z_{\tilde{\chi}^0}(j,1) + Z_{\tilde{\chi}^0}(j,3)Z_{\tilde{\chi}^0}(i,1))) \\
&+ (+C_B)(Z_{\tilde{\chi}^0}(i,4)Z_{\tilde{\chi}^0}(j,2) + Z_{\tilde{\chi}^0}(j,4)Z_{\tilde{\chi}^0}(i,2) \\
&- \frac{S_W}{C_W}(Z_{\tilde{\chi}^0}(i,4)Z_{\tilde{\chi}^0}(j,1) + Z_{\tilde{\chi}^0}(j,4)Z_{\tilde{\chi}^0}(i,1)))) \\
CL(4) = &-\mathrm{i}E_L/(2d0S_W)((+C_B)(Z^\star_{\tilde{\chi}^0}(i,3)Z^\star_{\tilde{\chi}^0}(j,2) + Z^\star_{\tilde{\chi}^0}(j,3)Z^\star_{\tilde{\chi}^0}(i,2) \\
&- \frac{S_W}{C_W}(Z^\star_{\tilde{\chi}^0}(i,3)Z^\star_{\tilde{\chi}^0}(j,1) + Z^\star_{\tilde{\chi}^0}(j,3)Z^\star_{\tilde{\chi}^0}(i,1))) \\
&+ (+S_B)(Z^\star_{\tilde{\chi}^0}(i,4)Z^\star_{\tilde{\chi}^0}(j,2) + Z^\star_{\tilde{\chi}^0}(j,4)Z^\star_{\tilde{\chi}^0}(i,2) \\
&- \frac{S_W}{C_W}(Z^\star_{\tilde{\chi}^0}(i,4)Z^\star_{\tilde{\chi}^0}(j,1) + Z^\star_{\tilde{\chi}^0}(j,4)Z^\star_{\tilde{\chi}^0}(i,1)))) \\
CR(4) = &+\mathrm{i}E_L/(2d0S_W)((+C_B)(Z_{\tilde{\chi}^0}(i,3)Z_{\tilde{\chi}^0}(j,2) + Z_{\tilde{\chi}^0}(j,3)Z_{\tilde{\chi}^0}(i,2) \\
&- \frac{S_W}{C_W}(Z_{\tilde{\chi}^0}(i,3)Z_{\tilde{\chi}^0}(j,1) + Z_{\tilde{\chi}^0}(j,3)Z_{\tilde{\chi}^0}(i,1))) \\
&+ (+S_B)(Z_{\tilde{\chi}^0}(i,4)Z_{\tilde{\chi}^0}(j,2) + Z_{\tilde{\chi}^0}(j,4)Z_{\tilde{\chi}^0}(i,2) \\
&- \frac{S_W}{C_W}(Z_{\tilde{\chi}^0}(i,4)Z_{\tilde{\chi}^0}(j,1) + Z_{\tilde{\chi}^0}(j,4)Z_{\tilde{\chi}^0}(i,1))))
\end{aligned}
$$

For chargino annihilation:

$$
\begin{aligned}
CL(5) &= -\frac{E_L}{S_W}C_B(V^\star_{\tilde{\chi}^\pm}(i,1)Z^\star_{\tilde{\chi}^0}(j,4) + \frac{1}{\sqrt{2}}(Z^\star_{\tilde{\chi}^0}(j,2) + \frac{S_W}{C_W}Z^\star_{\tilde{\chi}^0}(j,1))V^\star_{\tilde{\chi}^\pm}(i,2)) \\
CR(5) &= -\frac{E_L}{S_W}S_B(U_{\tilde{\chi}^\pm}(i,1)Z_{\tilde{\chi}^0}(j,3) - \frac{1}{\sqrt{2}}(Z_{\tilde{\chi}^0}(j,2) + \frac{S_W}{C_W}Z_{\tilde{\chi}^0}(j,1))U_{\tilde{\chi}^\pm}(i,2)) \\
CL(6) &= -\frac{E_L}{S_W}S_B(V^\star_{\tilde{\chi}^\pm}(i,1)Z^\star_{\tilde{\chi}^0}(j,4) + \frac{1}{\sqrt{2}}(Z^\star_{\tilde{\chi}^0}(j,2) + \frac{S_W}{C_W}Z^\star_{\tilde{\chi}^0}(j,1))V^\star_{\tilde{\chi}^\pm}(i,2)) \\
CR(6) &= \frac{E_L}{S_W}C_B(U_{\tilde{\chi}^\pm}(i,1)Z_{\tilde{\chi}^0}(j,3) - \frac{1}{\sqrt{2}}(Z_{\tilde{\chi}^0}(j,2) + \frac{S_W}{C_W}Z_{\tilde{\chi}^0}(j,1))U_{\tilde{\chi}^\pm}(i,2))
\end{aligned}
$$

For chargino annihilation:

$$
\begin{aligned}
CL(1) &= -\frac{E_L}{S_W\sqrt{2}}(-S_A V^{\star}_{\tilde{\chi}^\pm}(i,1)U^{\star}_{\tilde{\chi}^\pm}(j,2) + C_A V^{\star}_{\tilde{\chi}^\pm}(i,2)U^{\star}_{\tilde{\chi}^\pm}(j,1))\\
CR(1) &= -\frac{E_L}{S_W\sqrt{2}}(-S_A V_{\tilde{\chi}^\pm}(j,1)U_{\tilde{\chi}^\pm}(i,2) + C_A V_{\tilde{\chi}^\pm}(j,2)U_{\tilde{\chi}^\pm}(i,1))\\
CL(2) &= -\frac{E_L}{S_W\sqrt{2}}(C_A V^{\star}_{\tilde{\chi}^\pm}(i,1)U^{\star}_{\tilde{\chi}^\pm}(j,2) + S_A V^{\star}_{\tilde{\chi}^\pm}(i,2)U^{\star}_{\tilde{\chi}^\pm}(j,1))\\
CR(2) &= -\frac{E_L}{S_W\sqrt{2}}(C_A V_{\tilde{\chi}^\pm}(j,1)U_{\tilde{\chi}^\pm}(i,2) + S_A V_{\tilde{\chi}^\pm}(j,2)U_{\tilde{\chi}^\pm}(i,1))\\
CL(3) &= -\mathrm{i}\frac{E_L}{S_W\sqrt{2}}(-S_B V^{\star}_{\tilde{\chi}^\pm}(i,1)U^{\star}_{\tilde{\chi}^\pm}(j,2) - C_B V^{\star}_{\tilde{\chi}^\pm}(i,2)U^{\star}_{\tilde{\chi}^\pm}(j,1))\\
CR(3) &= \mathrm{i}\frac{E_L}{S_W\sqrt{2}}(-S_B V_{\tilde{\chi}^\pm}(j,1)UCha(i,2) - C_B V_{\tilde{\chi}^\pm}(j,2)UCha(i,1))\\
CL(4) &= -\mathrm{i}\frac{E_L}{S_W\sqrt{2}}(C_B V^{\star}_{\tilde{\chi}^\pm}(i,1)U^{\star}_{\tilde{\chi}^\pm}(j,2) - S_B V^{\star}_{\tilde{\chi}^\pm}(i,2)U^{\star}_{\tilde{\chi}^\pm}(j,1))\\
CR(4) &= \mathrm{i}\frac{E_L}{S_W\sqrt{2}}(C_B V_{\tilde{\chi}^\pm}(j,1)UCha(i,2) - S_B V_{\tilde{\chi}^\pm}(j,2)UCha(i,1))
\end{aligned}
$$

B.2. Neutralino/chargino-Vector boson

[26] For chargino annihilation

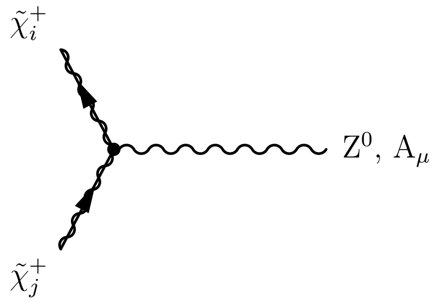

$$
\begin{aligned}
Z^0 &: \quad \mathrm{i}\gamma^\mu(A_L P_L + A_R P_R)\\
A_\mu &: \quad \mathrm{i}A_{PL}\gamma^\mu
\end{aligned}
$$

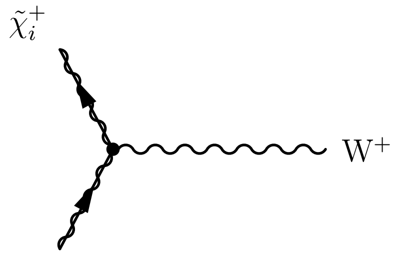

$i\gamma^\mu(A_L P_L + A_R P_R)$

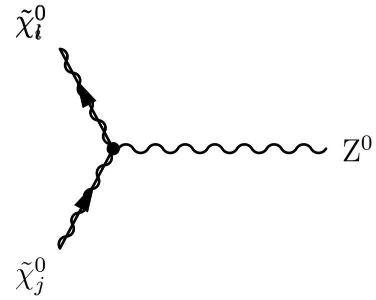

$i\gamma^\mu(A_L P_L + A_R P_R)$

$$A_{PL} = -E_L \delta_{i,j}$$
$$AL = E_L/(S_W * C_W) * (-VCha(indj,1) * VChaC(indi,1) - 1/2d0 * VCha(indj,2) * VChaC(indi,2$$
$$AR = E_L/(S_W * C_W) * (-UChaC(indj,1) * UCha(indi,1) - 1/2d0 * UChaC(indj,2) * UCha(indi,2$$

For neutralino-chargino coannihilation:

$$AL = \frac{E_L}{S_W} * (ZNeu(indj,2) * VChaC(indi,1) - 1/sqrt2 * ZNeu(indj,4) * VChaC(indi,2))$$
$$AR = \frac{E_L}{S_W} * (ZNeuC(indj,2) * UCha(indi,1) + 1/sqrt2 * ZNeuC(indj,3) * UCha(indi,2))$$

For neutralino annihilation:

$$AL = E_L/(2 * S_W * C_W) * (-ZNeu(indj,3) * ZNeuC(indi,3) + ZNeu(indj,4) * ZNeuC(indi,4))$$
$$AR(2) = E_L/(2 * S_W * C_W) * (ZNeuC(indj,3) * ZNeu(indi,3) - ZNeuC(indj,4) * ZNeu(indi,4))$$

B.3. Vector boson-Higgs-Higgs

In the calculation the coupling was given as J_{LR} this gives the prefactor of the couplings mentioned next to the following images:

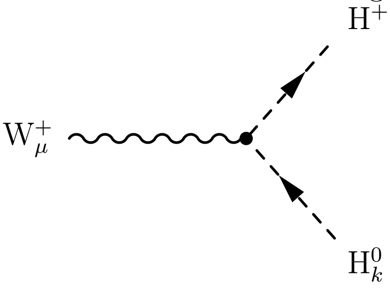

$$h^0, H^0: \qquad -\mathrm{i}\tfrac{g}{2} c_k (k_2 - k_3)^\mu$$

$$A^0: \qquad \tfrac{g}{2}(k_2 - k_3)^\mu$$

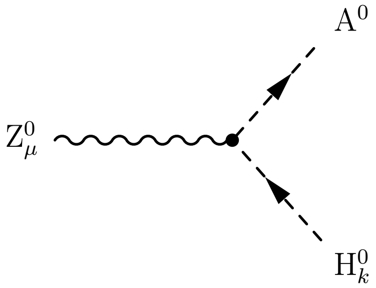

$$\tfrac{g}{2\cos(\theta_W} c_k (k_2 - k_3)^\mu$$

$$c1 = \cos(\alpha - \beta) \qquad c_2 = \sin(\alpha - \beta) \tag{B.1}$$

B.4. Higgs-vector boson-vektor boson

In the calculation the coupling was given as L_{LR} this gives the prefactor of the couplings mentioned next to the following images:

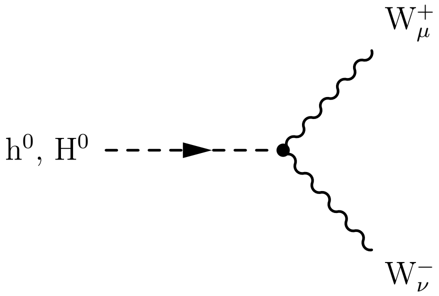

h^0 : $\quad \mathrm{i}g\sin(\beta-\alpha)g^{\mu\nu}$

H^0 : $\quad \mathrm{i}g\cos(\beta-\alpha)g^{\mu\nu}$

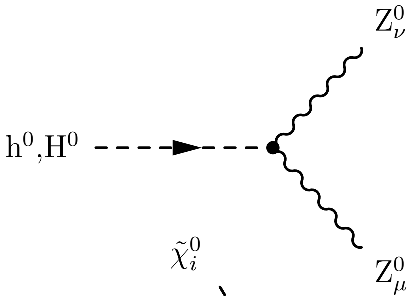

h^0 : $\quad \mathrm{i}\frac{g}{\cos(\theta_W)}\sin(\beta-\alpha)g^{\mu\nu}$

H^0 : $\quad \mathrm{i}\frac{g}{\cos(\theta_W)}\cos(\beta-\alpha)g^{\mu\nu}$

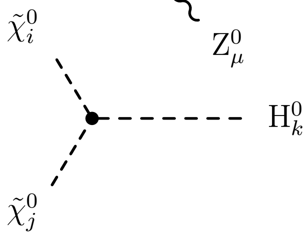

$-\mathrm{i}I_{LR}(i,j,k)$

B.5. Higgs Higgs Higgs

$$ILR(1,1,1) = -3 * \frac{E_L M_Z}{2C_W S_W} * C2A * SAB$$
$$ILR(1,1,2) = -\frac{E_L M_Z}{2C_W S_W} * (2 * S2A * SAB - CAB * C2A)$$
$$ILR(1,2,2) = \frac{E_L M_Z}{2C_W S_W} * (2 * S2A * CAB + SAB * C2A)$$
$$ILR(1,3,3) = -\frac{E_L M_Z}{2C_W S_W} * C2B * SAB$$
$$ILR(1,3,4) = -\frac{E_L M_Z}{2C_W S_W} * S2B * SAB$$
$$ILR(1,4,4) = \frac{E_L M_Z}{2C_W S_W} * C2B * SAB$$
$$ILR(1,5,5) = \frac{E_L}{S_W} * (M_W * SBA + M_Z/(2 * C_W) * C2B * SAB)$$
$$ILR(1,5,6) = \frac{E_L}{2S_W} * (M_W * CBA - M_Z/C_W * S2B * SAB)$$
$$ILR(1,6,6) = \frac{E_L}{(2C_W S_W} * M_Z * C2B * SAB$$
$$ILR(2,2,2) = -3 * \frac{E_L M_Z}{2C_W S_W} * C2A * CAB$$
$$ILR(2,3,3) = \frac{E_L M_Z}{2C_W S_W} * C2B * CAB$$
$$ILR(2,3,4) = \frac{E_L M_Z}{2C_W S_W} * S2B * CAB$$
$$ILR(2,4,4) = -\frac{E_L M_Z}{2C_W S_W} * C2B * CAB$$
$$ILR(2,5,5) = -\frac{E_L}{S_W} * (M_W * CBA - M_Z/(2 * C_W) * C2B * CAB)$$
$$ILR(2,5,6) = -\frac{E_L}{2S_W} * (M_W * SBA - M_Z/C_W * S2B * CAB)$$
$$ILR(2,6,6) = -\frac{E_L}{(2C_W S_W} * M_Z * C2B * CAB$$
$$ILR(3,5,6) = \mathrm{i} * \frac{E_L}{2S_W} * M_W$$

B.6. Short forms

M_W is the mass of the W-boson, M_Z is the mass of the Z-boson

$$
\begin{aligned}
&C_W = \cos\theta_W\\
&S_W = \sin\theta_W\\
&SBA = (\sin\beta\cos\alpha - \cos\beta\sin\alpha)\\
&CAB = (\cos\alpha\cos\beta - \sin\alpha\sin\beta)\\
&SAB = (\sin\alpha\cos\beta + \cos\alpha\sin\beta)\\
&C2B = \cos\beta^2 - \sin\beta^2\\
&C2A = \cos\alpha^2 - \sin\alpha^2\\
&S2A = 2\sin\alpha\cos\alpha\\
&S2B = 2\tan\beta\cos\beta^2
\end{aligned}
$$

C. Amplitudes

C.1. NeuNeu2HH

The neutralino annihilation in the s-channel to Higgs final states

$$\mathrm{i}M_{s(H)} = \overline{v}(p_b)(-\mathrm{i})(C_L(i)P_L + C_R(i)P_R)u(p_a)\frac{\mathrm{i}}{(s-m_i^2)}(-\mathrm{i}I_{LR}(i,k,l)) \tag{C.1}$$

$$\begin{aligned}\mathrm{i}M_{s(V)} = &\overline{v}(p_b)(-\mathrm{i})\gamma^\sigma(A_L(i)P_L + A_R(i)P_R)u(p_a)\\ &\frac{\mathrm{i}\mathrm{g}^{\sigma\rho}}{(s-m_V^2)}(-\mathrm{i}J_{LR}(i,k,l)(k_1-k2)^\rho))\end{aligned} \tag{C.2}$$

$$\begin{aligned}\mathrm{i}M_{t(\chi)} = &\overline{v}(p_b)(-\mathrm{i})(Y_L(i)P_L + Y_R(i)P_R)\\ &\frac{\mathrm{i}(\not{k}_2 - \not{p}_b + m_\chi)}{(t-m_\chi^2)}(-\mathrm{i})(Z_L(i)P_L + Z_R(i)P_R)u(p_a)\end{aligned} \tag{C.3}$$

$$\mathrm{i}M_{t(\chi)} = \overline{v}(p_b)(-\mathrm{i})(W_L(i)P_L + W_R(i)P_R)\frac{\mathrm{i}(\not{p}_a - \not{k}_2 + m_\chi)}{(u-m_\chi^2)}(-\mathrm{i})(X_L(i)P_L + X_R(i)P_R)u(p_a) \tag{C.4}$$

C.2. NeuNeu2HV

$$\mathrm{i}M_{s(H)} = \frac{-\mathrm{i}}{s-m_i^2}(J_{LR} * \overline{v}(p_b)(C_R * P_R + C_L * P_L)u(p_a) * (2 * k_1 + k2)^\nu * \varepsilon_\nu^\star(k_2)) \tag{C.5}$$

$$\mathrm{i}M_{s(V)} = \frac{\mathrm{i}}{s-m_V^2}(L_{LR} * \overline{v}(p_b)\gamma^\mu(A_R * P_R + A_L * P_L)u(p_a)\mathrm{g}^{\mu\nu}\mathrm{g}^{\nu\rho}\varepsilon_\rho^\star(k_2)) \tag{C.6}$$

$$\begin{aligned}\mathrm{i}M_{t(\chi)} = &\frac{-\mathrm{i}}{(t-m_q^2)} * \overline{v}(p_b)\gamma^\nu(U_R * P_R + U_L * P_L)(m_q - \not{k}_1 + \not{p}_a)\\ &(Z_R * P_R + Z_L * P_L)u(p_a)\varepsilon_\nu^\star(k_2))\end{aligned} \tag{C.7}$$

$$\begin{aligned}\mathrm{i}M_{u(\chi)} = &\frac{-\mathrm{i}}{u-m_q^2} * \overline{v}(p_b)(W_R * P_R + W_L * P_L)(m_q - \not{k}_2 + \not{p}_a)\gamma^\mu\\ &(T_R * P_R + T_L * P_L)u(p_a)\varepsilon_\mu^\star(k_2))\end{aligned} \tag{C.8}$$

C.3. NeuNeu2VV

$$\mathrm{i}M_{s(H)} = \frac{\mathrm{i}}{(s-m_i^2)} L_{LR}\overline{v}(p_b)(C_R P_R + C_L P_L)u(p_a)\mathrm{g}^{\mu\nu}\varepsilon_\mu^\star(k_1)\varepsilon_\nu^\star(k_2)) \tag{C.9}$$

$$\begin{aligned}\mathrm{i}M_{s(V)} =& \frac{\mathrm{i}}{(s-MV^2)} V_{VV}\overline{v}(p_b)\gamma^\rho.(-(A_R P_R) + A_L P_L)u(p_a)\varepsilon_\mu^\star(k_1)\varepsilon_\nu^\star(k_2) \\ & (\mathrm{g}^{\rho\sigma}(-\not{k}_1 - 2\not{k}_2)^\mu \mathrm{g}^{\nu\sigma} + \mathrm{g}^{\nu\sigma}(2\not{k}_1 + \not{k}_2)^\nu + \mathrm{g}^{\mu\nu}(\not{k}_1 - \not{k}_2)^\sigma))\end{aligned} \tag{C.10}$$

$$\begin{aligned}\mathrm{i}M_{t(\chi)} =& \frac{-\mathrm{i}}{s-m_\chi^2}\overline{v}(p_b)\gamma^\nu.(U_R * P_R + U_L * P_L)(m_\chi - \not{k}_2 + \not{p}_b) \\ & \gamma^\mu(V_R * P_R + V_L * P_L)u(p_a) * \varepsilon_\mu^\star(k_1)\varepsilon_\nu^\star(k_2))\end{aligned} \tag{C.11}$$

$$\begin{aligned}\mathrm{i}M_{u(\chi)} =& \frac{-\mathrm{i}}{(s-m_\chi^2)} * \overline{v}(p_b)\gamma^\mu.(S_R P_R + S_L P_L)(m_\chi - \not{k}_2 + \not{p}_a) \\ & \gamma^\nu(T_R P_R + T_L P_L)u(p_a)\varepsilon_\mu^\star(k_1)\varepsilon_\nu^\star(k_2))\end{aligned} \tag{C.12}$$

C.4. Ghosts

$$\mathrm{i}M_{s(h)} = \frac{-\mathrm{i}}{(s-m_i^2)} G_{GH}\overline{v}_{p_b}(C_L P_L + C_R P_R)u(p_a) \tag{C.13}$$

$$\mathrm{i}M_{s(h)} = \frac{-\mathrm{i}}{(s-m_V^2)} G_{GV}(k_1+k_2)^\nu\overline{v}_{p_b}\gamma^\mu(A_L P_L + A_R P_R)u(p_a) \tag{C.14}$$

D. Square amplitude

D.1. NeuNeu2HH

$$\left|M_{s(h)}\right|^2 = \frac{I_{LR}^2}{(s-m_i)^2}\left[(s-2m_{\tilde{\chi}^0}^2)(C_L C_L^\star + C_R C_R^\star) - 4m_{\tilde{\chi}^0}(C_L C_R^\star + C_R C_L^\star)\right]. \tag{D.1}$$

$$\begin{aligned}\left|M_{s(V)}\right|^2 = &-\frac{1}{(m_V^2-s)(s-m_V c^2)} J_{LR}\cdot J_{LR}^\star \\ &(A_L\cdot A_L^\star(m_1^2(m_3^2+3m_4^2-s+t-u)+m_2^2(3m_3^2+m_4^2-s-t+u) \\ &+m_3^4-2m_3^2m_4^2-2m_3^2s+m_4^4-2m_4^2s+s^2-t^2+2tu-u^2) \\ &+2m_1m_2A_R^\star(-2m_3^2-2m_4^2+s))+A_R(2m_1m_2A_L^\star(-2m_3^2-2m_4^2+s) \\ &+A_R^\star(m_1^2(m_3^2+3m_4^2-s+t-u)+m_2^2(3m_3^2+m_4^2-s-t+u)+m_3^4 \\ &-2m_3^2m_4^2-2m_3^2s+m_4^4-2m_4^2s+s^2-t^2+2tu-u^2)))\end{aligned} \tag{D.2}$$

$$\begin{aligned}\left|M_{t(\chi)}\right|^2 = &\frac{1}{(m_\chi^2-t)(t-m_\chi^2)} YR^\star(m_chiZ_R^\star(YR(m_\chi(m_1^2+m_2^2-s)Z_R \\ &-m_1(m_1^2-2m_2^2+m_4^2-t)Z_L)+m_2YL(Z_R(2m_1^2+m_2^2+m_4^2-s-u) \\ &+2m_1m_\chi Z_L))+Z_L^\star(m_2YL(m_\chi Z_L(2m_1^2+m_2^2+m_4^2-s-u) \\ &+2m_1(-m_1^2+m_2^2+t)Z_R)+YR(Z_L(-m_1^4+m_1^2(3m_2^2-3m_4^2+t+u) \\ &+m_2^4+m_2^2(m_4^2-s-2u)-m_4^4+m_4^2s+m_4^2t+m_4^2u-tu) \\ &-m_1m_\chi(m_1^2-2m_2^2+m_4^2-t)Z_R)))+YL^\star(m_\chi Z_L^\star(YL(m_\chi(m_1^2+m_2^2-s)Z_L \\ &-m_1(m_1^2-2m_2^2+m_4^2-t)Z_R)+m_2YR(Z_L(2m_1^2+m_2^2+m_4^2-s-u) \\ &+2m_1m_\chi Z_R))+Z_R^\star(m_2YR(m_\chi Z_R(2m_1^2+m_2^2+m_4^2-s-u) \\ &+2m_1(-m_1^2+m_2^2+t)Z_L)+YL(Z_R(-m_1^4+m_1^2(3m_2^2-3m_4^2+t+u)+m_2^4 \\ &+m_2^2(m_4^2-s-2u)-m_4^4+m_4^2s+m_4^2t+m_4^2u-tu) \\ &-m_1m_\chi(m_1^2-2m_2^2+m_4^2-t)Z_L))))\end{aligned} \tag{D.3}$$

$$
\begin{aligned}
\left|M_{u(\chi)}\right|^2 = \frac{1}{(m\chi^2-u)(u-m_\chi^2)})(W_R^\star(m_\chi XR^\star(W_R(m_1XL(2m_1^2+m_2^2+m_4^2-s-t) \\
+ m_\chi(m_1^2+m_2^2-s)XR) + m_2W_L((m_1^2-m_4^2+u)XR+2m_1m_qXL)) \\
+ XL^\star(m_2W_L(m_\chi(m_1^2-m_4^2+u)XL+2m_1uXR) \\
+ W_R(m_1m_\chi XR(2m_1^2+m_2^2+m_4^2-s-t) \\
+ XL(2m_1^4+m_1^2(m_2^2-m_4^2-s-t+u)-m_2^2m_4^2-m_4^4+m_4^2s+m_4^2t+m_4^2u-tu)))) \\
+ W_L^\star(m_\chi XL^\star(W_L(m_1XR(2m_1^2+m_2^2+m_4^2-s-t)+m_\chi(m_1^2+m_2^2-s)XL) \\
+ m_2W_R((m_1^2-m_4^2+u)XL+2m_1m_\chi XR)) \\
+ XR^\star(m_2W_R(m_\chi(m_1^2-m_4^2+u)XR+2m_1uXL) \\
+ W_L(m_1m_\chi XL(2m_1^2+m_2^2+m_4^2-s-t) \\
+ XR(2m_1^4+m_1^2(m_2^2-m_4^2-s-t+u) \\
- m_2^2m_4^2-m_4^4+m_4^2s+m_4^2t+m_4^2u-tu)))))
\end{aligned}
\tag{D.4}
$$

$$
\begin{aligned}
\left|M_{s(h)}M_{s(V)}^\star\right| = \frac{1}{(m_h^2-s)(s-m_V^2)})I_{LR}J_{LR}^\star \\
(C_L(m_2A_L^\star(-m_3^2+m_4^2+t-u) \\
+ m_1A_R^\star(-m_1^2+m_2^2+m_3^2-m_4^2+t-u)) \\
+ C_R(m_1A_L^\star(-m_1^2+m_2^2+m_3^2-m_4^2+t-u) \\
+ m_2A_R^\star(-m_3^2+m_4^2+t-u)))
\end{aligned}
\tag{D.5}
$$

$$
\begin{aligned}
\left|M_{s(h)}M_{t(\chi)}^\star\right| = \frac{1}{(m_i^2-s)(m_\chi^2-t)})I_{LR} \\
(C_L(YL^\star(m_1(m_1^2-2m_2^2+m_4^2-t)Z_R^\star \\
- m_\chi(m_1^2+m_2^2-s)Z_L^\star) \\
- m_2YR^\star((2m_1^2+m_2^2+m_4^2-s-u)Z_L^\star+2m_1m_\chi Z_R^\star)) \\
+ C_R(YR^\star(m_1(m_1^2-2m_2^2+m_4^2-t)Z_L^\star-m_\chi(m_1^2+m_2^2-s)Z_R^\star) \\
- m_2YL^\star((2m_1^2+m_2^2+m_4^2-s-u)Z_R^\star+2m_1m_\chi Z_L^\star)))
\end{aligned}
\tag{D.6}
$$

$$
\begin{aligned}
\left|M_{s(h)}M_{u(\chi)}^\star\right| = -(1/((m_i^2-s)(m_\chi^2-u)))I_{LR} \\
(C_L(W_L^\star(m_1(2m_1^2+m_2^2+m_4^2-s-t)XR^\star+m_\chi(m_1^2+m_2^2-s)XL^\star) \\
+ m_2W_R^\star((m_1^2-m_4^2+u)XL^\star+2m_1m_\chi XR^\star)) \\
+ C_R(W_R^\star(m_1(2m_1^2+m_2^2+m_4^2-s-t)XL^\star \\
+ m_\chi(m_1^2+m_2^2-s)XR^\star)+m_2W_L^\star((m_1^2-m_4^2+u)XR^\star \\
+ 2m_1m_\chi XL^\star)))
\end{aligned}
\tag{D.7}
$$

$$\begin{aligned}\left|M_{s(V)}M^{\star}_{t(\chi)}\right| = &-(1/(2(m_\chi^2-t)(m_V^2-s)))J_{LR}\\
&(A_L(2m_2YL^{\star}(m_1Z_R^{\star}(-m_1^2+m_2^2+2m_3^2+2m_4^2-s+t-u)\\
&+m_\chi(-m_3^2+m_4^2+t-u)Z_L^{\star})+YR^{\star}(2m_1m_\chi Z_R^{\star}(-m_1^2+m_2^2+m_3^2-m_4^2+t-u)\\
&+Z_L^{\star}(-m_1^4+m_1^2(m_2^2+m_3^2-6m_4^2+s+u)\\
&+m_2^2(-3m_3^2+s+2t-3u)\\
&+2m_3^2m_4^2+m_3^2s-m_3^2t-m_3^2u-2m_4^4+3m_4^2s\\
&+m_4^2t+m_4^2u-s^2+t^2-2tu+u^2)))\\
&+A_R(2m_2YR^{\star}(m_1Z_L^{\star}(-m_1^2+m_2^2+2m_3^2+2m_4^2-s+t-u)\\
&+m_\chi(-m_3^2+m_4^2+t-u)Z_R^{\star})+YL^{\star}(Z_R^{\star}(-m_1^4+m_1^2(m_2^2+m_3^2-6m_4^2+s+u)\\
&+m_2^2(-3m_3^2+s+2t-3u)+2m_3^2m_4^2+m_3^2s-m_3^2t-m_3^2u-2m_4^4+3m_4^2s\\
&+m_4^2t+m_4^2u-s^2+t^2-2tu+u^2)-2m_1m_\chi Z_L^{\star}(m_1^2-m_2^2-m_3^2+m_4^2-t+u))))\end{aligned} \tag{D.8}$$

$$\begin{aligned}\left|M_{s(V)}M^{\star}_{u(\chi)}\right| = &-(1/(2(m_\chi^2-u)(m_V^2-s)))J_{LR}\\
&(A_L(W_R^{\star}(2m_1m_\chi XR^{\star}(-m_1^2+m_2^2+m_3^2-m_4^2+t-u)\\
&-XL^{\star}(m_1^4-m_1^2(m_2^2+m_3^2+4m_4^2-s+2t-3u)\\
&-m_2^2(m_3^2+2m_4^2-s+u)+2m_3^2m_4^2+m_3^2s-m_3^2t-m_3^2u-2m_4^4\\
&+3m_4^2s+m_4^2t+m_4^2u-s^2+t^2-2tu+u^2))\\
&-2m_2W_L^{\star}(m_1(2m_3^2+2m_4^2-s-t+u)XR^{\star}+m_\chi(m_3^2-m_4^2-t+u)XL^{\star}))\\
&+A_R(W_L^{\star}(-2m_1m_\chi XL^{\star}(m_1^2-m_2^2-m_3^2+m_4^2-t+u)\\
&-XR^{\star}(m_1^4-m_1^2(m_2^2+m_3^2+4m_4^2-s+2t-3u)-m_2^2(m_3^2+2m_4^2-s+u)\\
&+2m_3^2m_4^2+m_3^2s-m_3^2t-m_3^2u-2m_4^4\\
&+3m_4^2s+m_4^2t+m_4^2u-s^2+t^2-2tu+u^2))\\
&-2m_2W_R^{\star}(m_1(2m_3^2+2m_4^2-s-t+u)XL^{\star}\\
&+m_\chi(m_3^2-m_4^2-t+u)XR^{\star})))\end{aligned} \tag{D.9}$$

$$
\begin{aligned}
\left|M_{t(\chi)}M^\star_{u(\chi)}\right|^2 = {} & (1/((m_\chi^2 - u)(m_\chi^2 - t))) \\
& (W_L^\star(m_\chi XL^\star(YL(m_1(m_1^2 - 2m_2^2 + m_4^2 - t)Z_R - m_\chi(m_1^2 + m_2^2 - s)Z_L) \\
& - m_2 YR(Z_L(2m_1^2 + m_2^2 + m_4^2 - s - u) + 2m_1 m_\chi Z_R)) \\
& + XR^\star(m_2 YR(m_1 Z_L(-3m_1^2 - m_2^2 + s + t + u) \\
& - m_\chi(m_1^2 - m_4^2 + u)Z_R) - YL(m_1 m_\chi Z_L(2m_1^2 + m_2^2 + m_4^2 - s - t) \\
& + Z_R(m_1^2(m_2^2 + 2m_4^2 - u) + u(m_2^2 + t) + m_4^4 - m_4^2(s + t + u))))) \\
& - W_R^\star(m_\chi XR^\star(YR(m_\chi(m_1^2 + m_2^2 - s)Z_R \\
& - m_1(m_1^2 - 2m_2^2 + m_4^2 - t)Z_L) + m_2 YL(Z_R(2m_1^2 + m_2^2 + m_4^2 - s - u) \\
& + 2m_1 m_\chi Z_L)) + XL^\star(m_2 YL(m_1 Z_R(3m_1^2 + m_2^2 - s - t - u) \\
& + m_\chi(m_1^2 - m_4^2 + u)Z_L) + YR(m_1 m_\chi Z_R(2m_1^2 + m_2^2 + m_4^2 - s - t) \\
& + Z_L(m_1^2(m_2^2 + 2m_4^2 - u) + u(m_2^2 + t) + m_4^4 - m_4^2(s + t + u))))))
\end{aligned}
\tag{D.10}
$$

D.2. NeuNeu2HV

$$
\begin{aligned}
\left|M_{s(h)}\right|^2 = {} & -\frac{1}{(m_i^2 - s)(s - m_j^2)})J_{LR}J_{LR}c \\
& (2m_3^2 - m_4^2 + 2s)(C_L(C_L^\star(m_1^2 + m_2^2 - s) + 2C_R^\star m_1 m_2) \\
& + C_R(2C_L^\star m_1 m_2 + C_R^\star(m_1^2 + m_2^2 - s)))
\end{aligned}
\tag{D.11}
$$

$$
\begin{aligned}
\left|M_{s(V)}\right|^2 = {} & (2L_{LR}L_{LR}^\star \\
& (A_L(A_L c(m_1^2 + m_2^2 - s) - 4A_R c m_1 m_2) + A_R(A_R c(m_1^2 + m_2^2 - s) \\
& - 4A_L c m_1 m_2)))/((m_V^2 - s)(s - m_V c^2))
\end{aligned}
\tag{D.12}
$$

$$
\begin{aligned}
\left|M_{t(\chi)}\right|^2 = {} & (1/((m_\chi^2 - t)(t - m_\chi^2))) \\
& 2(m_1^4(U_L U_L^\star Z_R Z_R^\star + U_R U_R^\star Z_L Z_L^\star) + m_1^3(m_\chi U_L U_L^\star Z_L^\star Z_R \\
& + m_\chi U_R U_R^\star Z_L Z_R^\star + m_\chi U_L U_L^\star Z_L Z_R^\star \\
& + m_\chi U_R U_R^\star Z_L^\star Z_R) + m_1^2(2m_2^2(U_L U_L^\star Z_R Z_R^\star + U_R U_R^\star Z_L Z_L^\star) \\
& + m_\chi(m_\chi(U_L U_L^\star Z_L Z_L^\star + U_R U_R^\star Z_R Z_R^\star) - 2m_2(U_L U_R^\star Z_R Z_R^\star \\
& + U_L^\star U_R Z_L Z_L^\star)) - 2m_2 m_\chi(U_L U_R^\star Z_L Z_L^\star \\
& + U_L^\star U_R Z_R Z_R^\star) - (s+u)(U_L U_L^\star Z_R Z_R^\star \\
& + U_R U_R^\star Z_L Z_L^\star)) + m_1(2m_2^2(m_\chi U_L U_L^\star Z_L^\star Z_R \\
& + m_\chi U_R U_R^\star Z_L Z_R^\star + m_\chi U_L U_L^\star Z_L Z_R^\star \\
& + m_\chi U_R U_R^\star Z_L^\star Z_R) - 4m_2(m_\chi^2 U_L U_R^\star Z_L Z_R^\star + m_\chi m_\chi U_L^\star U_R Z_L^\star Z_R \\
& + t U_L U_R^\star Z_L^\star Z_R + t U_L^\star U_R Z_L Z_R^\star) + (m_3^2 - s - u)(m_\chi U_L U_L^\star Z_L^\star Z_R \\
& + m_\chi U_R U_R^\star Z_L Z_R^\star + m_\chi U_L U_L^\star Z_L Z_R^\star + m_\chi U_R U_R^\star Z_L^\star Z_R)) \\
& + m_2^2(m_\chi m_\chi(U_L U_L^\star Z_L Z_L^\star \\
& + U_R U_R^\star Z_R Z_R^\star) - (2m_3^2 - t)(U_L U_L^\star Z_R Z_R^\star + U_R U_R^\star Z_L Z_L^\star)) \\
& + 2m_2(m_3^2 - t)(m_\chi U_L U_R^\star Z_R Z_R^\star + m_\chi U_L^\star U_R Z_L Z_L^\star \\
& + m_\chi U_L U_R^\star Z_L Z_L^\star + m_\chi U_L^\star U_R Z_R Z_R^\star) \\
& - m_3^4 U_L U_L^\star Z_R Z_R^\star - m_3^4 U_R U_R^\star Z_L Z_L^\star + m_3^2 s U_L U_L^\star Z_R Z_R^\star \\
& + m_3^2 s U_R U_R^\star Z_L Z_L^\star + m_3^2 t U_L U_L^\star Z_R Z_R^\star + m_3^2 t U_R U_R^\star Z_L Z_L^\star \\
& + m_3^2 u U_L U_L^\star Z_R Z_R^\star + m_3^2 u U_R U_R^\star Z_L Z_L^\star \\
& - m_\chi m_\chi s U_L U_L^\star Z_L Z_L^\star - m_\chi m_\chi s U_R U_R^\star Z_R Z_R^\star \\
& - t u U_L U_L^\star Z_R Z_R^\star - t u U_R U_R^\star Z_L Z_L^\star)
\end{aligned}
\tag{D.13}
$$

$$
\begin{aligned}
\left|M_{u(\chi)}\right|^2 = &-(1/((m_\chi^2-t)(m_\chi^2-u))) \\
&2(-2m_1^4(T_LU_R^\star WLZ_L^\star + T_RU_L^\star WRZ_R^\star) \\
&+ m_1^3(m_\chi(T_LU_L^\star WRZ_R^\star + T_RU_R^\star WLZ_L^\star) - 4m_\chi(T_LU_R^\star WLZ_R^\star \\
&+ T_RU_L^\star WRZ_L^\star)) + m_1^2(m_2^2(-(T_LU_R^\star WLZ_L^\star \\
&+ T_RU_L^\star WRZ_R^\star)) + m_2(m_\chi(T_LU_L^\star WLZ_L^\star + T_RU_R^\star WRZ_R^\star) \\
&- 2m_\chi(T_LU_R^\star WRZ_L^\star + T_RU_L^\star WLZ_R^\star)) + 2m_3^2(T_LU_R^\star WLZ_L^\star \\
&+ T_RU_L^\star WRZ_R^\star) - m_4^2T_LU_R^\star WLZ_L^\star - m_4^2T_RU_L^\star WRZ_R^\star + m_\chi m_\chi T_LU_L^\star WRZ_L^\star \\
&+ m_\chi m_\chi T_RU_R^\star WLZ_R^\star + sT_LU_R^\star WLZ_L^\star + sT_RU_L^\star WRZ_R^\star \\
&- tT_LU_R^\star WLZ_L^\star - tT_RU_L^\star WRZ_R^\star) + m_1(2m_2^2(m_\chi(T_LU_L^\star WRZ_R^\star \\
&+ T_RU_R^\star WLZ_L^\star) - m_\chi(T_LU_R^\star WLZ_R^\star + T_RU_L^\star WRZ_L^\star)) \\
&+ m_2(-(2m_3^2+2m_4^2-s-t-u)(T_LU_L^\star WLZ_R^\star + tRU_R^\star WRZ_L^\star) \\
&- 4m_\chi m_\chi(T_LU_R^\star WRZ_R^\star + T_RU_L^\star WLZ_L^\star)) \\
&+ m_3^2m_\chi(T_LU_L^\star WRZ_R^\star + T_RU_R^\star WLZ_L^\star) \\
&- 2m_4^2m_\chi T_LU_R^\star WLZ_R^\star - 2m_4^2m_\chi T_RU_L^\star WRZ_L^\star + 2m_\chi sT_LU_R^\star WLZ_R^\star \\
&+ 2m_\chi sT_RU_L^\star WRZ_L^\star + 2m_\chi tT_LU_R^\star WLZ_R^\star \\
&+ 2m_\chi tT_RU_L^\star WRZ_L^\star - m_\chi sT_LU_L^\star WRZ_R^\star - m_\chi sT_RU_R^\star WLZ_L^\star \\
&- m_\chi T_LuU_L^\star WRZ_R^\star - m_\chi T_RuU_R^\star WLZ_L^\star) + m_2^2(m_3^2(T_LU_R^\star WLZ_L^\star + T_RU_L^\star WRZ_R^\star) \\
&+ m_\chi m_\chi(T_LU_L^\star WRZ_L^\star + T_RU_R^\star WLZ_R^\star) - t(T_LU_R^\star WLZ_L^\star + T_RU_L^\star WRZ_R^\star)) \\
&+ m_2(2m_\chi(m_3^2-t)(T_LU_R^\star WRZ_L^\star + T_RU_L^\star WLZ_R^\star) + m_4^2(-m_\chi)(T_LU_L^\star WLZ_L^\star \\
&+ T_RU_R^\star WRZ_R^\star) + m_\chi u(T_LU_L^\star WLZ_L^\star + T_RU_R^\star WRZ_R^\star)) + m_3^2m_4^2T_LU_R^\star WLZ_L^\star \\
&+ m_3^2m_4^2T_RU_L^\star WRZ_R^\star - m_3^2sT_LU_R^\star WLZ_L^\star - m_3^2sT_RU_L^\star WRZ_R^\star \\
&- m_3^2tT_LU_R^\star WLZ_L^\star - m_3^2tT_RU_L^\star WRZ_R^\star - m_4^2tT_LU_R^\star WLZ_L^\star - m_4^2tT_RU_L^\star WRZ_R^\star \\
&- m_\chi m_\chi sT_LU_L^\star WRZ_L^\star - m_\chi m_\chi sT_RU_R^\star WLZ_R^\star + stT_LU_R^\star WLZ_L^\star + stT_RU_L^\star WRZ_R^\star \\
&+ t^2T_LU_R^\star WLZ_L^\star + t^2T_RU_L^\star WRZ_R^\star)
\end{aligned}
\tag{D.14}
$$

$$
\begin{aligned}
\left|M_{s(h)}M_{s(V)}^\star\right| = &-\frac{1}{(m_i^2-s)(s-m_Vc^2)})J_{LR}L_{LR}^\star \\
&(A_Lc(C_Lm_2(-3m_1^2-2m_3^2-m_4^2+2t+u) \\
&+ C_Rm_1(m_1^2+2m_2^2+2m_3^2+m_4^2-t-2u)) \\
&+ A_Rc(C_Lm_1(m_1^2+2m_2^2+2m_3^2+m_4^2-t-2u) \\
&+ C_Rm_2(-3m_1^2-2m_3^2-m_4^2+2t+u)))
\end{aligned}
\tag{D.15}
$$

$$
\begin{aligned}
\left|M_{s(h)}M^{\star}_{t(\chi)}\right| = &-\frac{1}{2(m_i^2-s)(m_\chi^2-t)} \\
& J_{LR}(C_L(m_1^4U_R^{\star}Z_L^{\star}+m_1^3(2m_\chi U_R^{\star}Z_R^{\star}-6m_2U_L^{\star}Z_R^{\star}) \\
& + m_1^2Z_L^{\star}(5m_2^2U_R^{\star}-6m_2m_\chi U_L^{\star}+U_R^{\star}(7m_3^2+s-5u)) \\
& + 2m_1Z_R^{\star}(2m_2^2m_\chi U_R^{\star}+m_2U_L^{\star}(m_3^2-2m_4^2+s+2t+u) \\
& + m_\chi U_R^{\star}(2m_3^2+m_4^2-t-2u))+Z_L^{\star}(m_2^2U_R^{\star}(3m_3^2+s-u) \\
& + 2m_2m_\chi U_L^{\star}(-2m_3^2-m_4^2+2t+u)-U_R^{\star}(m_3^2(3s-t+u) \\
& - m_4^2(s+t-u)+s^2+t^2-u^2)))+C_R(m_1^4U_L^{\star}Z_R^{\star} \\
& + 2m_1^3Z_L^{\star}(m_\chi U_L^{\star}-3m_2U_R^{\star})+m_1^2Z_R^{\star}(5m_2^2U_L^{\star} \\
& - 6m_2m_\chi U_R^{\star}+U_L^{\star}(7m_3^2+s-5u))+2m_1Z_L^{\star}(2m_2^2m_\chi U_L^{\star} \\
& + m_2U_R^{\star}(m_3^2-2m_4^2+s+2t+u)+m_\chi U_L^{\star}(2m_3^2+m_4^2-t-2u)) \\
& + Z_R^{\star}(m_2^2U_L^{\star}(3m_3^2+s-u)+2m_2m_\chi U_R^{\star}(-2m_3^2-m_4^2+2t+u) \\
& - U_L^{\star}(m_3^2(3s-t+u)-m_4^2(s+t-u)+s^2+t^2-u^2))))
\end{aligned}
\tag{D.16}
$$

$$
\begin{aligned}
\left|M_{s(h)}M^{\star}_{u(\chi)}\right| = &-\frac{1}{(2(m_i^2-s)(m_\chi^2-t)}) \\
& J_{LR}(C_L(m_1^4U_R^{\star}Z_L^{\star}+m_1^3(2m_\chi U_R^{\star}Z_R^{\star}-6m_2U_L^{\star}Z_R^{\star}) \\
& + m_1^2Z_L^{\star}(5m_2^2U_R^{\star}-6m_2m_\chi U_L^{\star}+U_R^{\star}(7m_3^2+s-5u)) \\
& + 2m_1Z_R^{\star}(2m_2^2m_\chi U_R^{\star}+m_2U_L^{\star}(m_3^2-2m_4^2+s+2t+u) \\
& + m_\chi U_R^{\star}(2m_3^2+m_4^2-t-2u))+Z_L^{\star}(m_2^2U_R^{\star}(3m_3^2+s-u) \\
& + 2m_2m_\chi U_L^{\star}(-2m_3^2-m_4^2+2t+u) \\
& - U_R^{\star}(m_3^2(3s-t+u)-m_4^2(s+t-u)+s^2+t^2-u^2))) \\
& + C_R(m_1^4U_L^{\star}Z_R^{\star}+2m_1^3Z_L^{\star}(m_\chi U_L^{\star}-3m_2U_R^{\star}) \\
& + m_1^2Z_R^{\star}(5m_2^2U_L^{\star}-6m_2m_\chi U_R^{\star}+U_L^{\star}(7m_3^2+s-5u)) \\
& + 2m_1Z_L^{\star}(2m_2^2m_\chi U_L^{\star}+m_2U_R^{\star}(m_3^2-2m_4^2+s+2t+u) \\
& + m_\chi U_L^{\star}(2m_3^2+m_4^2-t-2u))+Z_R^{\star}(m_2^2U_L^{\star}(3m_3^2+s-u) \\
& + 2m_2m_\chi U_R^{\star}(-2m_3^2-m_4^2+2t+u)-U_L^{\star}(m_3^2(3s-t+u) \\
& - m_4^2(s+t-u)+s^2+t^2-u^2))))
\end{aligned}
\tag{D.17}
$$

$$
\begin{aligned}
\left|M_{s(V)}M^{\star}_{t(\chi)}\right| = &(1/((m_\chi^2-t)(m_V^2-s)))2L_{LR} \\
& (A_L(m_1^3U_L^{\star}Z_R^{\star}+m_1^2Z_L^{\star}(m_\chi U_L^{\star}-2m_2U_R^{\star}) \\
& + m_1Z_R^{\star}(2m_2^2U_L^{\star}-4m_2m_\chi U_R^{\star}+U_L^{\star}(m_3^2-s-u)) \\
& + Z_L^{\star}(m_2^2m_\chi U_L^{\star}+2m_2U_R^{\star}(m_3^2-t)-m_\chi sU_L^{\star})) \\
& + A_R(m_1^3U_R^{\star}Z_L^{\star}+m_1^2(m_\chi U_R^{\star}Z_R^{\star}-2m_2U_L^{\star}Z_R^{\star}) \\
& + m_1Z_L^{\star}(2m_2^2U_R^{\star}-4m_2m_\chi U_L^{\star}+U_R^{\star}(m_3^2-s-u)) \\
& + Z_R^{\star}(m_2^2m_\chi U_R^{\star}+2m_2U_L^{\star}(m_3^2-t)-m_\chi sU_R^{\star})))
\end{aligned}
\tag{D.18}
$$

$$
\begin{aligned}
\left|M_{s(V)}M^\star_{u(\chi)}\right| = &\frac{1}{(m_\chi^2-t)(m_V^2-s)})2L_{LR} \\
&(A_L(m_1^3U_L^\star Z_R^\star + m_1^2 Z_L^\star(m_\chi U_L^\star - 2m_2U_R^\star) \\
&+ m_1 Z_R^\star(2m_2^2U_L^\star - 4m_2m_\chi U_R^\star + U_L^\star(m_3^2-s-u)) \\
&+ Z_L^\star(m_2^2m_\chi U_L^\star + 2m_2U_R^\star(m_3^2-t) - m_\chi sU_L^\star)) \\
&+ m_1 Z_L^\star(2m_2^2U_R^\star - 4m_2m_\chi U_L^\star + U_R^\star(m_3^2-s-u)) \\
&+ Z_R^\star(m_2^2m_\chi U_R^\star + 2m_2U_L^\star(m_3^2-t) - m_\chi sU_R^\star)))
\end{aligned} \tag{D.19}
$$

$$
\begin{aligned}
\left|M_{t(\chi)}M^\star_{u(\chi)}\right|^2 = &\frac{1}{(m_\chi^2-t)(t-m_\chi^2)} \\
&2(m_1^4(U_LU_L^\star Z_RZ_R^\star + U_RU_R^\star Z_LZ_L^\star) \\
&+ m_1^3(m_\chi U_LU_L^\star Z_L^\star Z_R + m_\chi U_RU_R^\star Z_LZ_R^\star \\
&+ m_\chi U_LU_L^\star Z_LZ_R^\star + m_\chi U_RU_R^\star Z_L^\star Z_R) \\
&+ m_1^2(2m_2^2(U_LU_L^\star Z_RZ_R^\star + U_RU_R^\star Z_LZ_L^\star) \\
&+ m_\chi(m_\chi(U_LU_L^\star Z_LZ_L^\star + U_RU_R^\star Z_RZ_R^\star) \\
&- 2m_2(U_LU_R^\star Z_RZ_R^\star + U_L^\star U_RZ_LZ_L^\star)) - 2m_2m_\chi(U_LU_R^\star Z_LZ_L^\star \\
&+ U_L^\star U_RZ_RZ_R^\star) - (s+u)(U_LU_L^\star Z_RZ_R^\star + U_RU_R^\star Z_LZ_L^\star)) \\
&+ m_1(2m_2^2(m_\chi U_LU_L^\star Z_L^\star Z_R + m_\chi U_RU_R^\star Z_LZ_R^\star \\
&+ m_\chi U_LU_L^\star Z_LZ_R^\star + m_\chi U_RU_R^\star Z_L^\star Z_R) \\
&- 4m_2(m_\chi m_\chi U_LU_R^\star Z_LZ_R^\star + m_\chi m_\chi U_L^\star U_RZ_L^\star Z_R \\
&+ tU_LU_R^\star Z_L^\star Z_R + tU_L^\star U_RZ_LZ_R^\star) \\
&+ (m_3^2-s-u)(m_\chi U_LU_L^\star Z_L^\star Z_R + m_\chi U_RU_R^\star Z_LZ_R^\star \\
&+ m_\chi U_LU_L^\star Z_LZ_R^\star + m_\chi U_RU_R^\star Z_L^\star Z_R)) \\
&+ m_2^2(m_\chi m_\chi(U_LU_L^\star Z_LZ_L^\star + U_RU_R^\star Z_RZ_R^\star) \\
&- (2m_3^2-t)(U_LU_L^\star Z_RZ_R^\star + U_RU_R^\star Z_LZ_L^\star)) \\
&+ 2m_2(m_3^2-t)(m_\chi U_LU_R^\star Z_RZ_R^\star + m_\chi U_L^\star U_RZ_LZ_L^\star \\
&+ m_\chi U_LU_R^\star Z_LZ_L^\star + m_\chi U_L^\star U_RZ_RZ_R^\star) \\
&- m_3^4U_LU_L^\star Z_RZ_R^\star - m_3^4U_RU_R^\star Z_LZ_L^\star \\
&+ m_3^2sU_LU_L^\star Z_RZ_R^\star + m_3^2sU_RU_R^\star Z_LZ_L^\star \\
&+ m_3^2tU_LU_L^\star Z_RZ_R^\star + m_3^2tU_RU_R^\star Z_LZ_L^\star \\
&+ m_3^2uU_LU_L^\star Z_RZ_R^\star + m_3^2uU_RU_R^\star Z_LZ_L^\star \\
&- m_\chi m_\chi sU_LU_L^\star Z_LZ_L^\star - m_\chi m_\chi sU_RU_R^\star Z_RZ_R^\star \\
&- tuU_LU_L^\star Z_RZ_R^\star - tuU_RU_R^\star Z_LZ_L^\star)
\end{aligned} \tag{D.20}
$$

D.3. NeuNeu2VV

$$
\begin{aligned}
\left|M_{s(h)}\right|^2 = & \frac{1}{((m_i^2 - s)(s - m_j^2))}(4L_{LR}L_{LR}^\star \\
& (C_L(C_L^\star(m_1^2 + m_2^2 - s) + 2C_R^\star m_1 m_2) \\
& + C_R(2C_L^\star m_1 m_2 + C_R^\star(m_1^2 + m_2^2 - s))))
\end{aligned} \tag{D.21}
$$

$$
\begin{aligned}
\left|M_{s(V)}\right|^2 = & \frac{1}{(M_V^2 - s)^2}V_{VV}^2 \\
& (A_L(A_L^\star(-9m_1^4 + m_1^2(-9m_2^2 - 5m_3^2 + 8m_4^2 - 3s + 20t + 7u) \\
& + m_2^2(17m_3^2 + 4m_4^2 - 3s - 2t + 11u) + 2m_3^4 - 22m_3^2m_4^2 - 15m_3^2 s \\
& + 9m_3^2 t + 9m_3^2 u + 2m_4^4 - 15m_4^2 s + 9m_1 + 9m_4^2 t + 9m_4^2 u + 3s^2 - 11t^2 \\
& + 4tu - 11u^2) + 2A_R c m_1 m_2(17m_3^2 + 17m_4^2 + 5s)) \\
& + A_R(2A_L c m_1 m_2(17m_3^2 + 17m_4^2 + 5s) \\
& + A_R^\star(-9m_1^4 + m_1^2(-9m_2^2 - 5m_3^2 + 8m_4^2 - 3s + 20t + 7u) \\
& + m_2^2(17m_3^2 + 4m_4^2 - 3s - 2t + 11u) + 2m_3^4 - 22m_3^2m_4^2 - 15m_3^2 s \\
& + 9m_3^2 t + 9m_3^2 u + 2m_4^4 - 15m_4^2 s + 9m_4^2 t \\
& + 9m_4^2 u + 3s^2 - 11t^2 + 4tu - 11u^2)))
\end{aligned} \tag{D.22}
$$

$$
\begin{aligned}
\left|M_{t(\chi)}\right|^2 = &-\frac{1}{(m_\chi^2 - s)(s - m_\chi^2)} \\
&4(m_1^4(U_L U_L^\star V_L V_L^\star + U_R U_R^\star V_R V_R^\star) \\
&+ 2m_1^3(4m_2 U_L U_R^\star V_L V_R^\star + 4m_2 U_L^\star U_R V_L^\star V_R \\
&+ m_\chi U_L U_L^\star V_L V_R^\star + m_\chi U_R U_R^\star V_L^\star V_R \\
&+ m_\chi U_L U_L^\star V_L^\star V_R + m_\chi U_R U_R^\star V_L V_R^\star) \\
&- m_1^2(3m_2^2(U_L U_L^\star V_L V_L^\star + U_R U_R^\star V_R V_R^\star) \\
&+ 4m_2(m_\chi U_L U_R^\star V_L V_L^\star + m_\chi U_L^\star U_R V_R V_R^\star \\
&+ m_\chi U_L U_R^\star V_R V_R^\star + m_\chi U_L^\star U_R V_L V_L^\star) \\
&- 3m_4^2(U_L U_L^\star V_L V_L^\star + U_R U_R^\star V_R V_R^\star) \\
&+ m_\chi m_\chi U_L U_L^\star V_R V_R^\star + m_\chi m_\chi U_R U_R^\star V_L V_L^\star \\
&+ tU_L U_L^\star V_L V_L^\star + tU_R U_R^\star V_R V_R^\star + uU_L U_L^\star V_L V_L^\star \\
&+ uU_R U_R^\star V_R V_R^\star) - 2m_1(4m_2^3(U_L U_R^\star V_L V_R^\star \\
&+ U_L^\star U_R V_L^\star V_R) + 2m_2^2(m_\chi U_L U_L^\star V_L V_R^\star \\
&+ m_\chi U_R U_R^\star V_L^\star V_R + m_\chi U_L U_L^\star V_L^\star V_R \\
&+ m_\chi U_R U_R^\star V_L V_R^\star) + 4m_2(m_\chi m_\chi U_L U_R^\star V_L^\star V_R \\
&+ m_\chi m_\chi U_L^\star U_R V_L V_R^\star + tU_L U_R^\star V_L V_R^\star \\
&+ tU_L^\star U_R V_L^\star V_R) - (m_4^2 - t)(m_\chi U_L U_L^\star V_L V_R^\star \\
&+ m_\chi U_R U_R^\star V_L^\star V_R + m_\chi U_L U_L^\star V_L^\star V_R \\
&+ m_\chi U_R U_R^\star V_L V_R^\star)) - m_2^4(U_L U_L^\star V_L V_L^\star \\
&+ U_R U_R^\star V_R V_R^\star) - 2m_2^3(m_\chi U_L U_R^\star V_L V_L^\star \\
&+ m_\chi U_L^\star U_R V_R V_R^\star + m_\chi U_L U_R^\star V_R V_R^\star \\
&+ m_\chi U_L^\star U_R V_L V_L^\star) - m_2^2(m_4^2(U_L U_L^\star V_L V_L^\star \\
&+ U_R U_R^\star V_R V_R^\star) + m_\chi m_\chi U_L U_L^\star V_R V_R^\star \\
&+ m_\chi m_\chi U_R U_R^\star V_L V_L^\star - s(U_L U_L^\star V_L V_L^\star \\
&+ U_R U_R^\star V_R V_R^\star) - 2uU_L U_L^\star V_L V_L^\star - 2uU_R U_R^\star V_R V_R^\star) \\
&- 2m_2(m_4^2 - s - u)(m_\chi U_L U_R^\star V_L V_L^\star + m_\chi U_L^\star U_R V_R V_R^\star \\
&+ m_\chi U_L U_R^\star V_R V_R^\star + m_\chi U_L^\star U_R V_L V_L^\star) \\
&+ m_4^4 U_L U_L^\star V_L V_L^\star + m_4^4 U_R U_R^\star V_R V_R^\star \\
&- m_4^2 s U_L U_L^\star V_L V_L^\star - m_4^2 s U_R U_R^\star V_R V_R^\star \\
&- m_4^2 t U_L U_L^\star V_L V_L^\star - m_4^2 t U_R U_R^\star V_R V_R^\star \\
&- m_4^2 u U_L U_L^\star V_L V_L^\star - m_4^2 u U_R U_R^\star V_R V_R^\star \\
&+ m_\chi m_\chi s U_L U_L^\star V_R V_R^\star + m_\chi m_\chi s U_R U_R^\star V_L V_L^\star \\
&+ tu U_L U_L^\star V_L V_L^\star + tu U_R U_R^\star V_R V_R^\star)
\end{aligned}
\tag{D.23}
$$

$$
\begin{aligned}
\left|M_{u(\chi)}\right|^2 = -&\frac{1}{(m_\chi^2-s)(s-m_\chi^2)} \\
&4(-2m_1^4(S_LS_L^\star T_LT_L^\star + S_RS_R^\star T_RT_R^\star) + 4m_1^3(m_\chi S_LS_L^\star T_LT_R^\star \\
&+ m_\chi S_RS_R^\star T_L^\star T_R + m_\chi S_LS_L^\star T_L^\star T_R + m_\chi S_RS_R^\star T_LT_R^\star) \\
&+ m_1^2(m_2^2(-(S_LS_L^\star T_LT_L^\star + S_RS_R^\star T_RT_R^\star)) + 2m_2(m_\chi S_LS_R^\star T_LT_L^\star \\
&+ m_\chi S_L^\star S_RT_RT_R^\star + m_\chi S_LS_R^\star T_RT_R^\star + m_\chi S_L^\star S_RT_LT_L^\star) \\
&+ m_4^2(S_LS_L^\star T_LT_L^\star + S_RS_R^\star T_RT_R^\star) - m_\chi m_\chi S_LS_L^\star T_RT_R^\star \\
&- m_\chi m_\chi S_RS_R^\star T_LT_L^\star + sS_LS_L^\star T_LT_L^\star + sS_RS_R^\star T_RT_R^\star \\
&+ S_LS_L^\star tT_LT_L^\star - S_LS_L^\star T_LT_L^\star u + S_RS_R^\star tT_RT_R^\star - S_RS_R^\star T_RT_R^\star u) \\
&+ 2m_1(m_2^2(m_\chi S_LS_L^\star T_LT_R^\star + m_\chi SRS_R^\star T_L^\star T_R + m_\chi S_LS_L^\star T_L^\star T_R \\
&+ m_\chi S_RS_R^\star T_LT_R^\star) - 4m_2(m_\chi m_\chi S_LS_R^\star T_L^\star T_R \\
&+ m_\chi m_\chi S_L^\star S_RT_LT_R^\star + S_LS_R^\star T_LT_R^\star u + S_L^\star S_RT_L^\star T_Ru) \\
&+ (m_4^2-s-t)(m_\chi S_LS_L^\star T_LT_R^\star + m_\chi S_RS_R^\star T_L^\star T_R + m_\chi S_LS_L^\star T_L^\star T_R \\
&+ m_\chi S_RS_R^\star T_LT_R^\star)) + m_2^2(m_4^2(S_LS_L^\star T_LT_L^\star \\
&+ S_RS_R^\star T_RT_R^\star) - m_\chi m_\chi(S_LS_L^\star T_RT_R^\star + S_RS_R^\star T_LT_L^\star)) \\
&- 2m_2(m_4^2-u)(m_\chi S_LS_R^\star T_LT_L^\star + m_\chi S_L^\star S_RT_RT_R^\star \\
&+ m_\chi S_LS_R^\star T_RT_R^\star + m_\chi S_L^\star S_RT_LT_L^\star) + m_4^4S_LS_L^\star T_LT_L^\star \\
&+ m_4^4S_RS_R^\star T_RT_R^\star - m_4^2sS_LS_L^\star T_LT_L^\star - m_4^2sS_RS_R^\star T_RT_R^\star \\
&- m_4^2S_LS_L^\star tT_LT_L^\star - m_4^2S_LS_L^\star T_LT_L^\star u \\
&- m_4^2S_RS_R^\star tT_RT_R^\star - m_4^2S_RS_R^\star T_RT_R^\star u \\
&+ m_\chi m_\chi sS_LS_L^\star T_RT_R^\star + m_\chi m_\chi sS_RS_R^\star T_LT_L^\star + S_LS_L^\star tT_LT_L^\star u \\
&+ S_RS_R^\star tT_RT_R^\star u)
\end{aligned}
\tag{D.24}
$$

$$
\begin{aligned}
\left|M_{s(h)}M_{s(V)}^\star\right| = &\frac{1}{(m_i^2-s)(s-MV^2)} \\
&5L_{LR}V_{VV}(A_Lc(C_Lm_2(m_3^2-m_4^2-t+u) \\
&+ C_Rm_1(m_1^2-m_2^2-m_3^2+m_4^2-t+u)) \\
&+ A_Rc(C_Lm_1(-m_1^2+m_2^2+m_3^2-m_4^2+t-u) \\
&+ C_Rm_2(-m_3^2+m_4^2+t-u)))
\end{aligned}
\tag{D.25}
$$

$$
\begin{aligned}
\left|M_{s(h)}M^{\star}_{t(\chi)}\right| = \frac{1}{(m_i^2-s)(s-m_\chi^2)} \\
& 2L_{LR}(C_L(m_1^3U_R^\star V_R^\star - 2m_1^2V_L^\star(m_2U_L^\star + m_\chi U_R^\star) \\
& - m_1V_R^\star(2m_2^2U_R^\star + 4m_2m_\chi U_L^\star \\
& + U_R^\star(t-m_4^2)) + V_L^\star(m_2^3(-U_L^\star) - 2m_2^2m_\chi U_R^\star + m_2U_L^\star(-m_4^2+s+u) \\
& + 2m_\chi sU_R^\star)) + C_R(m_1^3U_L^\star V_L^\star - 2m_1^2V_R^\star(m_2U_R^\star + m_\chi U_L^\star) \\
& - m_1V_L^\star(2m_2^2U_L^\star + 4m_2m_\chi U_R^\star + U_L^\star(t-m_4^2)) + V_R^\star(m_2^3(-U_R^\star) \\
& - 2m_2^2m_\chi U_L^\star + m_2U_R^\star(-m_4^2+s+u) + 2m_\chi sU_L^\star)))
\end{aligned}
\tag{D.26}
$$

$$
\begin{aligned}
\left|M_{s(h)}M^{\star}_{u(\chi)}\right| = \frac{1}{(m_i^2-s)(s-m_\chi^2)} \\
& 2L_{LR}(C_L(2m_1^3S_R^\star T_R^\star + m_1^2T_L^\star(m_2S_L^\star - 2m_\chi S_R^\star) \\
& + m_1T_R^\star(m_2^2S_R^\star - 4m_2m_\chi S_L^\star + S_R^\star(m_4^2-s-t)) + T_L^\star(-2m_2^2m_\chi S_R^\star \\
& + m_2S_L^\star(u-m_4^2) + 2m_\chi sS_R^\star)) + C_R(2m_1^3S_L^\star T_L^\star \\
& + m_1^2(m_2S_R^\star T_R^\star - 2m_\chi S_L^\star T_R^\star) + m_1T_L^\star(m_2^2S_L^\star - 4m_2m_\chi S_R^\star \\
& + S_L^\star(m_4^2-s-t)) + T_R^\star(-2m_2^2m_\chi S_L^\star + m_2S_R^\star(u-m_4^2) + 2m_\chi sS_L^\star)))
\end{aligned}
\tag{D.27}
$$

$$
\begin{aligned}
\left|M_{s(V)}M^{\star}_{t(\chi)}\right| = \frac{1}{(m_\chi^2-s)(s-MV^2)} \\
& 2V_{VV}(A_R(m_1^4U_R^\star V_R^\star - m_1^3V_L^\star(m_2U_L^\star + 2m_\chi U_R^\star) \\
& + m_1^2V_R^\star(-11m_2^2U_R^\star - 9m_2m_\chi U_L^\star + U_R^\star(-3m_3^2 + 2m_4^2 + s - 2t + 3u)) \\
& + m_1V_L^\star(m_2^3U_L^\star - 7m_2^2m_\chi U_R^\star + m_2U_L^\star(2m_3^2 + 2m_4^2 - s + t - u) \\
& + m_\chi U_R^\star(-7m_3^2 - 2m_4^2 + 2t + 7u)) + V_R^\star(-2m_2^4U_R^\star \\
& + m_2^2U_R^\star(-4m_3^2 - 7m_4^2 + 2s + 3t + 8u) + m_2m_\chi U_L^\star(-2m_3^2 - 7m_4^2 + 2t + 7u) \\
& + U_R^\star(-m_3^2(m_4^2 - 2s + t - 2u) + m_4^4 \\
& + m_4^2(s - 2t + u) - (t+2u)(s-t+u)))) - A_L(m_1^4U_L^\star V_L^\star \\
& - m_1^3V_R^\star(m_2U_R^\star + 2m_\chi U_L^\star) + m_1^2V_L^\star(-11m_2^2U_L^\star - 9m_2m_\chi U_R^\star \\
& + U_L^\star(-3m_3^2 + 2m_4^2 + s - 2t + 3u)) + m_1V_R^\star(m_2^3U_R^\star - 7m_2^2m_\chi U_L^\star \\
& + m_2U_R^\star(2m_3^2 + 2m_4^2 - s + t - u) + m_\chi U_L^\star(-7m_3^2 - 2m_4^2 + 2t + 7u)) \\
& + V_L^\star(-2m_2^4U_L^\star + m_2^2U_L^\star(-4m_3^2 - 7m_4^2 + 2s + 3t + 8u) \\
& + m_2m_\chi U_R^\star(-2m_3^2 - 7m_4^2 + 2t + 7u) + U_L^\star(-m_3^2(m_4^2 - 2s + t - 2u) + m_4^4 \\
& + m_4^2(s - 2t + u) - (t+2u)(s-t+u)))))
\end{aligned}
\tag{D.28}
$$

$$
\begin{aligned}
\left|M_{s(V)}M^{\star}_{u(\chi)}\right| = \frac{1}{m_\chi^2 - s)(s - MV^2)} \\
&2V_{VV}(A_L(8m_1^4 S_L^\star T_L^\star - 7m_1^3 m_\chi S_L^\star T_R^\star \\
&+ m_1^2 T_L^\star(4m_2^2 S_L^\star - 9m_2 m_\chi S_R^\star + S_L^\star(5m_3^2 + 5m_4^2 - 3s - 9t - u)) \\
&+ m_1 T_R^\star(-2m_2^2 m_\chi S_L^\star + m_2 S_R^\star(-2m_3^2 - 2m_4^2 + s + t - u) \\
&+ m_\chi S_L^\star(-2m_3^2 - 7m_4^2 + 7t + 2u)) + T_L^\star(2m_2^2 S_L^\star(m_3^2 - t) \\
&+ m_2 m_\chi S_R^\star(-7m_3^2 - 2m_4^2 + 7t + 2u) + S_L^\star(m_3^2(m_4^2 - 2s - 2t + u) \\
&- m_4^4 - m_4^2(s + t - 2u) + (2t + u)(s + t - u)))) \\
&+ A_R(-8m_1^4 S_R^\star T_R^\star + 7m_1^3 m_\chi S_R^\star T_L^\star \\
&+ m_1^2 T_R^\star(-4m_2^2 S_R^\star + 9m_2 m_\chi S_L^\star + S_R^\star(-5m_3^2 - 5m_4^2 + 3s + 9t + u)) \\
&+ m_1 T_L^\star(2m_2^2 m_\chi S_R^\star + m_2 S_L^\star(2m_3^2 + 2m_4^2 - s - t + u) \\
&+ m_\chi S_R^\star(2m_3^2 + 7m_4^2 - 7t - 2u)) + T_R^\star(2m_2^2 S_R^\star(t - m_3^2) \\
&+ m_2 m_\chi S_L^\star(7m_3^2 + 2m_4^2 - 7t - 2u) + S_R^\star(-m_3^2(m_4^2 - 2s - 2t + u) \\
&+ m_4^4 + m_4^2(s + t - 2u) - (2t + u)(s + t - u)))))
\end{aligned}
\tag{D.29}
$$

$$
\begin{aligned}
\left|M_{t(\chi)}M^\star_{u(\chi)}\right| = {} & \frac{1}{(m_\chi^2-s)(s-m_\chi^2)} \\
& 4(3m_1^4(S_L^\star T_L^\star U_L V_L + S_R^\star T_R^\star U_R V_R) + m_1^3(-3m_2(S_L^\star T_L^\star U_R V_R \\
& + S_R^\star T_R^\star U_L V_L) + m_\chi(S_L^\star T_R^\star U_L V_L + S_R^\star T_L^\star U_R V_R) \\
& + 2m_\chi(S_L^\star T_L^\star U_L V_R + S_R^\star T_R^\star U_R V_L)) + m_1^2(4m_2^2(S_L^\star T_L^\star U_L V_L \\
& + S_R^\star T_R^\star U_R V_R) + m_2(m_\chi(S_L^\star T_L^\star U_R V_L + S_R^\star T_R^\star U_L V_R) \\
& - 2m_\chi(S_L^\star T_R^\star U_R V_R + S_R^\star T_L^\star U_L V_L)) + m_\chi m_\chi S_L^\star T_R^\star U_L V_R \\
& + m_\chi m_\chi S_R^\star T_L^\star U_R V_L - 4s(S_L^\star T_L^\star U_L V_L + S_R^\star T_R^\star U_R V_R) \\
& - S_L^\star t T_L^\star U_L V_L - S_L^\star T_L^\star u U_L V_L - S_R^\star t T_R^\star U_R V_R - S_R^\star T_R^\star u U_R V_R) \\
& + m_1(m_2^3(-(S_L^\star T_L^\star U_R V_R + S_R^\star T_R^\star U_L V_L)) + m_2^2(m_\chi(S_L^\star T_L^\star U_L V_R \\
& + S_R^\star T_R^\star U_R V_L) - 2m_\chi(S_L^\star T_R^\star U_L V_L + S_R^\star T_L^\star U_R V_R)) \\
& + m_2(S_L^\star U_R(T_L^\star V_R(t+u) - 4m_\chi m_\chi T_R^\star V_L) + S_R^\star U_L(-4m_\chi m_\chi T_L^\star V_R \\
& + t T_R^\star V_L + T_R^\star u V_L) + s(S_L^\star T_L^\star U_R V_R + S_R^\star T_R^\star U_L V_L)) \\
& + m_4^2(m_\chi S_L^\star T_R^\star U_L V_L + m_\chi S_R^\star T_L^\star U_R V_R + \\
& m_\chi S_L^\star T_L^\star U_L V_R + m_\chi S_R^\star T_R^\star U_R V_L) \\
& - m_\chi S_L^\star t T_R^\star U_L V_L - m_\chi S_R^\star t T_L^\star U_R V_R - m_\chi s S_L^\star T_L^\star U_L V_R \\
& - m_\chi s S_R^\star T_R^\star U_R V_L - m_\chi S_L^\star t T_L^\star U_L V_R - m_\chi S_R^\star t T_R^\star U_R V_L) \\
& + m_2^4(S_L^\star T_L^\star U_L V_L + S_R^\star T_R^\star U_R V_R) - m_2^3 m_\chi(S_L^\star T_R^\star U_R V_R \\
& + S_R^\star T_L^\star U_L V_L) - m_2^2(S_L^\star U_L(-m_\chi m_\chi T_R^\star V_R + t T_L^\star V_L + T_L^\star u V_L) \\
& + S_R^\star U_R(T_R^\star V_R(t+u) - m_\chi m_\chi T_L^\star V_L) + 2s(S_L^\star T_L^\star U_L V_L \\
& + S_R^\star T_R^\star U_R V_R)) + m_2(m_4^2(-(m_\chi S_L^\star T_R^\star U_R V_R + m_\chi S_R^\star T_L^\star U_L V_L \\
& + m_\chi S_L^\star T_L^\star U_R V_L + m_\chi S_R^\star T_R^\star U_L V_R)) + m_\chi(s+u)(S_L^\star T_R^\star U_R V_R \\
& + S_R^\star T_L^\star U_L V_L) + m_\chi u(S_L^\star T_L^\star U_R V_L + S_R^\star T_R^\star U_L V_R)) \\
& + s(S_L^\star U_L(-m_\chi m_\chi T_R^\star V_R + t T_L^\star V_L + T_L^\star u V_L) + S_R^\star U_R(T_R^\star V_R(t+u) \\
& - m_\chi m_\chi T_L^\star V_L) + s(S_L^\star T_L^\star U_L V_L + S_R^\star T_R^\star U_R V_R)))
\end{aligned}
\tag{D.30}
$$

D.4. Ghosts

$$
\begin{aligned}
\left|M_{s(h)}\right|^2 = {} & \frac{1}{(m_i^2-s)(s-mj^2)}(G_{GH}G^\star_{GH}(C_L(C_L^\star(m_1^2+m_2^2-s)+2C_R^\star m_1 m_2) \\
& + C_R(2C_L^\star m_1 m_2 + C_R^\star(m_1^2+m_2^2-s))))
\end{aligned}
\tag{D.31}
$$

$$
\begin{aligned}
\left|M_{s(V)}\right|^2 = -\frac{1}{(m_V^2 - s)(s - m_V^2)} w_{wV} w_{wV}^{\star} \\
(AL(A_L^{\star}(2m_1^4 + m_1^2(2m_2^2 + 3m_3^2 + 3m_4^2 + s - 3t - 3u) + (m_3^2 + m_4^2 + s - t - u)(m_2^2 + m_3^2 + m_4^2 - \\
- 2A_R^{\star} m_1 m_2 s) + A_R(A_R^{\star}(2m_1^4 + m_1^2(2m_2^2 + 3m_3^2 + 3m_4^2 + s - 3t - 3u) \\
+ (m_3^2 + m_4^2 + s - t - u)(m_2^2 + m_3^2 + m_4^2 - s - t - u)) - 2A_L^{\star} m_1 m_2 s))
\end{aligned}
\tag{D.32}
$$

$$
\begin{aligned}
\left|M_{s(h)} M_{s(V)}^{\star}\right| = -\frac{1}{(m_i^2 - s)(s - m_V^2)} G_{GH} w_{wV}^{\star} \\
(A_L^{\star}(C_L m_2(-2m_1^2 - m_3^2 - m_4^2 + t + u) + C_R m_1(m_1^2 + m_2^2 + m_3^2 + m_4^2 - t - u)) \\
+ A_R^{\star}(C_L m_1(m_1^2 + m_2^2 + m_3^2 + m_4^2 - t - u) \\
+ C_R m_2(-2m_1^2 - m_3^2 - m_4^2 + t + u)))
\end{aligned}
\tag{D.33}
$$

E. Kinematic

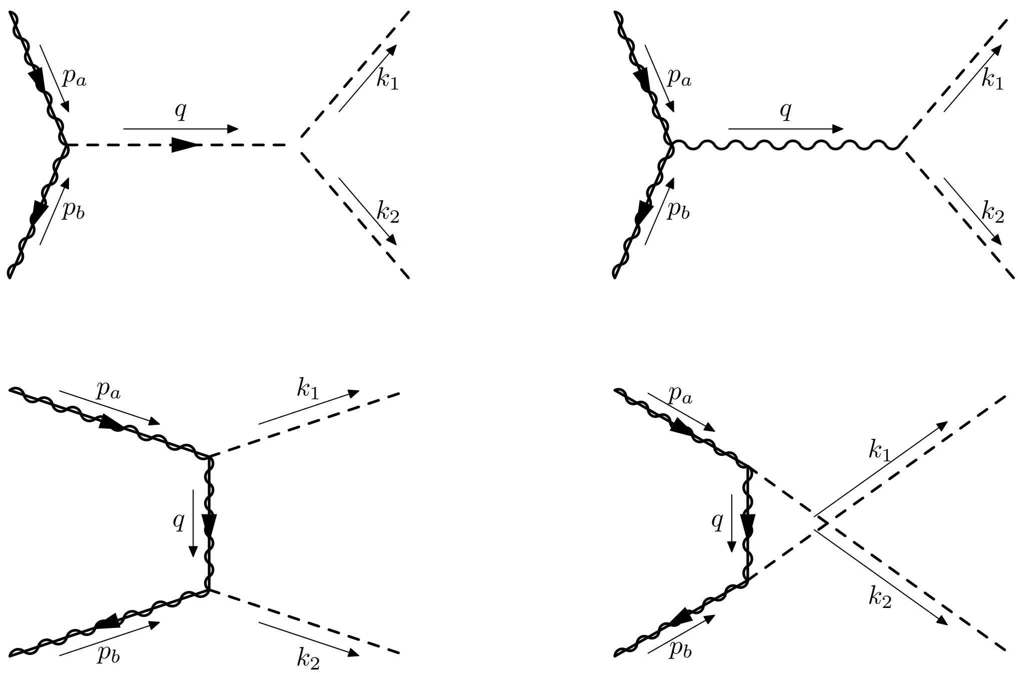

Figure E.1.: s-channel, t-channel and u-channel with fermion flux and the momentum direction

In figure E.1 the different channels of the calculated processes are shown. As a notation, it was used that the fermion flux goes from the upper spinor to the lower one. All initial momenta p_a and p_b were ingoing momenta, while the final momenta k_1 and k_2 were outgoing. Defining the Mandelstam variables [3] according to the chosen momenta convention, they are

$$\begin{aligned} s &= (p_b + p_a)^2 = (k_1 + k_2)^2 \\ t &= (p_a - k_1)^2 = (k_2 - p_b)^2 \\ u &= (p_b - k_1)^2 = (p_a - k_2)^2. \end{aligned} \tag{E.1}$$

F. Trapezoidal Method

The Trapezoidal Method [4] can be used for the calculation of an integral of the function $f(x)$. If you have a function f(x), like for example in figure F.1, you can calculate the space under the curve by approximating the curve by a straight line between two points on the curve. To improve the approximation the interval $[a, b]$ can be splitted in smaller intervals. To calculate the gray area, you can split the trapeze into a square $f(a) * (b - a)$ and a triangle $(f(b) - f(a))(b - a) \cdot 1/2$.

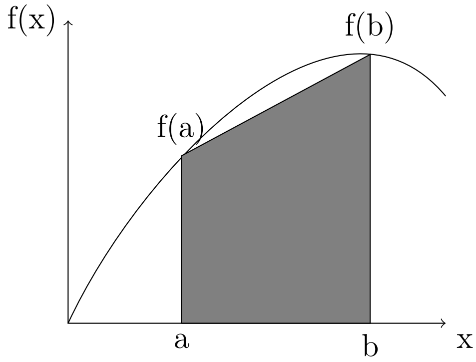

Figure F.1.: Illustration of the explanation of the Trapezoidal Method

G. Backward Euler Method

The backward Euler method [5] is used to over estimate the integral of a function $f(x)$. To integrate the function $f(x)$ between the points a and b one lay an recangle over the curve with the edge length of $b - a$ and $f(b)$ if $f(a) < f(b)$, see figure G.1. The area of the gray rectangle is then $(a - b)f(b)$. Again to improve the result the width between a and b can be splitted into smaller intervals.

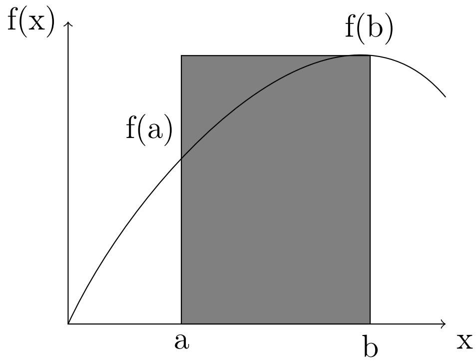

Figure G.1.: Illustration of the explanation of the Backward Euler Method

H. Simpson Integration

With the help of the Simpon's rule [6] one can numerically integrate a function. The function, which should be integrated, will be approximated via parabolic functions. To calculate an integral of the following form

$$\int_a^b f(x)dx \tag{H.1}$$

one has to partition the interval $[a, b]$ in N subintervals between $[x_i, x_{i+1}]$

$$\int_a^b f(x)dx = \sum_{i=0}^{N-1} \int_{x_i}^{x_{i+1}} f(x)dx. \tag{H.2}$$

The step width h for the subintervals is determined by the differ of the integration limits $[a, b]$ and the number of subintervals N

$$h = \frac{b-a}{N} \quad \rightarrow x_i = a + i \cdot h,\ x_{i+1} = a + (i+1) \cdot h. \tag{H.3}$$

The remaining integral can be approximated by the following function

$$\int_{x_i}^{x_{i+1}} f(x)dx = \frac{h}{6}\left[f(x_i) + 4 \cdot f\left(\frac{x_i + x_{i+1}}{2}\right) + f(x_{i+1})\right]. \tag{H.4}$$

List of Figures

Bibliography

[1] URL: http://apod.nasa.gov/apod/ap060824.html.

[2] URL: http://sci.esa.int/science-e-media/img/61/Planck_CMB_Mollweide_4k.jpg.

[3] URL: http://www.uni-muenster.de/Physik.KP/Lehre/KT2-SS04/mat/kt2_01_rel_kinematik.pdf.

[4] URL: http://mathworld.wolfram.com/TrapezoidalRule.html.

[5] URL: http://mathworld.wolfram.com/EulerForwardMethod.html.

[6] URL: http://mathworld.wolfram.com/SimpsonsRule.html.

[7] A. Pukhov A. Belyaev N.D. Christensen. 'CalcHEP 3.4 for collider physics within and beyond the Standard Model'. In: (2012). DOI: 10.1016/j.cpc.2013.01.014. URL: http://arxiv.org/abs/1207.6082.

[8] I. Aitchison. *Supersymmetry in Particle Physics*. Cambridge, 2007.

[9] I.J.R. Aitchison. 'Supersymmetry and the MSSM: An Elementary Introduction'. In: (2005). URL: arXiv:hep-ph/0505105.

[10] K. Begeman T.S. van Albada J.N.Bahcal and R. Sancisi. 'Distribution of dark matter in the spiral galaxy NGC 3198'. In: *Astrophysical Journal* 295.Part 1 (ISSN 0004-637X) (Aug. 1985). Provided by the SAO/NASA Astrophysics Data System, pp. 305–313. DOI: 10.1086/163375. URL: http://adsabs.harvard.edu/abs/1985ApJ...295..305V.

[11] M. Klasen B. Herrmann. 'Neutralino Annihilation into Massive Quarks with SUSY-QCD Corrections'. In: *Phys. Rev. D* (2009). DOI: 10.1103/PhysRevD.79.061701. URL: arXiv:0901.0481.

[12] K.Kovařík M.Meinecke P.Steppeler B.Herrmann M.Klasen. 'One-loop corrections to gaugino (co-)annihilation into quarks in the MSSM'. In: *Phys. Rev. D* (May 2014), p. 19. DOI: 10.1103/PhysRevD.89.114012.

[13] K.Kovařík B.Herrmann M.Klasen. 'SUSY-QCD effects on neutralino dark matter annihilation beyond scalar or gaugino mass unification'. In: *Phys. Rev. D* (2009). DOI: 10.1103/PhysRevD.80.085025. URL: arXiv:0907.0030.

[14] C.J.Borschensky. 'Einschränkungen an Annihilationsprozesse dunkler Materie aus dem seltenen $B_s \to \mu^+\mu^-$-Zerfall im Minimalen Supersymmetrischen Standardmodell'. MA thesis. Karlsruhe Institue of Technology, 2012.

[15] Planck Collaboration. 'Planck 2015 results. I. Overview of products and scientific results'. In: (). URL: `http://xxx.lanl.gov/abs/1502.01582`.

[16] Tom van Daal. 'Squark-Gluino Production Next-to-Leading Order Contributions to the Scattering Cross-Section in the Threshold Region'. PhD thesis. Radboud University Nijmegen, 2011.

[17] *Dark energy, dark matter*. URL: `http://science.nasa.gov/astrophysics/focus-areas/what-is-dark-energy/`.

[18] Anthony H. Gonzalez Maxim Markevitch Scott W. Randall Christine Jones Dennis Zaritsky Douglas Clowe Marusa Bradac. 'A direct empirical proof of the existence of dark matter'. In: *Astrophysical Journal* 648 (2006). DOI: `10.1086/508162`.

[19] A. P. A. S.langer F. Boudjema A. Pukhov A.Semenov G. BÃ©langer F. Boudjema. 'The micrOMEGAs user's manual, version 4.1'. In: (2014). URL: `http://lapth.cnrs.fr/micromegas/v4.1/manual4.1.pdf`.

[20] F.Boudjema A. Pukhov A.Semenov G.Belanger. 'micrOMEGAs: A program for calculating the relic density in the MSSM'. In: *Comput.Phys.Commun.* 149 (2002), pp. 103–120. DOI: `10.1016/S0010-4655(02)00596-9`.

[21] Dan Hooper. 'TASI 2008 Lectures on Dark Matter'. In: (2009). URL: `http://arxiv.org/abs/0901.4090`.

[22] A.J.G. Hey I.J.R. Aitchison. *Gauge theories in particle physics*. Vol. 1 and 2. Taylor & Francis.

[23] M. Klasen K. Kovařík Q. Le Boulc'h J. Harz B. Herrmann. 'Neutralino-stop co-annihilation into electroweak gauge and iggs bosons at one loop'. In: (2012). DOI: `10.1103/PhysRevD.87.054031`. URL: `arXiv:1212.5241`.

[24] M. Klasen K. Kovařík J. Harz B. Herrmann and M. Meinecke. 'SUSY-QCD corrections to stop annihilation into electroweak final states including Coulomb enhancement effects'. In: *Phys. Rev. D* 91 (2015).

[25] Karol Kovařík. 'Precise predictions for sfermion pair production at a linear collider'. PhD thesis. Comenius University, Bratislava, 2005.

[26] M. Kuroda. 'Complete Lagrangian of the MSSM'. In: (2005). URL: `http://arxiv.org/abs/hep-ph/9902340`.

[27] I.A. Stegun M. Abramowitz. *Handbook of Mathematical Functions*. 378. Dover Publications Inc., 1972.

[28] M.Milgrom. 'A Modification of the Newtonian dynamics as a possible alternative to the hidden mass hypothesis'. In: *Astrophysical Journal* 270 (1983), pp. 365–370. DOI: `10.1086/161130`.

[29] Moritz Meinecke. 'SUSY-QCD Corrections to the (Co) Annihilation of Neutralino Dark Matter within the MSSM'. PhD thesis. Westfälische Wilhelms-Universität Münster, 2015. URL: `http://pauli.uni-muenster.de/tp/fileadmin/Arbeiten/meinecke_phd.pdf`.

[30] P.Ullio L.Bergström M. Schelke E.A. Baltz P. Gondolo J. Edsjö. 'DarkMSSM: Computing Supersymmetric Dark Matter Properties Numerically'. In: *JCAP 0407* (2004). DOI: `10.1088/1475-7516/2004/07/008`.

[31] P.Gondolo and G.Gelmini. 'Cosmic Abundance of stable Patricles: Improved Analysis'. In: (1991).

[32] L.Bergstöm P.Ullio M.Schelke E.A. Baltz T.Bringmann G. Duda P.Gondolo J. Edsjö. 'Manual and long description of routines'. In: 806 (), pp. 322–324. URL: `http://fysik.su.se/~edsjo/darksusy/docs/Manual.pdf`.

[33] A. Pukhov. 'CalcHEP 2.3: MSSM, structure functions, event generation, batchs, and generation of matrix elements for other packages'. In: (). URL: `arXiv:hep-ph/0412191`.

[34] T.Hahn. 'FormCalc 8 User's Guide'. In: (2015).

[35] M.Perez-Victoria T.Hahn. 'AutomatMSSM One-Loop Claculation in 4 and D dimensions'. In: *Comput.Phys.Commun.* 118.153-165 (1999).

[36] F. Staub W. Porod. 'Spheno 3.1:Extensions including flavour, CP-phases and models beyond the MSSM'. In: *Comput.Phys.Commun.* 183 (2012), pp. 2458–2469. DOI: `10.1016/j.cpc.2012.05.021`.

[37] F. Zwicky. 'Die Rotverschiebung von extragalaktischen Nebeln'. In: *Helv. Phys. Acta* 6 (1933), pp. 110–127.

[38] P.Z.Skands *et al.* 'CompHEP 4.5 Status Report'. In: *PoS ACAT08:008* (2008). URL: `arXiv:0901.4757[hep-ph]`.

Statement

I hereby declare that the current thesis is authored by myself. There were neither other resources or tools used than the ones which are declared. Each part of the thesis where resources were used are provided with references.

Münster, 28th January 2016

Saskia Schmiemann